

**REPORT  
55**



# **ARCHAEAN FELSIC VOLCANISM IN PARTS OF THE EASTERN GOLDFIELDS REGION WESTERN AUSTRALIA**

**by P. A. Morris**



**GEOLOGICAL SURVEY OF WESTERN AUSTRALIA  
DEPARTMENT OF MINERALS AND ENERGY**



**GEOLOGICAL SURVEY OF WESTERN AUSTRALIA**

**REPORT 55**

**ARCHAEAN FELSIC VOLCANISM IN PARTS  
OF THE EASTERN GOLDFIELDS REGION  
WESTERN AUSTRALIA**

**by  
P. A. Morris**

**Perth 1998**

**MINISTER FOR MINES**  
**The Hon. Norman Moore, MLC**

**DIRECTOR GENERAL**  
**L. C. Ranford**

**DIRECTOR, GEOLOGICAL SURVEY OF WESTERN AUSTRALIA**  
**David Blight**

**Copy editor: D. P. Reddy**

**REFERENCE**

**The recommended reference for this publication is:**

MORRIS, P. A., 1998, Archaean felsic volcanism in parts of the Eastern Goldfields region, Western Australia: Western Australia Geological Survey, Report 55, 80p.

**National Library of Australia**  
**Cataloguing-in-publication entry**

Morris, P. A. (Paul Andrew), 1952–.  
Archaean felsic volcanism in parts of the Eastern Goldfields region, Western Australia

Bibliography.  
ISBN 0 7309 6612 7

1. Geology, Structural — Western Australia — Eastern Goldfields.
2. Volcanism — Western Australia — Eastern Goldfields.
3. Geochemistry — Western Australia — Eastern Goldfields.
4. Eastern Goldfields (W.A.).
  - I. Geological Survey of Western Australia.
  - II. Title. (Series: Report (Geological Survey of Western Australia); 55).

559.416

ISSN 0508-4741

The locations of points mentioned in this publication are referenced to the Australian Geodetic Datum 1984 (AGD84)

**Cover photograph:**

**Oligomictic dacite breccia, Morgans Island, near Kambalda.**

## Contents

Abstract .....	1
Introduction .....	1
Terminology .....	3
Regional geology .....	4
Felsic volcanism in the Kalgoorlie Terrane .....	4
The Black Flag Group in the Kalgoorlie area .....	4
East of White Flag Lake .....	5
Western side of White Flag Lake .....	8
Lakewood drilling .....	11
Drillcore from Boulder .....	21
Mount Shea .....	23
Gibson-Honman Rock .....	26
The Black Flag Group in the Kambalda–Mandilla–Widgiemooltha area .....	27
Morgans Island .....	27
Mandilla area .....	29
Diamond drillcore from the Kambalda area .....	29
Felsic volcanism in the northern Eastern Goldfields and Kanowna areas .....	33
Northern Eastern Goldfields region .....	33
Kanowna area .....	36
Perkolilli .....	36
Four Mile Hill .....	40
Diamond drilling near Kanowna .....	42
Gordon mining centre .....	42
Geochronology of felsic volcanic rocks .....	44
Kalgoorlie and Kanowna areas .....	44
Leonora area .....	44
Physical volcanology of felsic volcanic rocks .....	44
Black Flag Group .....	44
Dacite–rhyolite association .....	44
Andesite-dominated association .....	45
The Kanowna and northern Eastern Goldfields areas .....	46
Geochemistry of felsic volcanic rocks .....	46
Alteration and element mobility .....	47
Major- and trace-element variations .....	47
Rare-earth element chemistry .....	47
Discussion .....	51
Petrogenesis .....	52
Derivation of Black Flag Group dacites and rhyolites by fractional crystallization of andesite .....	52
Derivation of Black Flag Group andesite and dacite by partial melting of the same source .....	53
A review of relevant petrogenetic models .....	53
Petrogenetic models for felsic volcanic rocks in the Eastern Goldfields region .....	55
Summary and conclusions .....	60
Locus of melting .....	60
Mineralization potential .....	60
Interpretation of tectonic setting .....	61
Acknowledgements .....	63
References .....	64

## Appendix

Whole-rock chemistry of mafic, intermediate, and felsic volcanic rocks from parts of the Eastern Goldfields region .....	69
--	----

## Figures

1.	Distribution of major felsic volcanic associations in the Eastern Goldfields region of Western Australia .....	2
2.	Distribution of felsic volcanic rocks of the Black Flag Group and associated greenstones, east of White Flag Lake .....	6
3.	Rhyolite-dominated breccia with subordinate mafic clasts, Black Flag Group, east of White Flag Lake .....	7
4.	Laminated volcanoclastic sandstone, Black Flag Group, eastern side of White Flag Lake .....	7
5.	Distribution of intermediate and felsic volcanic and volcanoclastic rocks of the Black Flag Group and associated greenstones, western side of White Flag Lake .....	9
6.	Andesite flow, Black Flag Group, western side of White Flag Lake .....	10
7.	Volcanoclastic sandstone, Black Flag Group, White Flag Lake .....	10
8.	Distribution of intermediate and felsic volcanic rocks of the Black Flag Group and associated greenstones in the Kalgoorlie area .....	11
9.	Graphic log of diamond drillhole SE3 in the Black Flag Group at Lakewood .....	12
10.	Graphic log of the felsic part of diamond drillhole SE3, Black Flag Group, Lakewood .....	14
11.	Jigsaw-fit dacite breccia in the Black Flag Group, in diamond drillhole SE3 at Lakewood .....	15
12.	Disorganized dacite breccia in the Black Flag Group, in diamond drillhole SE3 at Lakewood .....	15
13.	Dacite at 621 m depth in the Black Flag Group, in diamond drillhole SE3 at Lakewood .....	16
14.	Dacite at 571 m depth in the Black Flag Group, in diamond drillhole SE3 at Lakewood .....	16
15.	Graphic log of diamond drillhole SE4 in the Black Flag Group at Lakewood .....	17
16.	Graphic log of diamond drillhole SE7 in the Black Flag Group at Lakewood .....	18
17.	Frequency histograms for thickness of Black Flag Group in diamond drillholes at Lakewood .....	21
18.	Idealized cross section of silicic lava extruded into shallow water .....	22
19.	Graphic log of diamond drillhole LED10 in the Black Flag Group at Kalgoorlie–Boulder .....	22
20.	Simplified geology of the Mount Shea area .....	24
21.	Crystal-rich matrix enclosing angular basalt fragments, Black Flag Group at Mount Shea .....	25
22.	Black Flag Group dacite from Gibson-Honman Rock .....	27
23.	Simplified Archaean geology of the Kambalda–Widgiemoorltha area .....	28
24.	Geological sketch map of Morgans Island .....	29
25.	Interpreted stratigraphy at Morgans Island .....	30
26.	Oligomictic breccia in Black Flag Group at locality 5, Morgans Island .....	31
27.	Pseudojigsaw-fit oligomictic breccia in Black Flag Group at locality 4, Morgans Island .....	31
28.	Rhyolite lava in Black Flag Group at locality 1, Morgans Island .....	32
29.	Graphic log of diamond drillholes DDH1–4 in the Black Flag Group at Loves Find .....	34
30.	Simplified geological map of the Kanowna area .....	37
31.	Moderately well sorted felsic fragmental unit at Perkolilli .....	38
32.	Glassy, spherulitic matrix to rhyolite clast in breccia unit from Perkolilli .....	38
33.	Eutaxitic texture developed in sample GSWA 114158 from Perkolilli .....	39
34.	Eutaxitic texture developed in clast from Perkolilli .....	40
35.	Quartz and feldspar phenocrysts in a partly devitrified groundmass in rhyolite at Four Mile Hill, Kanowna .....	41
36.	Simplified geology near the Gordon mining centre .....	43
37.	Harker variation diagrams for mafic, intermediate, and felsic rocks from Melita, Jeedamya, Kanowna, and the Black Flag Group .....	48
38.	Chondrite-normalized rare-earth element plots for rocks from the Black Flag Group and the Jeedamya, Melita, and Perkolilli (Kambalda) areas .....	50
39.	Zr/Nb versus SiO <sub>2</sub> (wt%) for mafic and intermediate rocks from Melita, Jeedamya, and the Black Flag Group .....	51
40.	MORB-normalized spider diagram for felsic volcanic rocks from Melita and Jeedamya .....	52
41.	Average dacite and results of andesite fractionation normalized to average Black Flag Group andesite .....	53
42.	Sr/Y versus Y for felsic and intermediate rocks of the Black Flag Group and felsic rocks from Melita, Jeedamya, and Kanowna .....	54
43.	Results of computer modelling for derivation of Black Flag Group andesite and SE dacite from tholeiitic basalt, and partial melting of tonalite and I-type granite .....	57
44.	Chondrite-normalized plot of La/Yb versus Yb for intermediate and felsic volcanic rocks of the Black Flag Group, and felsic rocks from Jeedamya, Melita, and Perkolilli .....	59
45.	Th/Yb versus chondrite-normalized Yb for intermediate and felsic volcanic rocks of the Black Flag Group, and felsic rocks from Jeedamya, Melita, and Perkolilli .....	61
46.	Zr/Y versus Y for intermediate and felsic volcanic rocks of the Black Flag Group, and felsic rocks from Jeedamya, Melita, and Perkolilli .....	61
47.	Tectonic cartoon for the Eastern Goldfields region at two stages in the late Archaean .....	62

## Tables

1. Grain-size classification of sedimentary, pyroclastic, and volcanoclastic rocks .....	3
2. Stratigraphic schemes for the Black Flag Group .....	4
3. Chronology of intermediate and felsic volcanic rocks from parts of the Eastern Goldfields region .....	36
4. Volcanological characteristics of the Black Flag Group and felsic volcanic rocks from the Melita, Jeedamyia, and Kanowna areas .....	46
5. Mineral compositions used in least-squares modelling of fractional crystallization of the Black Flag Group .....	52
6. Summary of least-squares modelling results for fractional crystallization of the Black Flag Group .....	52
7. Mineral/melt distribution coefficients for fractionation modelling of the Black Flag Group .....	53
8. Selected characteristics of high-Al TTD, average SE dacite, Jeedamyia rhyolite, and Melita rhyolite ....	54
9. Compositions of daughter liquids, parent liquids, and minerals used in modelling of partial melting ....	56
10. Results of least-squares and Rayleigh fractionation modelling of two potential source compositions (I-type granite and tonalite) .....	58



### Digital dataset (in pocket)



Geochemical data for mafic, intermediate, and felsic volcanic rocks from parts of the Eastern Goldfields region (FELCHEM.CSV)



# Archaean felsic volcanism in parts of the Eastern Goldfields region, Western Australia

by

P. A. Morris

## Abstract

Two felsic volcanic rock associations can be distinguished on the basis of eruption style, lithology, and whole-rock geochemistry in the Eastern Goldfields region of Western Australia. One association, the Black Flag Group, forms a 200 km-long, north-northwesterly trending belt centred on Kalgoorlie–Boulder. The Black Flag Group consists of dacite and subordinate rhyolite lava lobes, andesite lavas, volcanoclastic breccias and sandstones, and carbonaceous shales. The dacites and rhyolites represent subaqueous extrusion of lava, with marginal breccias resulting from fragmentation of lava following contact with water. More-distal products represent redeposition of lava fragments. Andesites have been erupted as subaerial lava flows. The second association comprises volcanic rocks at Melita, Jeedamya, and Kanowna, and forms a belt parallel to and east of the Black Flag Group, with a strike length of more than 400 km. This association comprises a series of subaerially erupted tuffs and subordinate pyroclastic flows and lava. Both associations are bimodal in that although they are dominated by felsic volcanic rocks, they also have (subordinate) mafic and intermediate volcanic members.

Dacites and rhyolites of the Black Flag Group have higher  $\text{Na}_2\text{O}:\text{K}_2\text{O}$  ratios and are depleted in heavy rare-earth elements, Y, Zr, and Nb. They are also enriched in  $\text{Al}_2\text{O}_3$ , light rare-earth elements, and Sr relative to most felsic volcanic rocks with the same  $\text{SiO}_2$  contents from Melita, Jeedamya, and Perkolilli. Andesites of the Black Flag Group have similar rare-earth element and high field strength element patterns to dacites and rhyolites, but are decoupled on some bivariate plots and relatively enriched in heavy rare-earth elements despite having similar light rare-earth element contents. These andesites cannot be modelled as the unfractionated parent to dacite and rhyolite, but represent melting of the same material under different conditions. Alternatively, the high Cr, Ni, and magnesium number of these andesites may indicate partial melting of metasomatized mantle.

The chemistry of intermediate to felsic volcanic rocks of the Black Flag Group is consistent with the melting of amphibolite at a pressure of about 11 kb (at about 35 km depth) under anhydrous conditions. Alternatively, felsic volcanic rocks from Melita, Jeedamya, and Kanowna represent melting of a felsic source under hydrous conditions. To explain the spatial relations and chemistry of these two associations, a convergent margin with a westerly dipping lithospheric plate is proposed. Felsic volcanic rocks from Melita, Jeedamya, and Perkolilli represent melting at the base of the crust, whereas melting of the subducted oceanic plate (and possibly the overlying mantle wedge) can account for the Black Flag Group rocks.

**KEYWORDS:** felsic volcanic rocks, geochemistry, petrogenesis, tectonics, volcanology, Eastern Goldfields region

## Introduction

The aims of this report are to present geochemical and geological data for some felsic-dominated volcanic rock successions in the Eastern Goldfields region of Western Australia, discuss their volcanology and chemistry, and define the tectonic setting.

Although igneous, sedimentary, and metamorphic rocks with high modal proportions of quartz and feldspar

form up to 50% of outcropping greenstones in the Eastern Goldfields region (Fig. 1), little is known about the relative proportions of sedimentary versus igneous rocks, depositional or eruption processes, or the chemistry of the igneous component. This is due to two factors: firstly, the poor outcrop and variable preservation of diagnostic textural and mineralogical characteristics that belie the origin of these rocks; and secondly, the commonly perceived low economic potential of these rocks and their consequent neglect by the exploration industry. However,

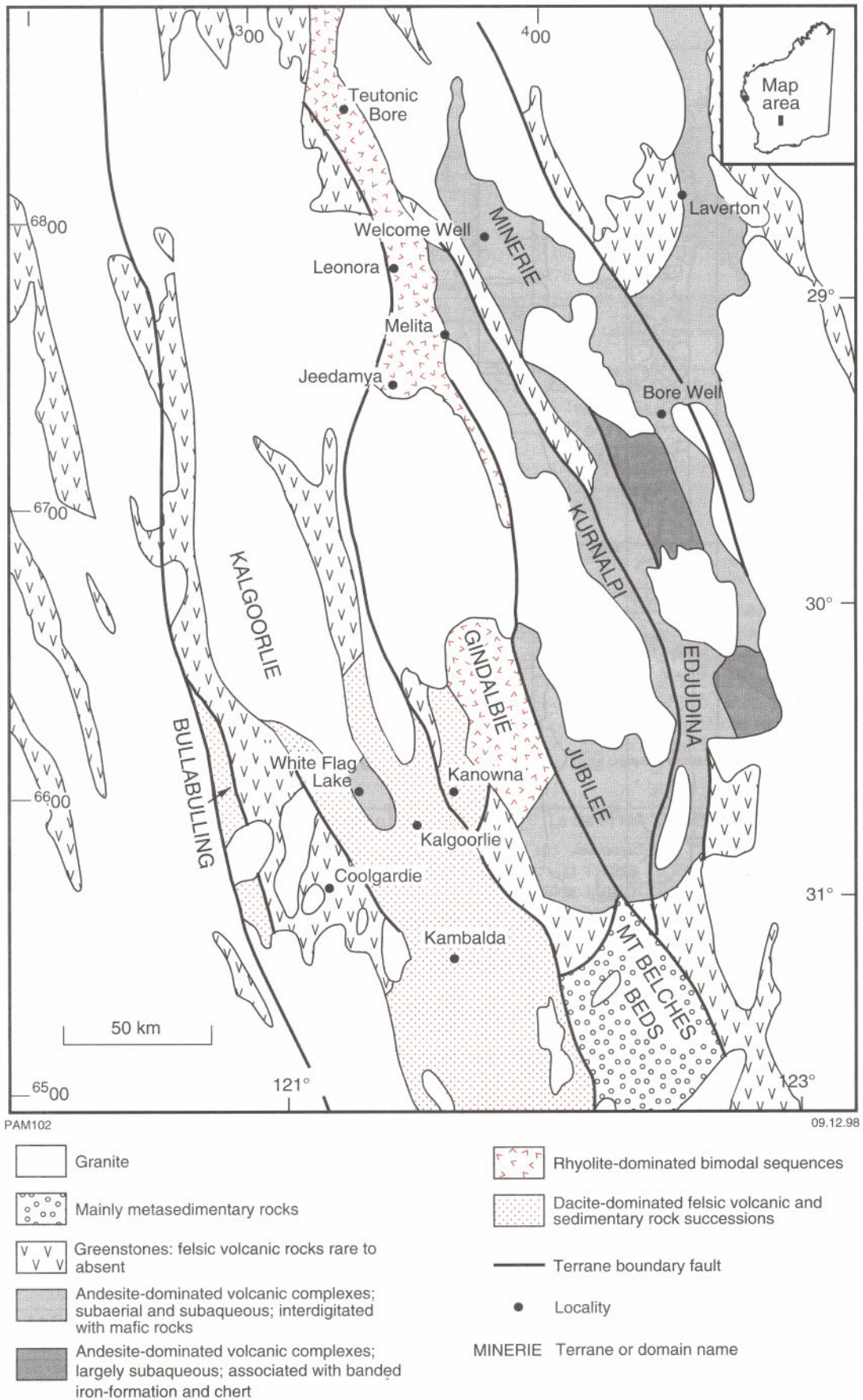


**Figure 1. Distribution of major felsic volcanic associations in the Eastern Goldfields region of Western Australia (after Hallberg et al., 1993)**

recent interest in felsic volcanic rocks and felsic volcanism has been stimulated by the identification of a significant gold resource hosted by felsic rocks at Kanowna Belle, east of Kalgoorlie, and global interest in volcanic-hosted massive sulfide (VHMS) deposits (Large, 1992; Cas, 1992). Kanowna Belle is estimated to contain measured and indicated resources of 1.60 million ounces of gold, and has estimated inferred resources of 2.27 million ounces of gold (Delta Gold NL, 1997).

In this report, the volcanology and chemistry of two areas of felsic volcanic rocks are discussed. One group of rocks, the Black Flag Group, belongs to a greenstone belt in which structural and stratigraphic relations are well known. The volcanology and chemistry of the Black Flag Group form a major part of this report.

The other group of rocks, found in a northwesterly trending belt east of the Black Flag Group, belongs to a greenstone succession whose structural and stratigraphic relations are not clear. The volcanology and chemistry of one of these felsic volcanic successions at Melita and Jeedamyia, southeast of Leonora (Witt, 1993a; Fig. 1), and its strike extension at Kanowna (Hallberg et al., 1993) are described.

## Terminology

In areas of low strain, greenstones retain their primary igneous or sedimentary textures and it is possible, in most cases, to assign a rock name based on hand specimen and thin section characteristics. The nomenclature of volcanic rocks follows the recommendations of the International Union of Geological Sciences Subcommittee on the Systematics of Igneous Rocks (Le Maitre, 1989):

- Basalts comprise (calcic) plagioclase and amphibole or chlorite (after pyroxene).
- Andesites are usually porphyritic rocks with zoned labradorite–oligoclase, amphibole (after pyroxene), and hornblende, with or without biotite.
- Dacites comprise quartz, (sodic) plagioclase, minor amounts of biotite, with or without hornblende and pyroxene.

- Rhyolites have phenocrysts of quartz and alkali feldspar, often with minor amounts of plagioclase and biotite.

When rocks are fine grained, contain a significant amount of glassy mesostasis, or have been modified by metamorphism or deformation, nomenclature based solely on texture and mineralogy is difficult. In these cases rock names have been assigned according to silica content following Gill (1981), where basalts have less than 53% SiO<sub>2</sub>, andesites 53 to 63 wt% SiO<sub>2</sub>, dacites 63 to 70 wt% SiO<sub>2</sub>, and rhyolites more than 70 wt% SiO<sub>2</sub>. There is good agreement between the petrographic and chemical classification schemes.

Clastic rock nomenclature is based on the Udden-Wentworth scale (Krumbein, 1934), with corresponding volcanic terminology where appropriate (Table 1).

Because greenstones of the Eastern Goldfields region are commonly characterized by poor outcrop and textural and mineralogical modification (by devitrification, metamorphism, and weathering), highly genetic terminology such as ‘ignimbrite’ and ‘lahar’ have been avoided. Instead, hand specimen and outcrop descriptions, contact relations, bed geometry, relationships to nearby facies, and the regional context are combined in an attempt to interpret possible modes of eruption, fragmentation, and deposition (Cas and Wright, 1987). The following terms are used in the sense of Cas and Wright (1987):

- Volcaniclastic — a non-genetic term for any fragmental aggregate of volcanic parentage, irrespective of origin.
- Epiclastic — a non-genetic term for deposits or rocks produced by normal surface fragmentation processes (weathering, gravitational collapse, physical abrasion) or finally deposited by normal surface processes (traction, suspension, mass flow) irrespective of their fragmentation mode.
- Pyroclastic — a genetic term for rocks formed by volcanic explosive activity *and* deposited by transport processes resulting from this activity.

**Table 1. Grain-size classification of sedimentary, pyroclastic, and volcaniclastic rocks**

<i>Udden-Wentworth scale<sup>(a)</sup></i>	<i>Pyroclastic fragments<sup>(b,c)</sup></i>	<i>Lithified pyroclastic deposit<sup>(b,c)</sup></i>	<i>Volcaniclastic rock<sup>(b)</sup></i>
Cobbles	Bombs and blocks	Agglomerate or pyroclastic breccia	Volcanic breccia or conglomerate
..... 64 mm .....			
Granules and pebbles	Lapilli	Lapillistone	Volcanic breccia or conglomerate
..... 2.0 mm .....			
Sand	Coarse ash	Tuff	Volcanic sandstone
..... 0.0625 mm .....			
Silt	Fine ash	Tuff	Volcanic siltstone (mudstone)

SOURCES: (a) Krumbein (1934)  
 (b) Fisher (1961)  
 (c) Fisher (1966)

The term ‘pyroclastic flow’ is used for ‘a hot, variably fluidized, gas-rich, high particle concentration mass-flow of pyroclastic debris’ (Cas and Wright, 1991). Cas and Wright (1987, 1991) summarize the following criteria for the recognition of pyroclastic deposits:

- presence of pyroclastically fragmented debris, such as diagnostic juvenile debris (radially jointed bombs, variably vesiculated fragments);
- facies characteristics indicating a (pyroclastic) mass flow mode of deposition. Three types of pyroclastic flow are recognized: pumice flow or ignimbrites; scoria and ash flow; block and ash flow;
- evidence for a hot state of emplacement, indicated by welding textures, clearly defined columnar jointing, gas-segregation pipes, syndepositional thermoremanent magnetization, red thermal oxidation colouration, and carbonized wood and vegetation.

Clearly, some criteria do not apply to Archaean situations and, in other cases, diagnostic criteria are usually modified or destroyed due to textural and mineralogical reconstitution.

## Regional geology

The eastern part of the Archaean Yilgarn Craton in Western Australia (Fig. 1) is composed of granitoid rocks and elongate bodies of metamorphosed igneous rocks (greenstones) dominated by basaltic lithologies. The best understood greenstone succession in the Eastern Goldfields region is the 400 × 80 km Kalgoorlie Terrane, which is a series of elongate structural and stratigraphic domains containing all or part of a common stratigraphy (Swager et al., 1990; Fig. 1). In the Kalgoorlie Terrane mafic and ultramafic rocks host important gold and nickel

deposits (Marston, 1984; Clout et al., 1990) and their geology is correspondingly well known. However, little is known about the upper part of the greenstone stratigraphy, which is dominated by a series of felsic volcanic, volcanoclastic, and epiclastic rocks of the Black Flag Group.

Elsewhere in the Eastern Goldfields region the greenstone stratigraphy is less well understood (Hallberg, 1985, 1986; Rattenbury, 1993; Witt, 1993a), and the stratigraphic positions of some well-exposed felsic volcanic successions (e.g. at Welcome Well, Melita, Bore Well; Fig. 1) are currently contentious. Some of these rocks form a large part of the Gindalbie Terrane immediately east of the Kalgoorlie Terrane (Fig. 1; Swager, 1995).

## Felsic volcanism in the Kalgoorlie Terrane

### The Black Flag Group in the Kalgoorlie area

Most published stratigraphies of the Black Flag Group (Table 2) record a felsic to intermediate volcanic and associated volcanoclastic succession overlain by dominantly epiclastic and volcanoclastic rocks, with only a minor volcanic component. However, Clout et al.’s (1990) stratigraphy of the structurally complex Kalgoorlie–Boulder succession has felsic volcanic rocks at the top of the stratigraphy. The wide variations in estimated stratigraphic thicknesses for the Black Flag Group probably reflect the rapid lateral facies changes characteristic of felsic volcanic deposits (Cas and Wright, 1987) and the structural repetition of greenstones (Swager, 1989; Swager and Griffin, 1990; Clout et al., 1990).

**Table 2. Stratigraphic schemes for the Black Flag Group**

<i>Reference</i>	<i>Stratigraphic scheme</i>
Woodall (1965)	<b>Black Flag Beds</b> Tuff, acid to intermediate lavas and agglomerate, sandstone, shale, slate, and quartzite. Thickness: 3000 m
Gemuts and Theron (1975)	<b>Gundockerta Group</b> Sequence 5: Greywacke, shale, siltstone, and conglomerate Sequence 4: Acid extrusive rocks, greywacke, shale, and conglomerate
Williams (1976)	<b>Gundockerta Group</b> Epiclastic assemblage, conglomerate, and felsic volcanic assemblages; subordinate mafic volcanic rocks
Keats (1987)	<b>Black Flag Beds</b> IIB: Clastic sedimentary rocks IIIA: Felsic to intermediate volcanic and subvolcanic rocks. Thickness: up to 2500 m
Hunter (1993)	<b>White Flag Formation</b> Intermediate volcanic rocks and minor flows. Thickness: 50 to 1500 m. <b>Spargoville Formation</b> Heterogeneous sequence of felsic volcanic rocks, flows, intrusions, and minor sedimentary rocks. Thickness: 1500 m
Clout et al. (1990)	Lower sequence of basalt, mudstone, turbiditic mudstone, siltstone, and sandstone. Overlain by felsic volcanic rocks and minor sedimentary rocks. Thickness: 1000 m
Roberts and Elias (1990)	<b>Morgans Island Epiclastic</b> Breccias, lavas, and tuffs. Thickness: 1000 m. <b>Newtown Felsics</b>

Keats (1987) and Hunter (1993) examined the Black Flag Group in detail. Keats (1987) divided the Black Flag Group of the Kalgoorlie area into a lower (IIIA) and an upper (IIIB) unit. At the base of unit IIIA, a 10–50 m-thick, locally sulfidic, graphitic shale is overlain by felsic to intermediate volcanic and subvolcanic rocks with an estimated stratigraphic thickness of 2500 m. Volcanic rocks comprise dacite with subordinate rhyolite, trachyte, and andesite as lava flows, tuffs, and coarse fragmental rocks. Keats (1987) suggested a close genetic relationship between volcanic and volcanoclastic rocks on the basis of similar lithologies. Unit IIIB is dominated by feldspathic clastic rocks with sedimentary structures consistent with deposition from a high-energy flow regime.

Hunter (1993) identified two formations within the Black Flag Group — the Spargoville Formation and the White Flag Formation. The lower, 50–1500 m-thick Spargoville Formation contains locally developed conglomerate consisting of mafic, ultramafic, and felsic volcanic clasts. The remainder comprises dacite and rhyodacite porphyry, tuff breccia, and clastic rocks. Volcanoclastic rocks consist of ash-flow tuffs with interbedded epiclastic rocks, accretionary lapilli, and locally developed crystalline rocks (terminology of Hunter, 1993). The overlying 1500 m-thick White Flag Formation is dominated by intermediate volcanoclastic rocks and locally developed volcanic flows. Eighty to ninety percent of the rocks are termed tuff breccias, and consist of porphyritic and amygdaloidal andesite.

Prominent outcrops of andesitic volcanic and volcanoclastic rocks west of White Flag Lake (northwest of Kalgoorlie) are part of the White Flag Formation, which Hunter (1993) placed at the top of the Black Flag Group. However, J. A. Hallberg (1993, pers. comm.) does not consider these rocks to be part of the Black Flag Group, placing them instead at the top of the Ora Banda stratigraphy. Thus there is some question as to the stratigraphic position of these rocks, although they lie in the same tectono-stratigraphic domain as dacite and rhyolite to the south at Gibson-Honman Rock, which shows strong lithological affinity with the Black Flag Group (Swager et al., 1990). Alternatively, the andesites may represent an isolated facies of volcanic activity. Support for this is provided by a localized outcrop of intermediate volcanic rocks in close stratigraphic proximity to underlying mafic and ultramafic volcanic rocks at Mount Shea, south of Kalgoorlie–Boulder (Keats, 1987).

Despite the usually poor outcrop in areas of low strain, there are well-preserved and laterally extensive outcrops where rock types can be identified and lateral relationships determined.

## East of White Flag Lake

Isolated outcrops of felsic volcanic, sedimentary, and ultramafic rocks form a northwesterly trending belt from west of the Kalgoorlie–Menzies Road towards Black Flag to east of White Flag Lake (Fig. 2). Hunter (1988) mapped the area at 1:100 000 scale as the Spargoville Formation, which he maintained was the lower part of the Black Flag Group.

East of the Kalgoorlie–Leonora railway line at Kalgoorlie (AMG (3136) 503088<sup>1</sup> on the KALGOORLIE<sup>2</sup> 1:100 000 map sheet; Fig. 2) there is a rubbly outcrop of conchoidally fractured, weakly porphyritic, pale-green to yellow felsic volcanic rock, with local development of globular features (possibly spherules) up to 5 mm in diameter. Scattered quartz and subordinate feldspar phenocrysts reach a maximum length of 1 mm. About 60 m north of this outcrop, a similar rock forms a breccia with subordinate angular mafic fragments up to 2 cm long (Fig. 3).

Petrographically, this felsic volcanic rock (AMG 503088, GSWA 110690<sup>3</sup>) comprises a cryptocrystalline aggregate of quartz and feldspar with scattered microphenocrysts of ?feldspar now pseudomorphed by quartz and spongy opaque grains. Secondary calcite patches are common and the rock is criss-crossed by a net vein system infilled with fine-grained sericite. On the basis of outcrop, hand specimen, and thin section characteristics the rock is identified as a once-glassy rhyolite or dacite lava. Sample GSWA 110689 (Fig. 2), collected north of GSWA 110690, is less altered and consists of subangular to rounded (locally cusped), fine-grained, felsic volcanic rock fragments up to 5 mm long of feldspar laths with minor amounts of quartz and rare pseudomorphs after ?amphibole. Locally, the rock fragments show pseudo-jigsaw-fit texture. The groundmass comprises cryptocrystalline quartz and feldspar (the latter as thin blades) with scattered opaque oxides. There is abundant secondary carbonate and sericite. The rock is identified as a brecciated rhyolite or dacite lava.

Unbrecciated rhyolite, lithologically similar to GSWA 110690 and 110689, outcrops in a breakaway to the southeast (AMG 513084). Immediately to the north is a 2 m-thick, poorly sorted, weakly foliated breccia (with a 315° strike and vertical dip) with angular, dominantly felsic volcanic rock fragments up to 5 cm in diameter. Clasts make up about 80% of this open- and closed-framework breccia. The lateral extent is unknown.

Immediately north of the breccia, matrix-supported pebbly sandstone is succeeded by fine- to medium-grained interbedded sandstone and shale. Low-angle cross-bedding and size grading indicate that the succession youngs to the northeast, placing the unbrecciated rhyolite at the base of the exposure. Clasts in the pebbly sandstone are dominantly of fine-grained felsic volcanic rock. Further north (AMG 515087), chaotically organized blocks of thinly bedded felsic volcanoclastic sandstone form a clast-supported breccia with little matrix. Individual blocks show size grading, cross-bedding, and slump structures. In thin section a sandstone unit from one of these blocks (GSWA 110691) has 1–4 mm-thick laminae (Fig. 4). Thicker laminae have size-graded angular quartz, feldspar (commonly perthitic), and plagioclase with subordinate

<sup>1</sup> Localities are specified by the Australian Map Grid (AMG) standard six-figure reference system whereby the first group of three figures (eastings) and the second group (northings) together uniquely define position, on this sheet (four-figure standard reference number), to within 100 m.

<sup>2</sup> Capitalized names refer to standard 1:100 000 map sheets.

<sup>3</sup> Six-digit sample numbers correspond to samples held in the Geological Survey of Western Australia's petrology collection

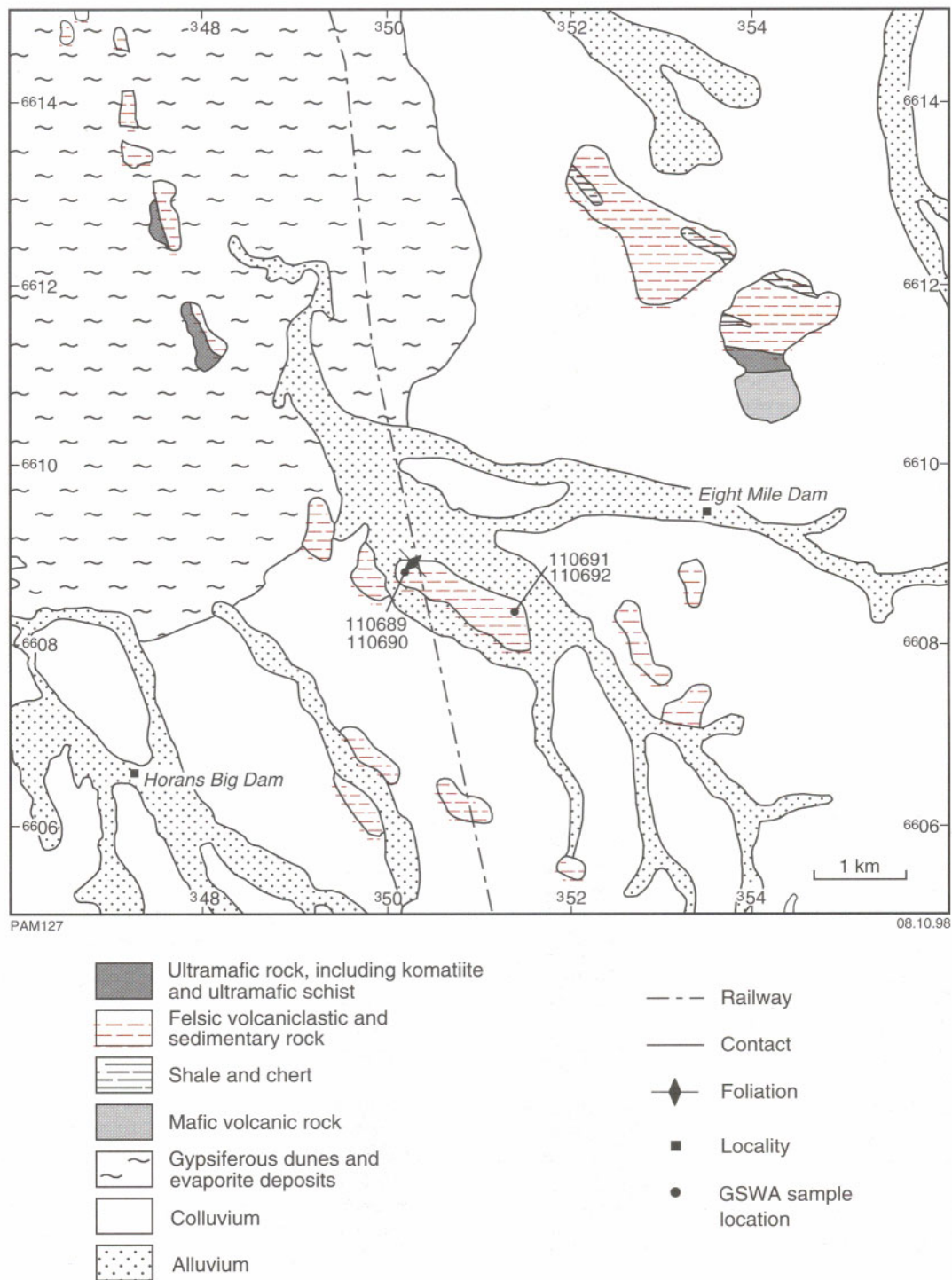
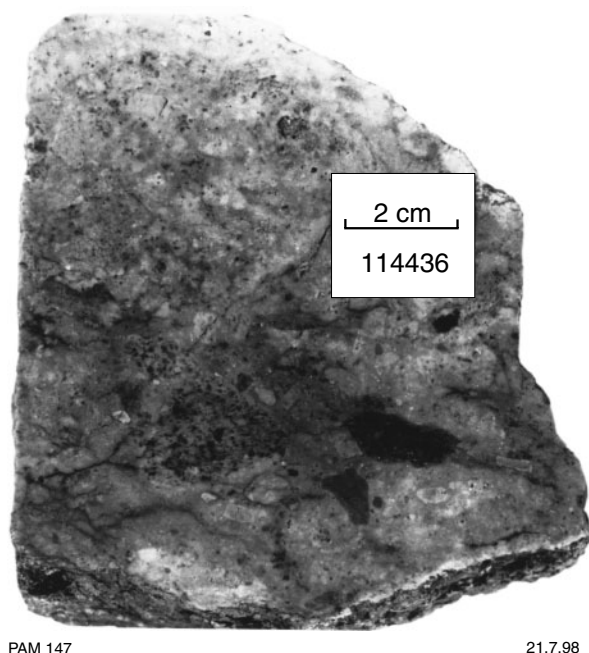


**Figure 2. Distribution of felsic volcanic rocks of the Black Flag Group (shown as felsic volcanoclastic and sedimentary rocks, shale, and chert) and associated greenstones, east of White Flag Lake (after Hunter, 1988)**

muscovite flakes and subangular to rounded granoblastic and cryptocrystalline quartz and feldspar rock fragments. All phases are less than 1 mm in diameter. Scattered granules or thin laminae of opaque oxide are accompanied by abundant secondary calcite. Finer grained laminae have cryptocrystalline quartz and feldspar with few rock fragments and less carbonate. Sample GSWA 110692, a

coarser grained sandstone from the same outcrop, is moderately well sorted with grains up to 1 mm in diameter of angular to subrounded quartz, rounded granoblastic quartz and feldspar rock fragments, and less common partly sericitized alkali feldspar. The latter phenocrysts are equant and show perthitic twinning. The matrix is subangular perthitic feldspar with subordinate locally



PAM 147

21.7.98

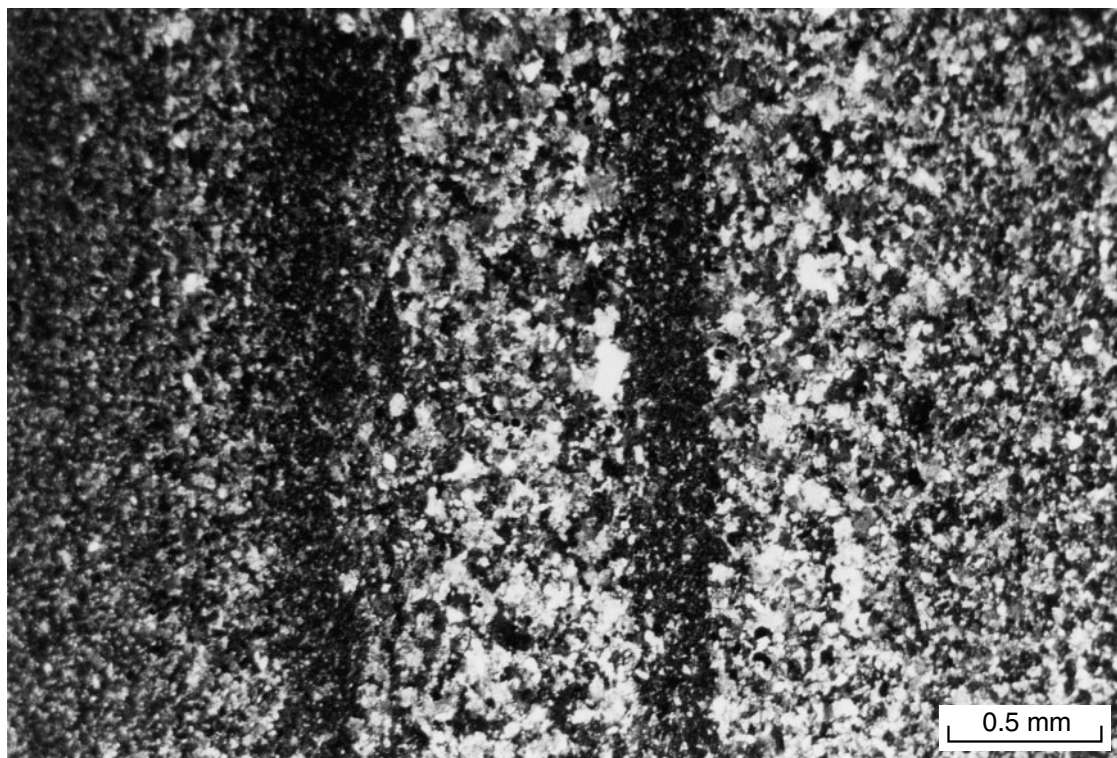
**Figure 3. Rhyolite-dominated breccia with subordinate mafic clasts, Black Flag Group, east of White Flag Lake; AMG (3136) 496117**

cusplate quartz and significant carbonate. Some fragments have shard-like outlines. The angularity of clasts, their limited compositional range, and the few rock fragments suggest that these sandstones represent reworking of a crystal-rich ash deposit.

Several explanations have been advanced for the origin of this unit as a whole, including dewatering of a loosely consolidated sedimentary succession, collapse of a volcanic cinder cone, and slumping of variably consolidated sediments (partial liquefaction) initiated by earthquake shock (Swager et al., 1990).

Northwest of this area (AMG 478128) a weakly brecciated and carbonated ultramafic unit (possibly part of the underlying Hannan Lake Serpentinite) is overlain by conglomerate of the Black Flag Group, which contains clasts of felsic volcanic rock with subordinate slate, ultramafic rock (now fuchsite), and chert. The breccia has both an open and closed framework, and locally developed cross-bedding indicates that it youngs to the east. The conglomerate-ultramafic contact is intruded by a quartz-feldspar porphyry.

Strongly weathered, vertically bedded shale, sandstone, and less common pebbly sandstone exposed in a breakaway (AMG 441160) have coarse- to fine-grained sandstone beds (20 to 30 cm thick) that fine upward to the



PAM 148

21.7.98

**Figure 4. Laminated volcaniclastic sandstone, Black Flag Group, eastern side of White Flag Lake. Coarser bands are dominated by quartz and feldspar. Finer bands comprise quartz, feldspar, and opaque oxides. Sample GSWA 110691; AMG (3136) 515083; plane polarized light**

northeast. The succession is locally folded, with fold axes plunging to the northwest. Lateral facies changes are shown by the transition from coarse sandstone to pebbly sandstone along strike.

### **Interpretation**

Facies represented on the eastern side of White Flag Lake include cohesive, locally brecciated rhyolite lava, oligomictic and polymictic breccia and conglomerate, and interbedded volcanoclastic sandstone and siltstone. Volcanoclastic rocks show a restricted range in clast type, and are dominated by weakly porphyritic felsic volcanic clasts. Both sandstones and siltstones are quartz and feldspar rich. In some instances (e.g. thinly bedded sandstones at AMG 515087) the angularity of framework components is consistent with only limited reworking of ash-grade material.

Cohesive and jigsaw-brecciated rhyolite (e.g. AMG 503088) are interpreted as the core and margin respectively of a subaqueous lava lobe, the breccia resulting from in situ quenching of lava in contact with water (Yamagishi, 1991; de Rosen Spence et al., 1980; Cas, 1992). Lithologically similar rhyolite (AMG 513084) is overlain by breccia composed largely of rhyolite fragments. The breccia could result from the erosion of the lava lobe with subsequent deposition as either a high-concentration turbidity current or a gravity flow. The overlying graded and cross-bedded sedimentary rocks are interpreted as more-distal turbidity current deposits. The chaotically arranged blocks of thinly bedded sandstone (AMG 513084) could represent slumped blocks of partially consolidated reworked ash. Slumping could have been triggered by volcanic activity, such as the extrusion of rhyolite lava.

### **Western side of White Flag Lake**

On the western side of White Flag Lake, the Spargoville and White Flag Formations (Hunter, 1993) form some of the best exposures of the Black Flag Group (Fig. 5). To the southwest, the succession is unconformably overlain by the Kurrawang Beds.

Felsic schists of the Spargoville Formation outcrop near Crown Dam and George Dam, along with several prominent 50–75 m-thick northwesterly striking chert ridges and locally developed dolerite. Hunter (1993) recorded southwesterly younging pillow lava in an interbedded porphyritic basalt unit. Thin lava units within the Spargoville Formation are weakly porphyritic, with scattered feldspar and subordinate amphibole phenocrysts.

The overlying White Flag Formation is well exposed on low hills immediately west of White Flag Lake (AMG 325100; Fig. 5). Here, rock types include volcanoclastic sandstone, conglomerate, and less common andesite lava flows. Volcanoclastic sandstones are size graded and cross-bedded (e.g. AMG 316101), and young to the west. They are largely composed of single grains of brown amphibole and feldspar, with subordinate lithic fragments. A 30–40 m-thick conglomerate unit contains

clasts up to 1 m in diameter of variably amygdaloidal plagioclase–amphibole andesite, as well as fewer clasts of fine-grained dacite. The conglomerate is largely clast supported. The matrix is composed of amphibole and plagioclase crystals and andesite fragments. A conglomerate unit 1 km to the northwest is largely composed of fine-grained dacite clasts, again with little matrix.

Petrographically the Spargoville Formation rocks are dominated by quartz and feldspar, whereas the White Flag Formation has less quartz, more feldspar, and conspicuous amphibole. A fine-grained felsic rock (GSWA 114470), outcropping about 500 m west-southwest of George Dam (Fig. 5), is a typical example of the Spargoville Formation. Granoblastic quartz grains show grain-size changes consistent with relict millimetre-scale bedding. The bedding is irregular and outlined by drusy carbonaceous material. Scattered voids up to 0.5 mm in diameter, with a bipyramidal form, could represent plucked quartz grains.

A porphyritic, weakly columnar jointed andesite flow on the shore of White Flag Lake (AMG 333100) belongs to the White Flag Formation, and is surrounded by poorly bedded volcanoclastic sandstone. It is strongly porphyritic, with roughly equal proportions of amphibole and feldspar. Amphibole phenocrysts (up to 3 mm in diameter in GSWA 114461) are euhedral and green to pale brown, some with ragged brown cores (Fig. 6). Oscillatory zoning is well developed and most grains are bordered by a thin, pale-brown inner rim then drusy opaque oxide. Grains are locally intergrown with feldspar. Feldspar phenocrysts are cloudy and partly sericitized. Some spongy grains have inclusions of opaque oxide, whereas others show weak oscillatory zoning. Most grains are simple-twinning alkali feldspar, although some are multiply twinned and have been optically determined as albite. The rock contains scattered opaque oxide. The groundmass consists of cryptocrystalline feldspar and granular amphibole, the latter locally altered to biotite. A visual estimate of GSWA 114472 (Fig. 6) is 35% phenocrysts and 65% groundmass.

The major components of White Flag Formation sandstones are amphibole and plagioclase (up to 2.5 mm long) that are optically identical to those in adjacent lava. They are accompanied by subordinate quartz and rock fragments. The crystal:matrix ratio ranges from about 30:70 (GSWA 114465) to 50:50 (GSWA 114473). Ratios of amphibole:feldspar range from 15:85 (GSWA 114463) to 25:75 (GSWA 114464). Both closed- and open-framework textures are present. Rock fragments consist of rounded, granoblastic quartz aggregates up to 0.4 mm in diameter. Monocrystalline quartz grains are anhedral and usually less than 5% in volume. The matrix has anhedral feldspar and amphibole crystals (some of which are broken), irregular calcite patches, and accessory epidote, chlorite, and opaque oxide in a cryptocrystalline quartzofeldspathic aggregate (Fig. 7).

### **Interpretation**

Felsic volcanic rocks at White Flag Lake illustrate the contrasting lithologies that make up the Black Flag Group,

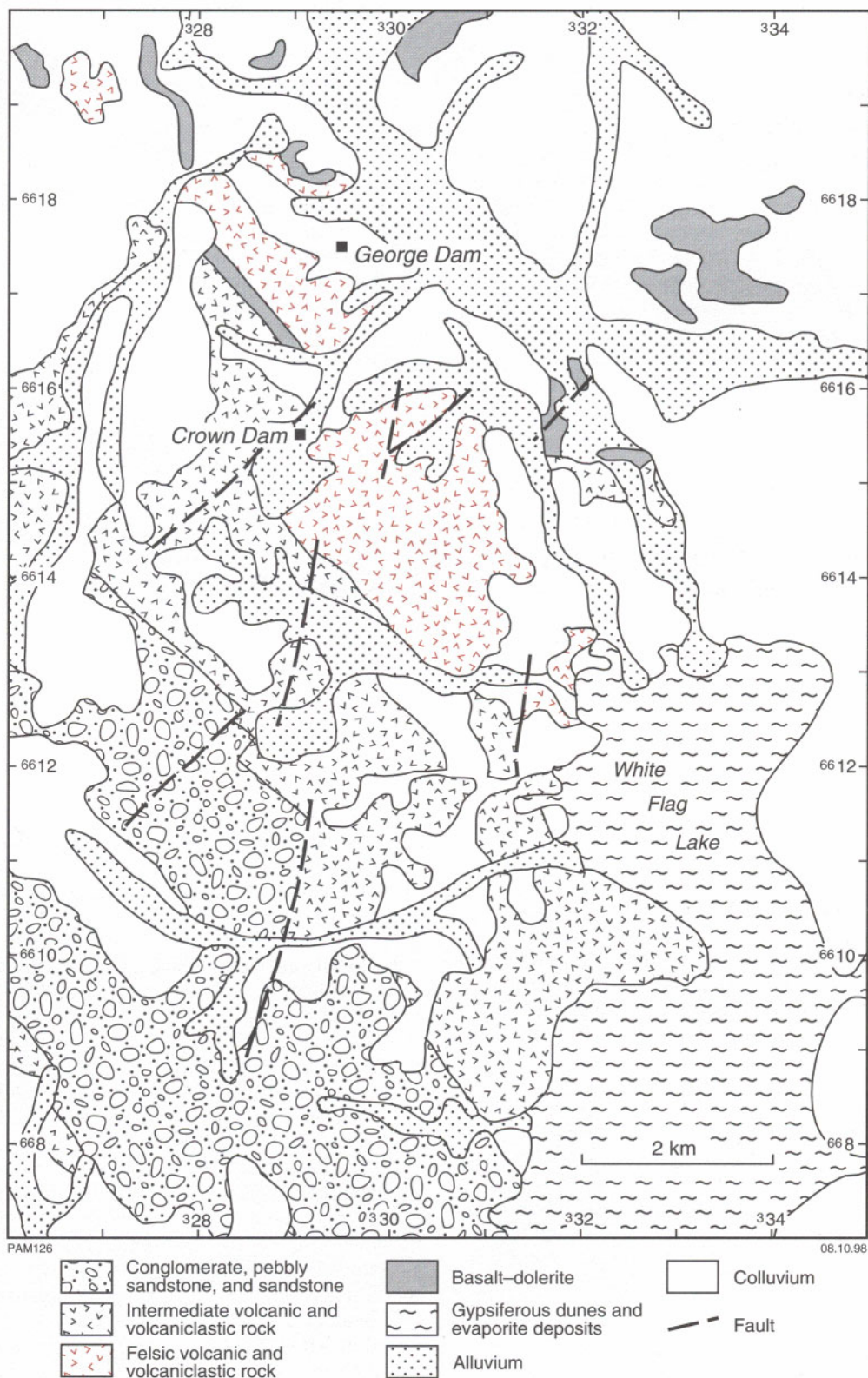


Figure 5. Distribution of intermediate and felsic volcanic and volcanoclastic rocks of the Black Flag Group and associated greenstones, western side of White Flag Lake (after Hunter, 1988)

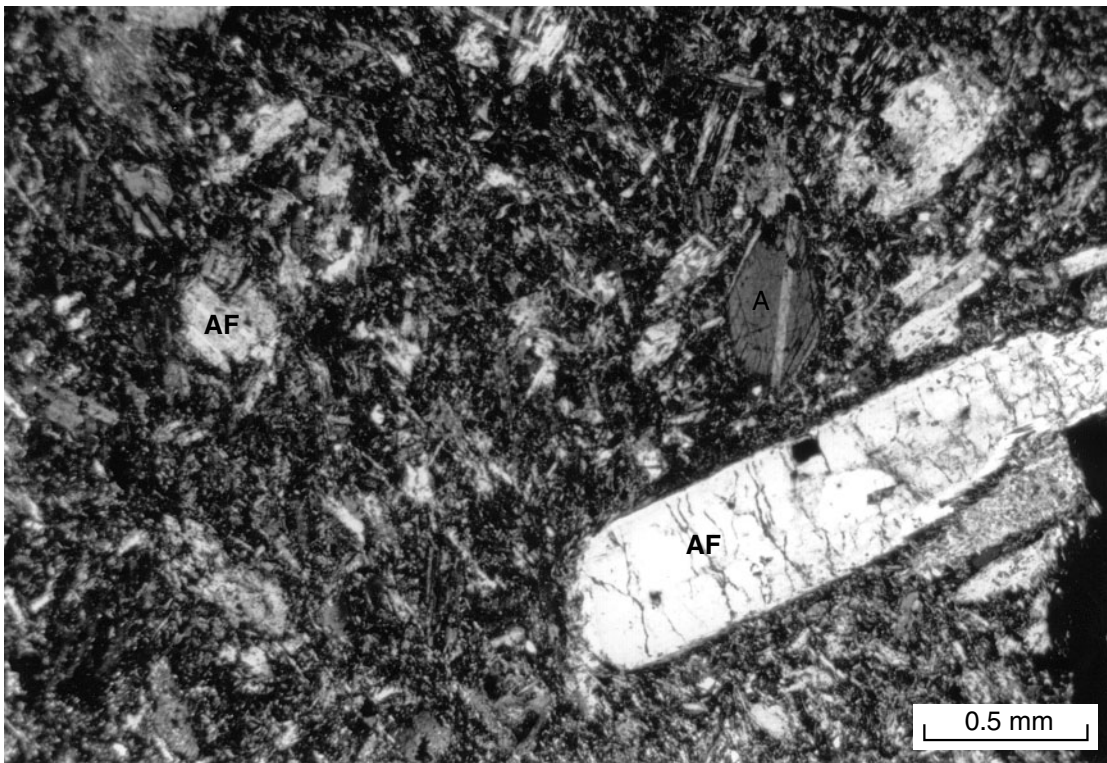


Figure 6. Andesite flow, Black Flag Group, western side of White Flag Lake. AF — alkali feldspar, A — amphibole. Sample GSWA 114472; AMG (3136) 330100; plane polarized light

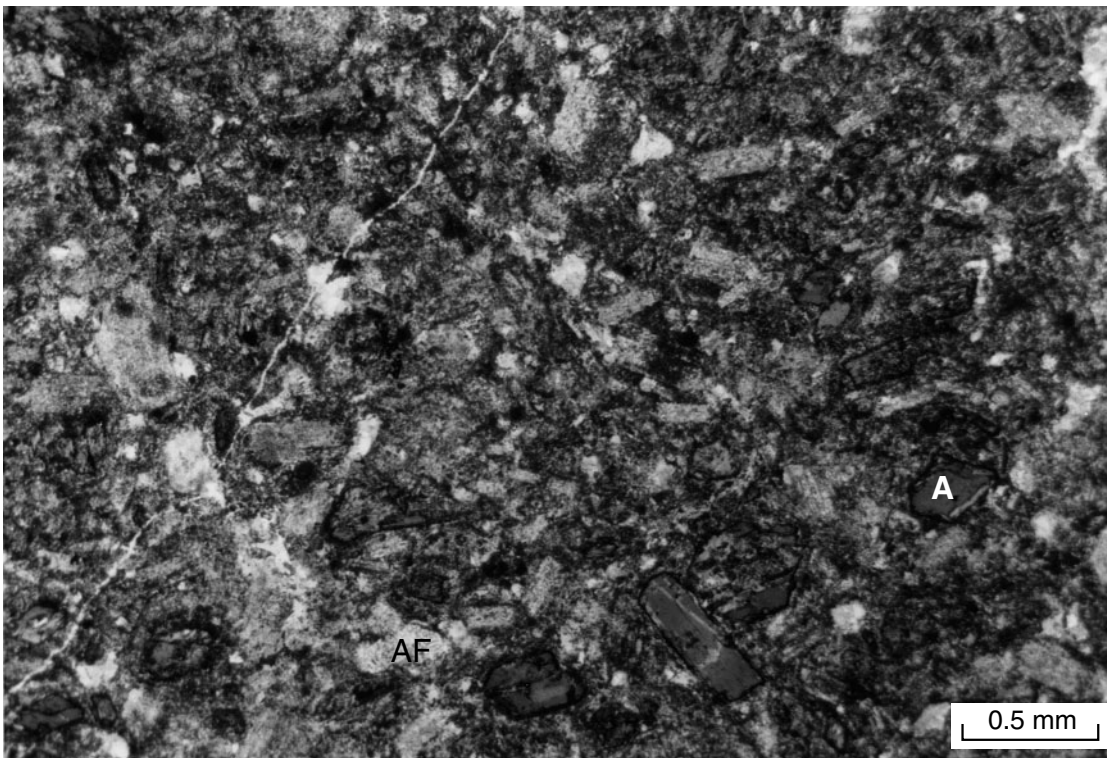


Figure 7. Volcaniclastic sandstone, Black Flag Group, White Flag Lake. AF — alkali feldspar, A — amphibole (note thin opaque rim). Sample GSWA 114464; AMG (3136) 283168; plane polarized light

with quartz- and feldspar-dominated assemblages accompanied by intermediate rocks with little quartz and roughly equal proportions of amphibole and feldspar. Both intermedial volcanic and volcanoclastic rocks of the White Flag Formation (Hunter, 1993) outcrop in the same areas and have similar types and proportions of minerals, consistent with a common magma source. Graded bedding, cross-bedding in intermediate to felsic rocks, and pillow structures in mafic lavas are consistent with subaqueous deposition, although at least one columnar-jointed flow attests to localized subaerial eruption. Degradation of lava flows resulted in the deposition of largely oligomictic conglomerates. One conglomerate has a dacite-dominated clast population and a quartzofeldspathic matrix, indicating reworking of the more-felsic volcanic rocks.

In the White Flag Formation the euhedral form of amphibole and plagioclase, few rock fragments, and the presence of sedimentary structures are consistent with the redeposition of crystal-rich volcanic deposits. Cas and Wright (1987) explained the crystal-rich nature of volcanoclastic rocks in terms of combined pyroclastic and epiclastic processes, where syneruption sorting of a crystal-rich pyroclastic eruption involves settling of dense crystal fragments and winnowing of fine ash from the eruption column. Up to 50% more crystal enrichment can be attained by transformed flow sorting from air into water, where subaqueous deposition effectively size sorts the deposit, elutriating the fine fraction and leaving a crystal-rich deposit.

## Lakewood drilling

A series of diamond drillholes transects the greenstone succession at Lakewood, about 10 km southeast of Kalgoorlie–Boulder. Locally the drilling is known as the Southend (SE) drilling program. These holes are of particular value to this study as they include significant thicknesses of the Black Flag Group, and Lakewood is sufficiently far from Kalgoorlie–Boulder to escape severe textural modification caused by carbonate metasomatism. Three drillholes (SE3, SE4, and SE7) have been logged and sampled for this study (Fig. 8). Drillholes SE4 and SE7 both contain the Black Flag Group and Golden Mile Dolerite, whereas SE3 contains only the Black Flag Group.

Travis et al. (1971) and Keats (1987) maintained that the Lakewood holes penetrated the western limb of the Kalgoorlie Syncline, terminating in the eastern limb. However, Clout et al. (1990) did not recognize either fold closure or axial-plane cleavage, and argued that the ‘core’ of the syncline is a series of rotated blocks of Golden Mile Dolerite and Black Flag Group rocks. In drillhole SE3, most bedded volcanoclastic rocks at the bottom of the hole show a downhole-facing direction, whereas those towards the top of the hole young upward, although there are local variations. This is consistent with Clout et al.’s (1990) observations of structural complexity, but could also represent regional folding. The exact stratigraphic position of the holes is still controversial. As the Golden Mile Dolerite cuts the Paringa Basalt – Black Flag Group contact and the base of the Black Flag Group is usually

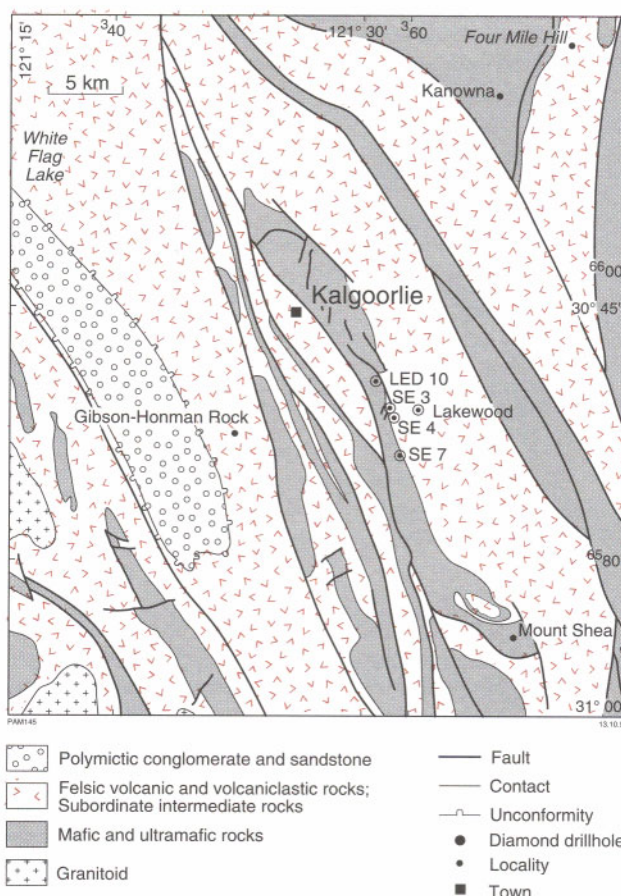


**Figure 8.** Distribution of intermediate and felsic volcanic rocks of the Black Flag Group and associated greenstones in the Kalgoorlie area. Also shown are diamond drillholes and other localities discussed in the text (modified from Swager et al., 1990)

sheared, it is unclear what part of the Black Flag Group stratigraphy is traversed by the SE drillholes. However, the dominance of felsic (versus intermediate) volcanic rocks and the assumption that the Golden Mile Dolerite intrudes the lower part of the Black Flag Group suggest that this drilling cuts the lower part of the Black Flag Group stratigraphy — corresponding to Hunter’s (1993) Spargoville Formation.

The lower half of core logged in drillhole SE3 (from about 670 to 1370 m) comprises volcanoclastic and epiclastic sedimentary rocks, whereas the upper half is dominantly volcanic material (Fig. 9).

Volcanoclastic and other sedimentary rocks consist of open- and closed-framework, largely dacitic, oligomictic and less common polymictic breccias, pebbly sandstone, massive poorly bedded sandstone, interbedded sandstone and shale, and thinly bedded carbonaceous and pyritic shale.

Breccias and pebbly sandstones have gradational contacts and similar clast compositions, comprising fine-



-  Cohesive lava
-  Flow-banded lava
-  Brecciated lava
-  Jigsaw brecciated lava
-  Breccia
-  Pebbly sandstone or breccia (open framework)
-  Pebbly sandstone or breccia (closed framework)
-  Sandstone
-  Cross-bedded sandstone
-  Siltstone (usually carbonaceous)
-  Carbonaceous sedimentary rock fragments
-  Dolerite (GMD = Golden Mile Dolerite)
-  Porphyry
-  Quartz vein

Grain size on base of log

- B boulder or cobble
- P pebble
- S sand
- S-M silt-mud
- Sharp contact
- ~ ~ Sheared contact
- ↑ Grading direction
-  Break in logging

PAM105A

14.10.98

grained felsic volcanic rock with less common fine-grained mafic and fuchsitic clasts and shale fragments. Felsic volcanic clasts are dacitic, angular, and up to 15 cm in diameter, although most are less than 10 cm in diameter. The matrix is a poorly sorted felsic sandstone with abundant felsic volcanic rock fragments.

Interbedded sandstones and siltstones have a range of sand:silt ratios, from 1:1 to 1:30. With decreasing proportions of sandstone, sandstone bed thicknesses decrease from centimetre to millimetre scale. Individual sandstone beds are normally graded.

Thinly bedded, locally sulfidic, carbonaceous shale contains pyrite as cubes and thin laminae parallel to bedding. Contorted folds result from loading by overlying sandstone.

From about 130 to 630 m depth the core is dominated by volcanic and related rocks (Fig. 10). Coherent dacite lava comprises almost 80% of this interval. In hand

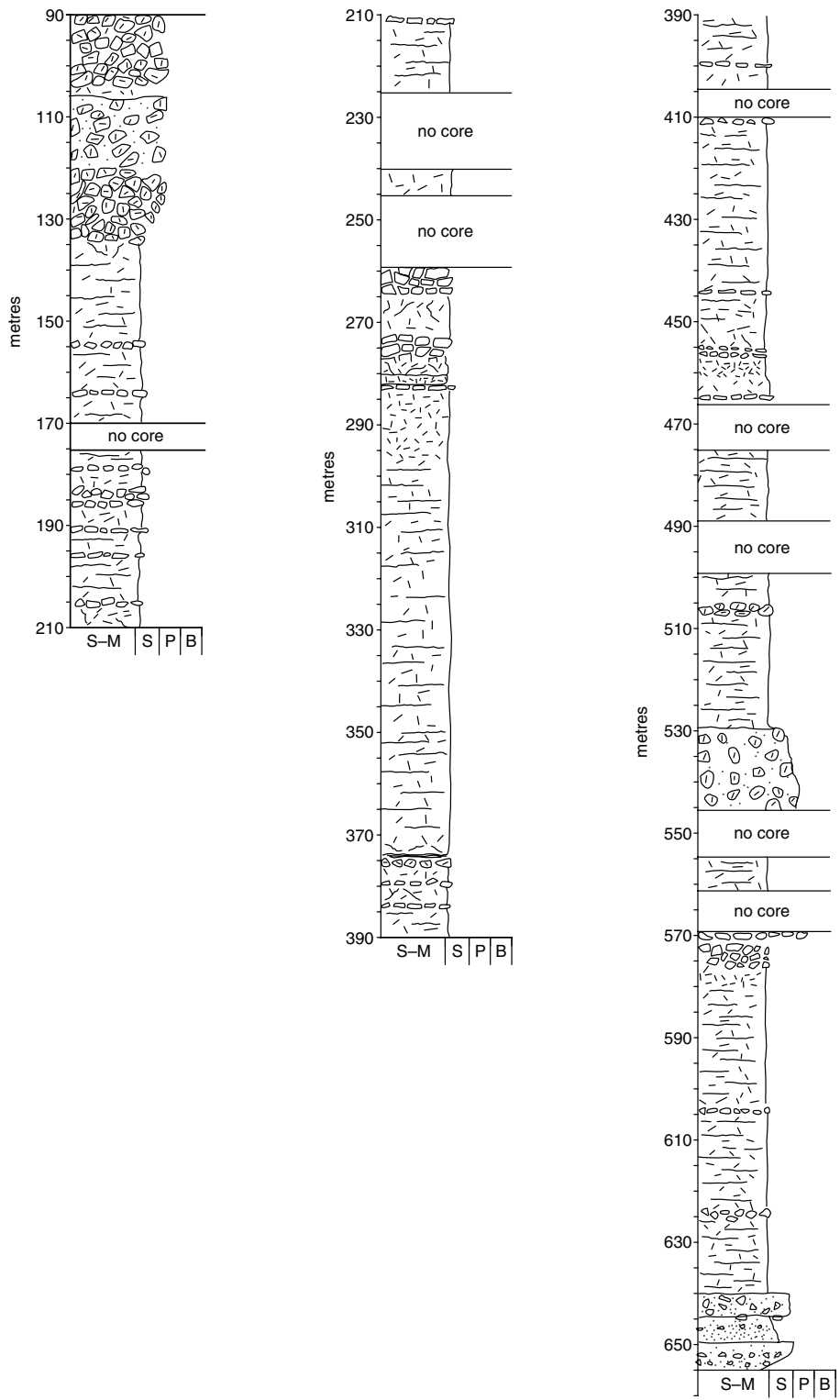
specimen, the lava shows centimetre-scale banding of alternating greenish mica-rich bands and buff-coloured quartzofeldspathic bands, the latter containing scattered phenocrysts of feldspar and subordinate quartz up to 2 mm in length. Flow banding around these phenocrysts is locally preserved and some of this banding has been contorted during flowage. More glassy parts (e.g. at 290 and 580 m depth) are less porphyritic and lack flow banding. Lithic fragments, up to a few millimetres long and of the same composition as the host, are unevenly distributed throughout the core. In some parts, flow banding is less well developed, and the core shows weak primary (i.e. igneous) brecciation superimposed on the banding (e.g. at 450 m depth).

Brecciated lava, with fragments showing an interlocking (jigsaw-fit) texture (Cas, 1992), are marginal to and gradational with coherent dacite lava. Breccia fragments range from 6 to 8 cm to millimetre size (Fig. 11). Disorganized, clast-supported oligomictic breccia (Fig. 12) is found within coherent dacite lava or adjacent to jigsaw-fit breccia (e.g. at 185 and 455 m). The clasts are lithologically identical to both coherent dacite lava and jigsaw-fit breccia.

Weakly polymictic breccias with variable amounts of matrix (e.g. at 125 m depth) have angular to subangular dacite clasts up to 15 cm in diameter with smaller, locally abundant, carbonaceous shale fragments. The matrix is a quartzofeldspathic sandstone. Some finer grained units show both normal and reverse grading. These breccias grade into interbedded volcanoclastic and epiclastic sandstone and siltstone.

In thin section, dacite lava from drillhole SE3 has quartz and feldspar phenocrysts in a flow-banded quartzofeldspathic groundmass (Fig. 13). Flow banding is highlighted by abundant sericite. Samples are variably carbonated. Based on simple versus polysynthetic twinning, the feldspar is about 80% alkali feldspar and 20% plagioclase. Feldspars are euhedral, cloudy, sericitized, and up to 6 mm long in GSWA 110619. Subordinate quartz is locally bipyramidal (up to 2 mm long) and some grains are embayed. Uncommon lithic fragments consist of granoblastic quartz and feldspar up to 4 mm long. Bedding-parallel, wispy, locally angular apophyses are infilled with either granoblastic aggregates of quartz and feldspar, carbonate plates, or chlorite. They are up to 5 mm long and 1 mm wide and usually concentrated in phenocryst-poor flow bands (Fig. 13). They are easily recognized by their drusy opaque-oxide dusting. They impart a vitriclastic texture to the rock, and could represent devitrified, flattened pumice fragments. However, some are not flattened and the opaque coating suggests that they were cavities rather than altered fragments.

Jigsaw-textured dacite lava comprises angular to subangular fragments, 1 to 10 mm in length. Fragments have tiny euhedra of alkali feldspar, rare plagioclase, and quartz in a micaceous and quartzofeldspathic groundmass. In GSWA 114122 (SE3 at 571 m depth; Fig. 14), there are signs of flowage around crystals. The vein material interstitial to the fragments consists of cryptocrystalline quartz and feldspar.



PAM107

01.09.98

**Figure 10. Graphic log of the felsic part of diamond drillhole SE3, Black Flag Group, Lakewood. See Figure 9 for legend**



**Figure 11. Jigsaw-fit dacite breccia in the Black Flag Group, in diamond drillhole SE3 at Lakewood (GSWA 114132, 183.18 m depth)**

In drillhole SE3, the sandstone in interbedded sandstone–siltstone successions is quartzofeldspathic. Angular, locally embayed quartz grains (up to 0.5 mm in length) and totally sericitized feldspar are accompanied by less common granoblastic quartzofeldspathic rock fragments. The matrix is a weakly granoblastic association of quartz and feldspar with sericite needles and significant carbonate.

The Black Flag Group in drillhole SE4 consists of volcanoclastic rocks and shale intruded by the Golden Mile

Dolerite (Fig. 15). Cohesive lava is restricted to the lower 60 m of the core, which comprises weakly flow banded dacite (with scattered phenocrysts of euhedral feldspar and quartz) and locally jigsaw-brecciated rhyolite. The spatial relationship of lava to breccia is the same as in drillhole SE3. The remainder of the Black Flag Group is pebbly sandstone and shale with sandstone interbeds, similar to units described in the lower part of drillhole SE3.

The matrix to volcanoclastic pebbly sandstone and breccia in drillhole SE3 consists of rounded lithic fragments up to 3 mm in diameter of granoblastic quartz, feldspar, sericite, and carbonate, with less common fragments of laminated shale. Interstitial to these fragments are granoblastic quartz, subhedral cloudy feldspar, and wispy sericite with abundant carbonate (up to 20 vol. %).

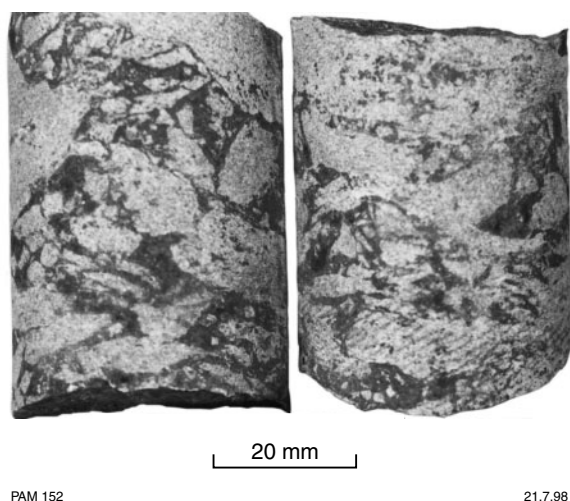
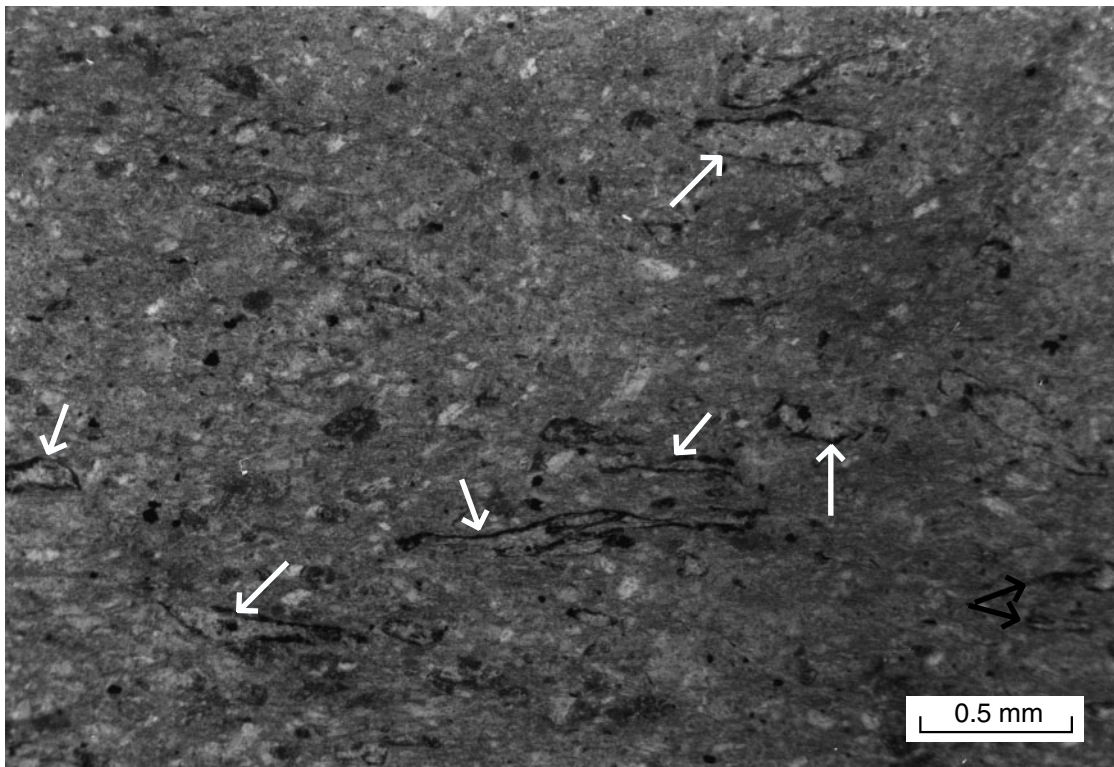


**Figure 12. Disorganized dacite breccia in the Black Flag Group, in diamond drillhole SE3 at Lakewood**

In drillhole SE4 sandstones comprise subangular to subrounded volcanic rock fragments (up to 5 mm in diameter) with a limited compositional range, consisting of euhedral amphibole (up to 0.4 mm in diameter) now replaced by biotite flakes and partly saussuritized alkali feldspar phenocrysts, and less common albitic plagioclase. The matrix is a cryptocrystalline association of quartz and feldspar with calcite plates, broken plagioclase and alkali feldspar crystals, rare angular monocrystalline quartz grains, and fine-grained non-porphyrific rock fragments.

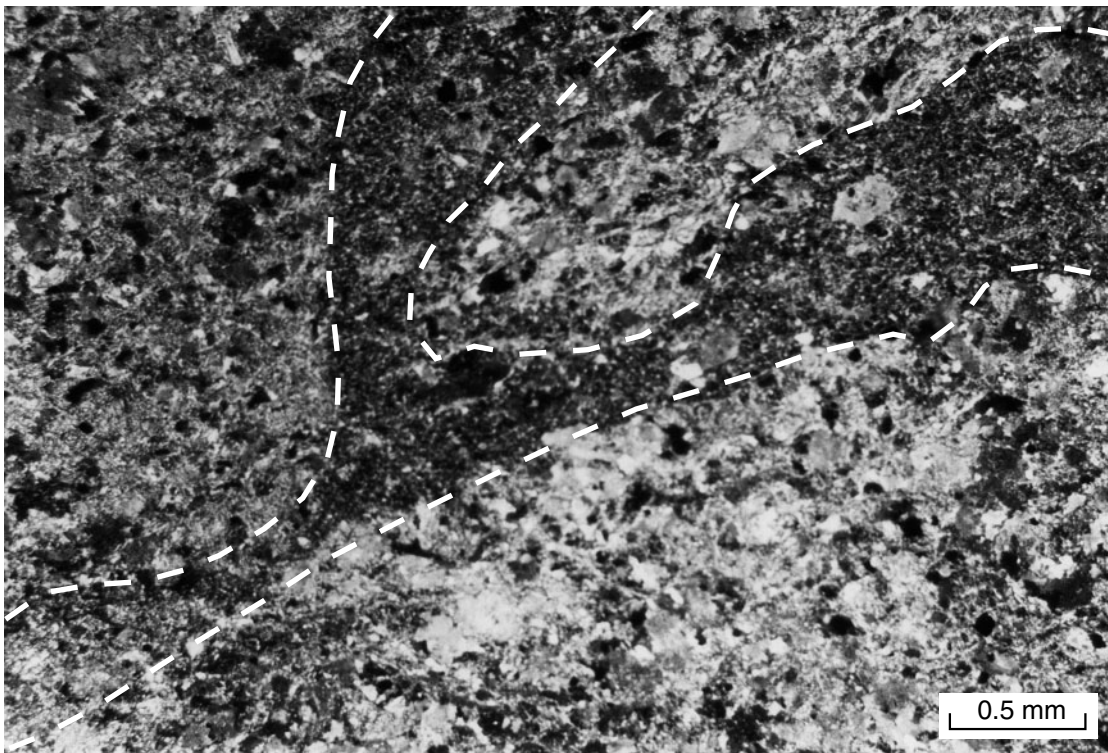
About 500 m of the Black Flag Group has been logged in drillhole SE7, part of which is shown in Figure 16. Cohesive dacite lava and breccia are present throughout, particularly in the lower 150 m. The cohesive lava is flow banded and contains scattered phenocrysts of feldspar and



PAM 153

21.7.98

Figure 13. Dacite at 621 m depth in the Black Flag Group, in diamond drillhole SE3 at Lakewood. Note opaque-lined apophyses (arrowed) parallel to flow banding. Sample GSWA 110619; plane polarized light



PAM 154

9.10.98

Figure 14. Dacite at 571 m depth in the Black Flag Group, in diamond drillhole SE3 at Lakewood. Note quench-textured brecciation, with fragments shown by broken line. Sample GSWA 114122; plane polarized light

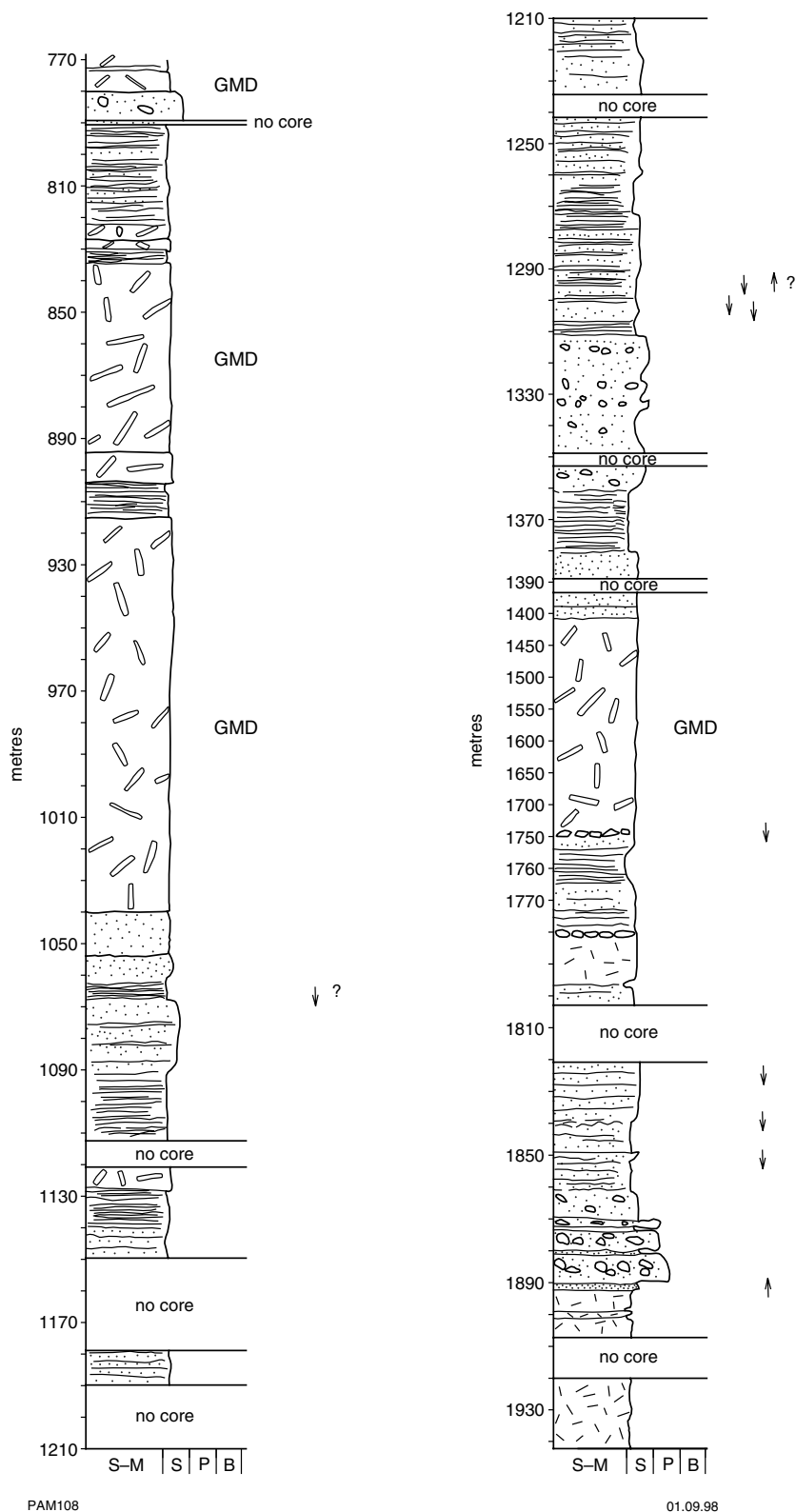


**Figure 15. Graphic log of diamond drillhole SE4 in the Black Flag Group at Lakewood. See Figure 9 for legend. GMD = Golden Mile Dolerite; AMG (3136) 583899**

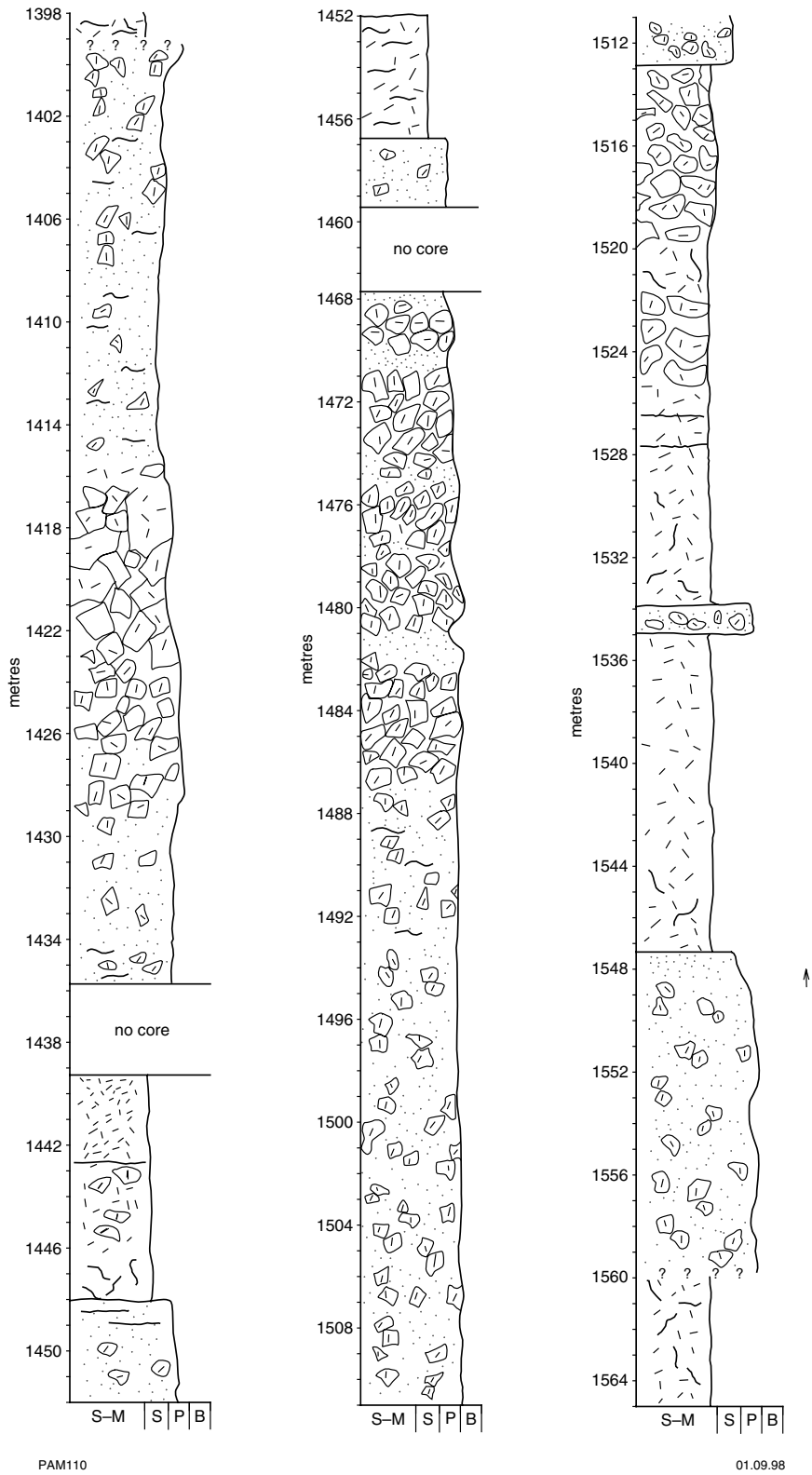
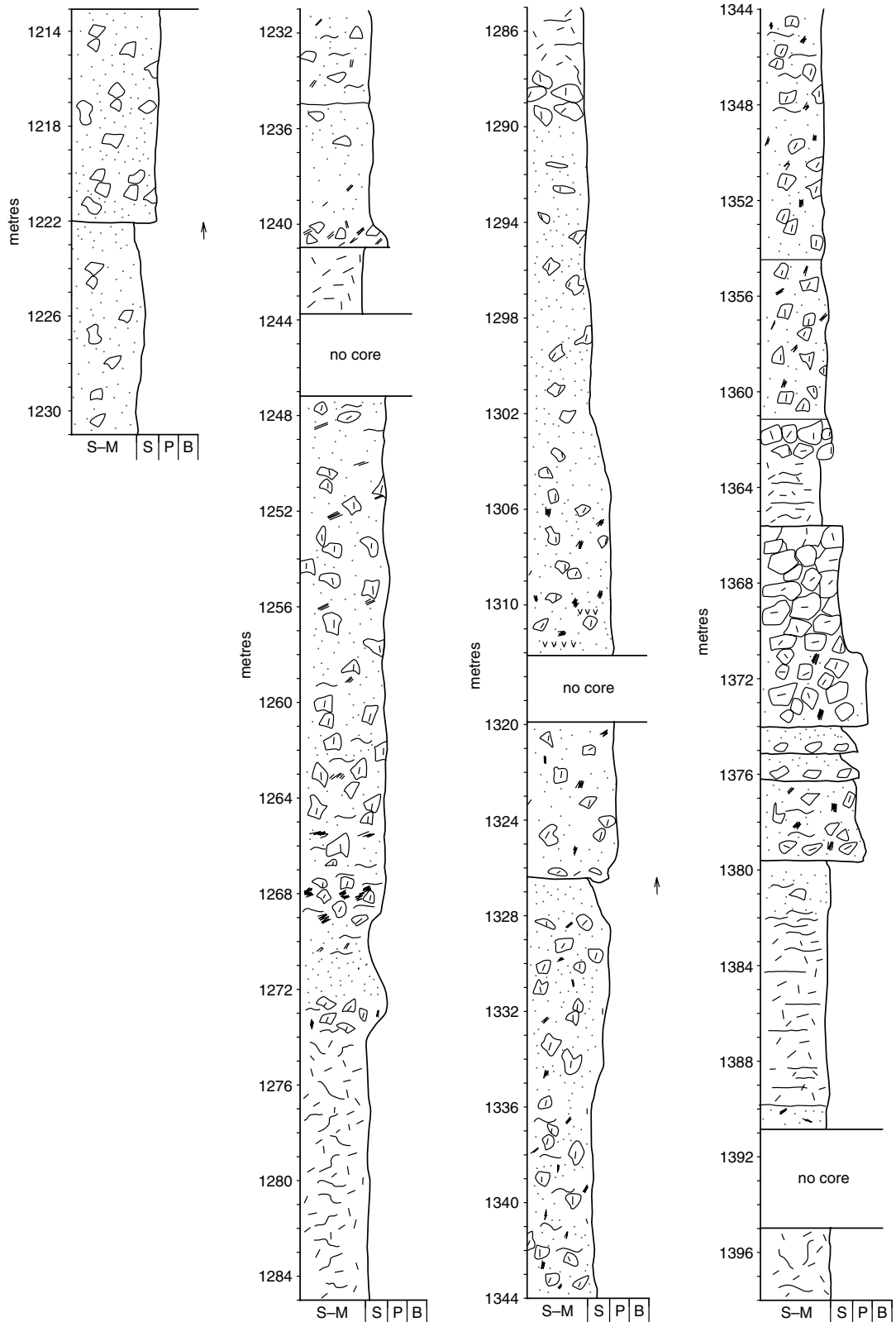


Figure 16. This page and opposite: Graphic log of diamond drillhole SE7 in the Black Flag Group at Lakewood. See Figure 9 for legend; AMG (3136) 589871



PAM111

12.08.96

quartz. Non-porphyrific zones (e.g. from 1716 to 1720 m) are fine grained, possibly originally glassy, and usually flow banded, whereas unbrecciated parts are much more strongly porphyritic and lack flow banding. Weakly flow banded dacite lava from 1274 to 1288 m contains angular dacite fragments up to 3 cm in diameter. Infilled spherical features at 1695 m are probably amygdales. Zones of jigsaw-fit breccia (e.g. at 1686 m, 1665 m, and 1659 m) are in sharp contact with cohesive lava. From 1650 to 1653 m and 1570 to 1578 m there are several thin (less than 1 m thick) repetitions of cohesive brecciated lava, whereas from 1525 to 1529 m cohesive lava units are bound by thin (less than 2 cm thick) chilled rims resembling pillow margins. Here, the adjacent lava is jigsaw brecciated with rare shale fragments, gradually becoming less organized. Further from the lava, breccias consist of 85% fine-grained volcanic rock fragments (lithologically identical to cohesive lava) and 15% shale. Some volcanic fragments exceed 50 cm in diameter. A similar unit is in sharp contact with pebbly sandstone at 1513 m. Variations of this clast-supported, largely oligomictic breccia are present within volcanoclastic sedimentary rocks at 1475 and 1483 m. At 1368 m there is a gradation from closed-framework, essentially oligomictic, felsic breccia through to fragmented, more-cohesive dacite, whereas a similar breccia is in sharp contact with cohesive lava at 1364 m (Fig. 16).

Volcanoclastic rocks show a variety of sedimentary structures, but a limited range in clast composition. At 1550 m breccia grades upward into coarse-grained sandstone, and fining-upward sandstone beds are well developed between 1374 and 1380 m. Poorly sorted, closed-framework breccias at 1468–1488 m comprise angular dacite rock fragments with a few shale fragments and little matrix. Other breccias have both closed and open framework (e.g. at 1560 m), but are still dominated by angular to subrounded dacitic rock fragments with subordinate shale and porphyritic volcanic rock fragments in a felsic sandstone matrix. At 1495 m, about 70% of the clasts are porphyritic volcanic rock fragments with subordinate fine-grained dacite fragments.

Dacite lava in drillhole SE7 is petrographically similar to that in SE3. Sample GSWA 114161 (from 1541 m depth) has anhedral quartz and feldspar phenocrysts with elongate granoblastic zones up to 1.5 mm long. Once-glassy zones are represented by matted chlorite flakes. Other rocks (e.g. GSWA 114162 from 1531 m depth) are weakly porphyritic, with uncommon anhedral plagioclase up to 1 mm long comprising less than 5 volume % of the rock. These phenocrysts are unzoned and have been optically determined as albite. The coarsely crystalline groundmass contains euhedral blocky plagioclase laths in a cryptocrystalline quartzofeldspathic matrix with secondary calcite.

More-coarsely porphyritic, unbrecciated, weakly flow banded units (e.g. GSWA 114176 from 1616 m) have abundant (about 35%) locally embayed, euhedral plagioclase and alkali feldspar phenocrysts (up to 1.5 mm in long) that are cloudy, unzoned, and accompanied by subordinate quartz. The groundmass is a granoblastic aggregate of quartz and feldspar with patches of chlorite, calcite, and minor amounts of sericite. Cavities

in GSWA 114177 (from 1614 m) are outlined by drusy magnetite and infilled with quartz, feldspar, and chlorite. Aphyric versions (e.g. GSWA 114181 from 1388 m) comprise disrupted bands of sericite, chlorite, and calcite with minor amounts of quartz and feldspar. Sample GSWA 114187 (from 1278 m) is brecciated and consists of rounded to subangular volcanic rock fragments up to 2 cm in diameter of feldspar laths in a sericite and carbonate matrix. Thin rock fragment spalls give a pseudojigsaw-fit appearance.

A dacite rock fragment in a poorly sorted, matrix-supported sandstone in drillhole SE7 (GSWA 114179 from 1492 m) is petrographically similar to cohesive dacite lava. The fragment is weakly flow banded and has a few cloudy anhedral alkali feldspar phenocrysts (up to 1.2 mm long) set in cryptocrystalline quartz and feldspar, with abundant calcite and sericite. Non-porphyrific, possibly originally glassy bands are now preserved as chlorite, feldspar, and opaque oxide. Localized elongate partings have thin opaque-oxide coatings.

Sandstones in drillhole SE7 (e.g. GSWA 114182 from 1379.8 m) consist of recrystallized felsic volcanic rock fragments (now granoblastic quartz and feldspar) in a fine-grained quartzofeldspathic matrix, with abundant secondary calcite and sericite. Some rock fragments are non-porphyrific (possibly originally glassy) and all samples examined were foliated. Three types of rock fragments are identified in GSWA 114184 (from 1342 m). The most common are rounded clasts up to 2 mm in diameter comprising euhedral stubby plagioclase, chlorite, and calcite grains. Less common are porphyritic fragments, up to 1 mm in diameter, dominated by anhedral to subhedral feldspar phenocrysts. The least common type comprises weakly interlocking feldspar grains with minor amounts of quartz.

Sample GSWA 114185 is a crystal-lithic sandstone with angular to rounded quartz grains (up to 0.5 mm in diameter), cloudy anhedral feldspar (alkali feldspar » plagioclase) up to 0.6 mm in diameter, and fine-grained volcanic rock fragments. The latter comprises aphyric cryptocrystalline rhyolite, weakly porphyritic dacite (with rare embayed quartz grains), and less common laminated shale. The framework is both open and closed, and the cryptocrystalline quartz and feldspar matrix contains abundant secondary calcite. Sample GSWA 114186 (from 1295 m) is dominated by aphyric to porphyritic felsic rock fragments up to 1 cm in diameter.

### **Interpretation**

Volcanoclastic rocks of the Black Flag Group in Lakewood drillcore show a limited range in clast type and mineralogy. Most clasts are of weakly porphyritic fine-grained dacite with less common shale and more strongly porphyritic dacite clasts. Fine-grained dacite clasts are identical to coherent dacite lava, whereas shale fragments are lithologically similar to bedded carbonaceous shale units elsewhere in the same holes. Porphyritic dacite clasts are mineralogically similar to cohesive dacite lava and could represent more slowly cooled variants. Thus, there is strong evidence that all clasts are of local derivation.

Dacite is flow banded and has a limited range in mineralogy. It is interpreted as subaqueous lava extruded as small-volume flows or lava lobes. Elongate, opaque-lined, bedding-parallel apophyses in lava (Fig. 13) could, on first inspection, be mistaken for fiammé, but their morphological diversity and the likelihood that the opaque dusting is a cavity lining are inconsistent with a vitriclastic origin. Similar features have been described from Archaean rhyolite flows in Quebec by de Rosen Spence et al. (1980), who identified them as vesicles flattened by flowage. Hausback (1987) described crystal-lined, planar, lithophysal cavities in the Miocene Providencia rhyodacite in Mexico, which he attributed to cavitation during the late stages of flow.

The spatial association with sedimentary rocks provides strong evidence that dacite was subaqueously erupted. The depth of water is not known, but Golding and Walter (1979) recorded evaporite minerals in shale from one SE hole, which they argued was consistent with deposition in shallow water. Glassy, less porphyritic dacite is often found adjacent to coherent flow-banded dacite lava. This glassy lava is brecciated and shows less well-developed flow banding, and in some cases it grades into jigsaw-textured breccia. The transition to glassy lava is consistent with more-rapid cooling, whereas jigsaw-fit breccia could result from in situ brecciation of lava with no accompanying clast rotation. This quench brecciation (Cas and Wright, 1987; Yamagishi, 1991; Cas, 1992) could result from lava coming into contact with water.

Chaotic disorganized breccia is often developed adjacent to jigsaw-textured breccia. Clasts are identical to dacite lava and jigsaw-fit breccia, but there are also scattered shale fragments. This breccia type is interpreted as spalled-off fragments from the dacite lava that have been redeposited by mass flow along with ripped-up shale clasts. More-distal parts of the same succession are represented by massive, unbedded, open- and closed-framework, polymictic breccias and sandstones that show both normal and reverse grading. They are interpreted as mass-flow and turbidity current deposits respectively. Carbonaceous and pyritic shale represent background sedimentation.

The proportions of lava and breccia types in 484 m of core dominated by volcanic rocks from drillhole SE3 have been estimated. Cohesive dacite lava accounts for 377 m (78%), of which 38 m (8%) comprises open- and closed-framework polymictic breccia, 32 m (7%) is jigsaw-textured breccia, 20 m (4%) is more-heterogeneous dacite and shale breccia, and 15 m (3%) is chaotic breccia. The size of individual dacite lava flows or lobes can be estimated by measuring the thickness of cohesive lava between jigsaw-textured horizons. Frequency histograms for lava lobe thickness and the thickness of the adjacent jigsaw-textured breccia are shown in Figure 17. In drillholes SE3 and SE7 most lobes are less than 15 m thick, although intersections of 40 to 45 m in SE7 and 85 to 90 m in SE3 indicate isolated thicker lobes. It is possible that these thicker lobes acted as feeders from which the thinner lobes budded off, similar to the diagrammatic interpretation offered by Pichler (1965) for the subaqueous extrusion of viscous rhyolite (Fig. 18).

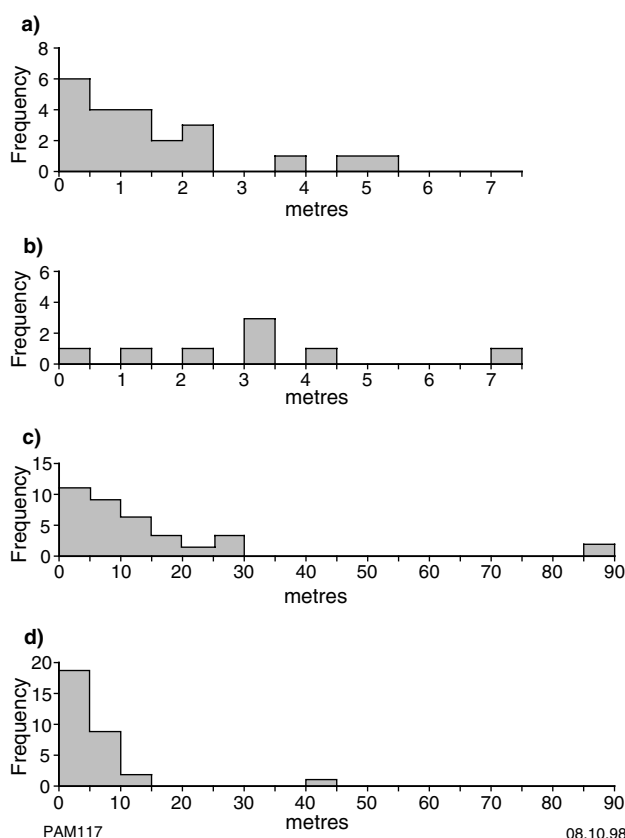
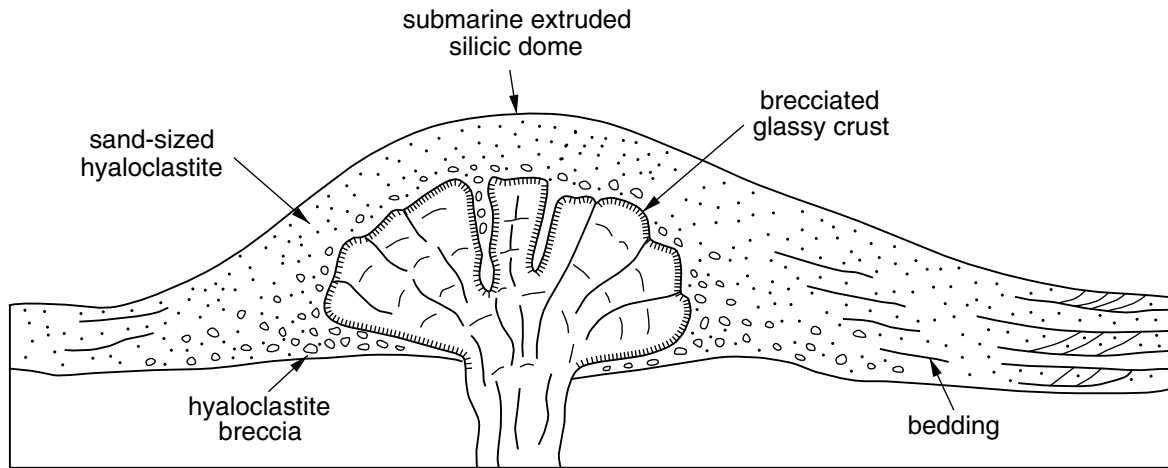


**Figure 17. Frequency histograms for thickness of Black Flag Group in diamond drillholes at Lakewood: a) thickness of jigsaw-textured breccia in SE3; b) thickness of jigsaw-textured breccia in SE7; c) thickness of cohesive dacite lava units in SE3; and d) thickness of cohesive dacite lava units in SE7**

## Drillcore from Boulder

Diamond drillhole LED10 intersected 385 m of the Black Flag Group southeast of Kalgoorlie–Boulder (Fig. 8). Unlike the SE drillholes from Lakewood, LED10 contains basaltic volcanic rocks and felsic porphyry, in addition to Golden Mile Dolerite and felsic volcaniclastic rocks (Fig. 19). Although the stratigraphic position of the hole is unknown, it is included in this discussion because of its quite different lithologies.

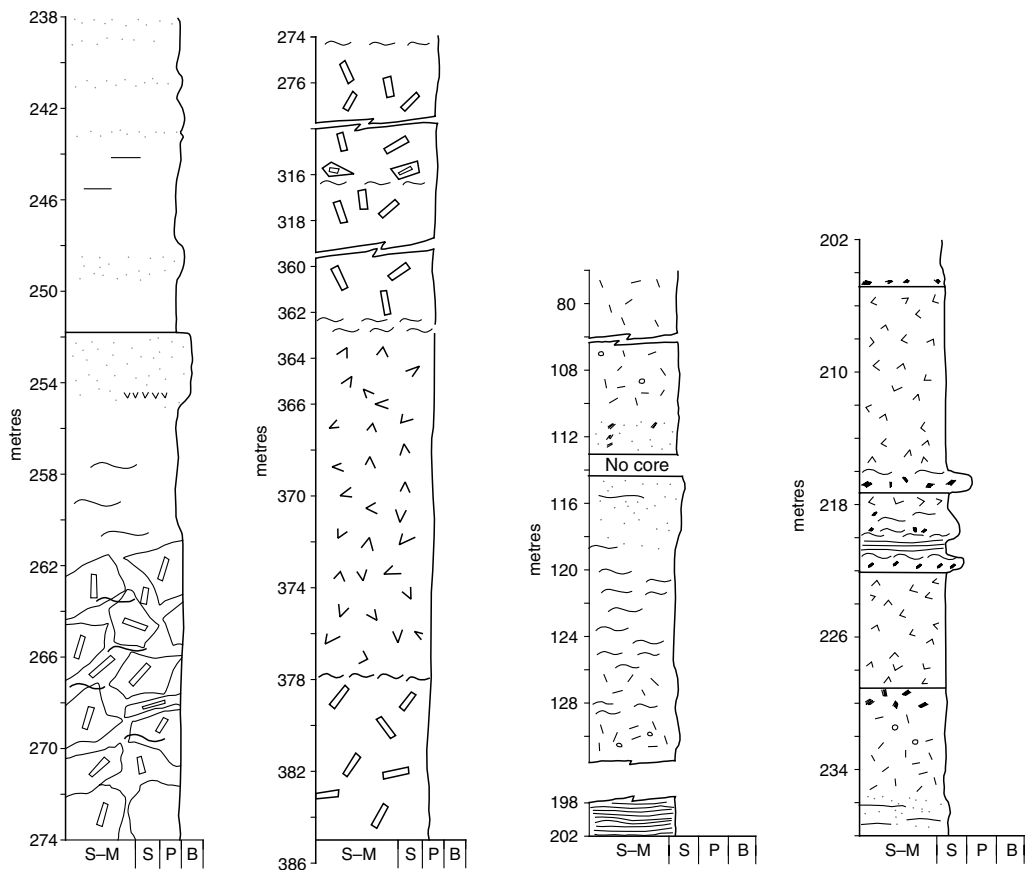
Sedimentary structures indicate that the stratigraphy in drillhole LED10 has been inverted. From 385 to 260 m depth locally brecciated Golden Mile Dolerite has a sheared upper contact with carbonaceous shale. Shale, with localized pyrite (as lenses and cubes) and sandstone interbeds, dominates the core from 260 to 130 m. From 130 to 78 m tectonically brecciated shale and quartzofeldspathic sandstone is interbedded with pillowed amygdaloidal basalt. From 78 m to the top of the hole there is sandstone with rip-up shale clasts. Basalt is fine grained, amygdaloidal, and usually non-porphyritic (e.g. GSWA 114492 from 230.4 m), although anhedral chlorite patches could be relict phenocrysts. The groundmass consists of fine-grained sericite and carbonate. Amygdales



PAM114

09.10.98

**Figure 18. Idealized cross section of silicic lava extruded into shallow water. Dome thickness is in the order of 200 m (after Pichler, 1965; and Cas and Wright, 1987)**



PAM113

09.10.98

**Figure 19. Graphic log of diamond drillhole LED10 in the Black Flag Group at Kalgoorlie-Boulder; AMG (3136) 792919. See Figure 9 for legend**

are up to 2 mm in diameter and infilled with quartz. Sample GSWA 114481 (from 94.5 m) has anhedral fragments, up to 0.5 mm in diameter, of quartz and feldspar in a groundmass of weakly granoblastic feldspar and chlorite with relict phenocryst feldspar. Accessory phases comprise opaque oxide with secondary calcite and sphene and localized calcite veins.

Quartzofeldspathic sandstones (e.g. GSWA 114491 from 252.8 m) are weakly foliated with sub-rounded quartz grains (up to 1 mm in diameter), cloudy sericitized alkali feldspar (up to 2 mm in diameter), and fine-grained granoblastic rock fragments composed of quartz and feldspar. The matrix has carbonate, sericite, and patches of granoblastic quartz and feldspar.

Porphyry units (e.g. GSWA 114493 from 229.8 m) are fresher, unfoliated, and less carbonated, with scattered alkali feldspar and albitic plagioclase grains up to 2 mm in diameter showing weak zoning. Relict amphibole is now replaced by calcite. The groundmass has quartz and feldspar with accessory carbonate, sericite, and scattered opaque oxide. Excellent amphibole cross sections are preserved in GSWA 114494 as drusy magnetite-lined cavities with carbonate infillings. The freshness and lack of foliation indicate that porphyry intrusion post-dates greenstone deformation.

### Interpretation

As its stratigraphic position is unknown, the value of this core in interpreting Black Flag Group volcanism is limited, but the variety of lithologies (felsic and mafic volcanic rocks and porphyries) indicates some diversity within the Black Flag Group. Amygdaloidal fine-grained basalt is present as clasts in a conglomerate on the western side of White Flag Lake, which is in the upper part of Hunter's (1993) Black Flag Group stratigraphy. Mafic volcanic rocks are also present in drillcore from the Black Flag Group in the Kambalda area (discussed below). Sedimentary rocks in drillhole LED10 are lithologically similar to those in SE drillholes from Lakewood, which contain felsic volcanic rocks typical of Hunter's (1993) lower Spargoville Formation. Thus, it is possible that the basalt represents an isolated facies of volcanism within the lower part of the Black Flag Group.

### Mount Shea

Based on outcrop mapping and drillhole information, Keats (1987) identified a zone of ultramafic and mafic volcanic flows and breccias and felsic igneous and sedimentary rocks (O'Beirne, 1968) extending south from Kalgoorlie–Boulder to Mount Shea (Figs 8 and 20). Well-exposed successions in the Feysville – Mount Shea area include intermediate and felsic volcanic rocks assigned to the Black Flag Group. Keats (1987) estimated that about 1.5 km southwest of Red Lake, felsic rocks comprise about 90% dacites and 10% andesites, as volcanic and subvolcanic rocks. At Mount Shea he argued that these rocks were interleaved with komatiite and basalt, which formed the upper parts of the mafic-dominated part of the greenstone stratigraphy (i.e. Hannan Lake Serpentinite and

Paringa Basalt). This was supported by Ahmat (1995a) who maintained that although some of the interleaving of mafic, ultramafic, and felsic lithologies may be structural, there was a strong possibility of coeval mafic and felsic volcanic activity. The Mount Shea area has been examined in this study to determine the extent of coeval mafic and felsic volcanism, the type of felsic igneous activity, and if similar felsic rocks are present elsewhere in the Black Flag Group.

There are several laterally continuous outcrops of igneous rocks in the Mount Shea area. Spoil around a shaft (AMG (3236) 673763 on the KANOWNA 1:100 000 map sheet; Fig. 20) contains fragments, up to 3 cm in diameter, of olivine-bearing, spinifex-textured ultramafic rock (Hannan Lake Serpentinite) in a felsic matrix. A felsic rock (AMG 672762) contains mafic rock fragments and amphibole phenocrysts. In thin section this rock comprises cloudy, sericitized, subhedral feldspar up to 2 mm long, and scattered amphibole up to 1 mm long now replaced by biotite flakes. One rounded 6 mm-long fragment is composed of biotite flakes. The groundmass comprises cryptocrystalline quartz and feldspar with biotite flakes and scattered quartz apophyses. The rock resembles an altered hornblende dacite. From this outcrop southwest towards Mount Shea the succession largely comprises mafic igneous rocks of the Paringa Basalt with units of felsic igneous rocks. The latter are coarsely porphyritic with euhedral feldspar crystals up to 0.3 mm long and acicular amphibole. They lack any structure such as graded bedding or flow features, but contain clasts of locally derived ultramafic rocks or high-magnesian basalt with rare autochthonous felsic fragments.

Another felsic rock has angular basaltic rock fragments up to 20 cm in diameter (but mostly less than 1 cm) enclosed in a crystal-rich felsic matrix (AMG 675753; Fig. 21). The basalt fragments have well-developed pyroxene spinifex texture typical of the underlying Paringa Basalt. In thin section they are angular and cusped comprising matted, locally bunched and radiating, colourless to pale-green amphibole (after pyroxene) and minor amounts of chlorite with interstitial feldspar. There are rare phenocrysts of twinned amphibole (after pyroxene). Finer grained glassier versions have feathery amphibole and unresolvable groundmass. Less common felsic rock fragments consist of fine-grained granoblastic quartz and feldspar enclosing scattered amphibole and feldspar phenocrysts. The matrix to these fragments is composed of cloudy to totally sericitized feldspar euhedra up to 0.5 mm long, felsic rock fragments (fine-grained granoblastic quartz and feldspar with feldspar microphenocrysts), and accessory amounts of quartz, calcite, and chlorite. Granoblastic quartz and feldspar are interstitial, with amphibole ghosts now composed of biotite and chlorite. Scattered partly resorbed euhedra of alkali feldspar are accompanied by small mafic rock fragments.

At the eastern end of a small island (AMG (3236) 670770), basalt breccia outcrops with easterly facing and younging felsic sedimentary rocks, rare andesite flows, and fine-grained feldspathic sandstones. The basalt breccia consists of angular fine-grained basalt fragments up to

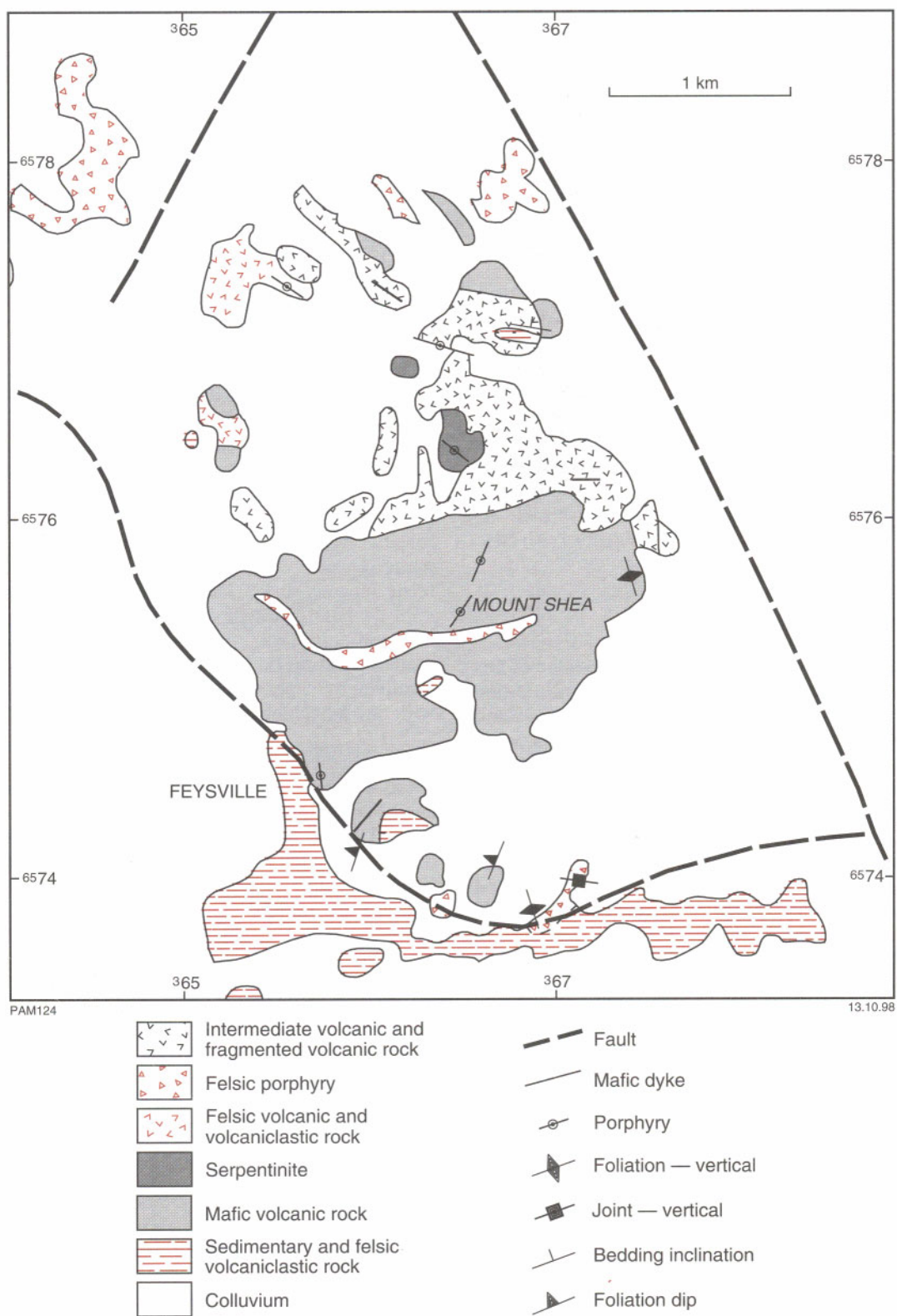
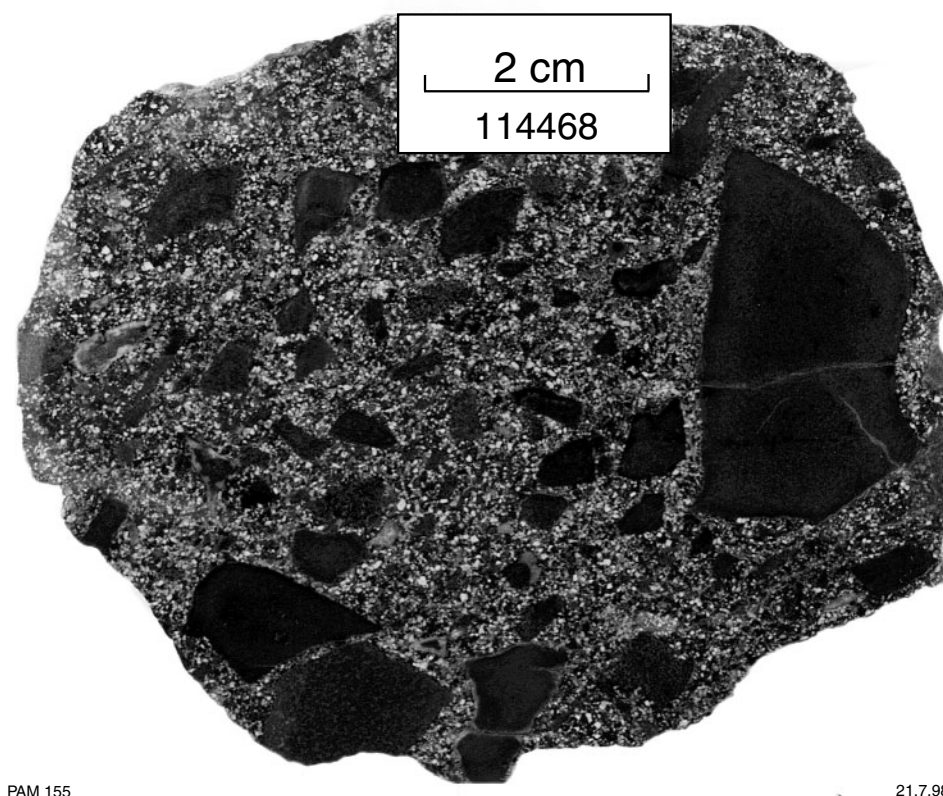


Figure 20. Simplified geology of the Mount Shea area (after Ahmat, 1995a)



PAM 155

21.7.98

**Figure 21. Crystal-rich matrix enclosing angular basalt fragments, Black Flag Group at Mount Shea; GSWA 114468; AMG (3236) 675753**

15 cm in diameter in a compositionally similar matrix. Within the sedimentary succession is a porphyritic rock with phenocrysts of amphibole and feldspar in a felsic groundmass. The amphibole is tabular, euhedral, and up to 3 mm (locally 7 mm) long. Subordinate feldspar (up to 3 mm long) are euhedral to subhedral, slightly resorbed, show intense oscillatory zoning, and is optically albite. Some grains are cloudy and others are totally sericitized. Aggregates of euhedral epidote grains less than 0.2 mm long are scattered throughout the thin section. The matrix is composed of anhedral feldspar and quartz with subhedral granular amphibole. Estimated modes are 30% phenocrysts (comprising 70% amphibole and 30% feldspar) and 70% matrix. The rock is identified as either a hornblende dacite flow or crystal tuff.

Another member of this succession is crystal rich, consisting of feldspar, amphibole, and rare rock fragments in a matrix of amphibole, quartz, and feldspar. The feldspar crystals are euhedral, up to 1 mm long, weakly zoned, cloudy, and slightly resorbed. Euhedral, tabular, pale-green to brown amphibole grains have weakly zoned rims. Irregularly shaped fragments up to 7 mm long are composed of interlocking amphibole flakes. They are possibly an alteration product after metastable rock fragments. The matrix is composed of fine-grained cryptocrystalline quartz and feldspar with fine-grained amphibole. The rock is interpreted as a reworked dacite tuff.

The remainder of this sedimentary succession comprises felsic sedimentary rocks. Sample GSWA 114445 is a fine-grained, altered rock containing ragged weakly pleochroic amphibole and spongy feldspar grains with patches of chlorite. Interstitial material comprises a cloudy and murky mixture of altered feldspar and chlorite and granoblastic quartz patches. Uncommon fragments of granoblastic quartz are rounded and up to 5 mm long.

North of the Mount Shea area, there are coarse-grained felsic rocks that Keats (1987) believed to be subvolcanic. In thin section (e.g. GSWA 114449) these rocks are coarsely porphyritic with quartz and feldspar phenocrysts in a felsic groundmass. Quartz grains are bipyramidal, subhedral, and locally aggregated, with individual grains up to 2 mm long. The feldspar is cloudy, multiply twinned, euhedral, up to 3 mm long, and is optically albite. The groundmass is a coarse-grained interlocking assemblage of quartz and feldspar (with more feldspar than quartz), with abundant sericite and scattered opaque oxide. The rock contrasts strongly in terms of both texture and mineralogy with felsic rocks within the mafic succession of the Mount Shea area.

### **Interpretation**

Ultramafic and mafic rocks in the Mount Shea area correlate with the Hannan Lake Serpentinite and the Paringa Basalt respectively. Graded bedding in the

sedimentary succession (AMG 669770) indicates younging to the east. Mafic and ultramafic rocks are intruded by porphyritic dacites that have phenocrysts of amphibole and plagioclase. Further to the east (i.e. above these mafic and ultramafic rocks), basalt breccia has a compositionally similar, coarsely crystalline felsic matrix. Both the porphyritic dacite and the felsic matrix to basalt breccia could represent forced intrusion of crystal-rich felsic magma (i.e. crystal mush). However, higher in the succession (AMG 669770) there is clear evidence for coeval extrusion of felsic and mafic magma, where a succession of quartzofeldspathic and dacitic sedimentary rocks and possible dacite flows is overlain by a basalt breccia.

Intrusive and extrusive felsic rocks in the Mount Shea area may represent a slice through an early phase of felsic volcanic activity at the inception of Black Flag Group volcanism. Lithologically similar felsic igneous rocks to those at Mount Shea (i.e. amphibole- and plagioclase-bearing volcanoclastic rocks and volcanic flows) are also found in the upper part of the Black Flag Group at White Flag Lake. Thus, there is some evidence that intermediate volcanism in the Black Flag Group is not confined to any single stratigraphic horizon.

The 'granitic' succession (Keats, 1987) southwest of Red Lake (AMG 635795) comprises coarsely porphyritic felsic rocks with a different mineralogy to porphyry intrusions at Mount Shea. Here the mineralogy comprises quartz and feldspar with no amphibole. The freshness of these rocks, their lack of deformation, and different mineralogy suggest that they post-date felsic igneous activity in the Mount Shea area further to the south.

## Gibson-Honman Rock

Gibson-Honman Rock is an approximately 1 km<sup>2</sup> outcrop of the Black Flag Group about 12 km southwest of Kalgoorlie–Boulder (Fig. 8), along strike from the intermediate and felsic volcanic and volcanoclastic rocks of the Black Flag Group at White Flag Lake. The outcrop at Gibson-Honman Rock consists of poorly sorted, weakly polymictic breccia, rare slate beds, and cohesive felsic lava. Breccia clasts are of fine-grained porphyritic volcanic rock (dacite or possibly rhyolite) and less common slate. Clasts of volcanic rocks reach a maximum diameter of 2 m, but most are less than 10 cm long. Shale clasts are elongate and up to 1 m long. Breccias are largely of open framework with a felsic volcanoclastic matrix.

Cohesive lava outcrops as 3–4 m-wide units that have lava-lobe form. They show weakly developed flow banding and have a few scattered phenocrysts of feldspar up to 3 mm long set in a cryptocrystalline groundmass. Parts of the unit are brecciated, and northeast of the outcrop the lava contains hornblende, is weakly amygdaloidal, and bordered by schistose sedimentary rock. The central part of the lobe association is more coarse grained, and bordered to the east by a 15 m-thick breccia unit.

All breccia clasts appear to be of local derivation. Rare lensoidal shale units are lithologically similar to shale clasts (although some shale 'units' may themselves be 3 to 4 m-long and 50 cm-wide shale rafts), and clasts of volcanic rocks are lithologically similar to lava lobes.

Three thin sections from the core to the margin of a lava unit from Gibson–Honman Rock have been examined. They are petrographically similar (Fig. 22). Euhedral alkali feldspar crystals range from microphenocryst grade to 6 mm in length and show well-developed cross-hatched twinning. They are slightly cloudy, and speckled with carbonate and sericite. Grain margins show weak oscillatory zoning. Grains are locally aggregated and intergrown. Euhedral phenocrysts of less common albitic plagioclase are up to 3 mm long. The groundmass is inhomogeneous, comprising weakly granoblastic quartz and feldspar (the former locally developed as microphenocrysts) and patches of coarse granoblastic quartz. One millimetre-diameter aggregates of a brown, tabular, pleochroic mineral (?oxybiotite) are scattered throughout. Sample GSWA 114498 from the core of the lava unit has about 25 volume % crystals. A sample from the lobe margin (GSWA 114500) contains similar types and amounts of phenocrysts to the core, but the groundmass is cryptocrystalline and the sample contains weathered-out ?amphibole forms, now lined with a brown alteration product and cored by calcite.

A volcanic clast from the mass-flow breccia (GSWA 114499) is petrographically similar to lava. It is dominated by single (occasionally intergrown) crystals of alkali feldspar up to 6 mm long. Also present are a few fine-grained felsic rock fragments up to 6 mm long and less common rock fragments composed of granoblastic quartz. The matrix is granoblastic quartz and sericite, and a brown alteration mineral possibly after amphibole or biotite.

## Interpretation

The spatial relationships of lava and breccia and the lithological similarity of volcanic clasts in the breccia to lava lobes suggest that breccia is derived from the lava by wastage and mass-flow deposition. Shale clasts represent rip-ups of the local substrate. This lava–breccia association is similar to that recorded in SE3 where dacite lava was extruded subaqueously and brecciated on contact with water. With lava movement the breccia was spalled off the lobe margin and accumulated as a gravity deposited mass-flow unit at the lobe foot. Shale clasts may represent fragments dislodged during lobe extrusion involving substrate inflation.

Lithologically, lava at Gibson-Honman Rock is more strongly porphyritic and texturally and mineralogically better preserved than felsic volcanic rocks examined in SE holes from Lakewood. The coarse-grained nature of the lava and the intergrowth of alkali feldspar prior to emplacement are consistent with either extrusion of the lava as a crystal mush or intrusion and cooling at a high level. The suggestion that the lava margin was once partly glassy favours the former interpretation.

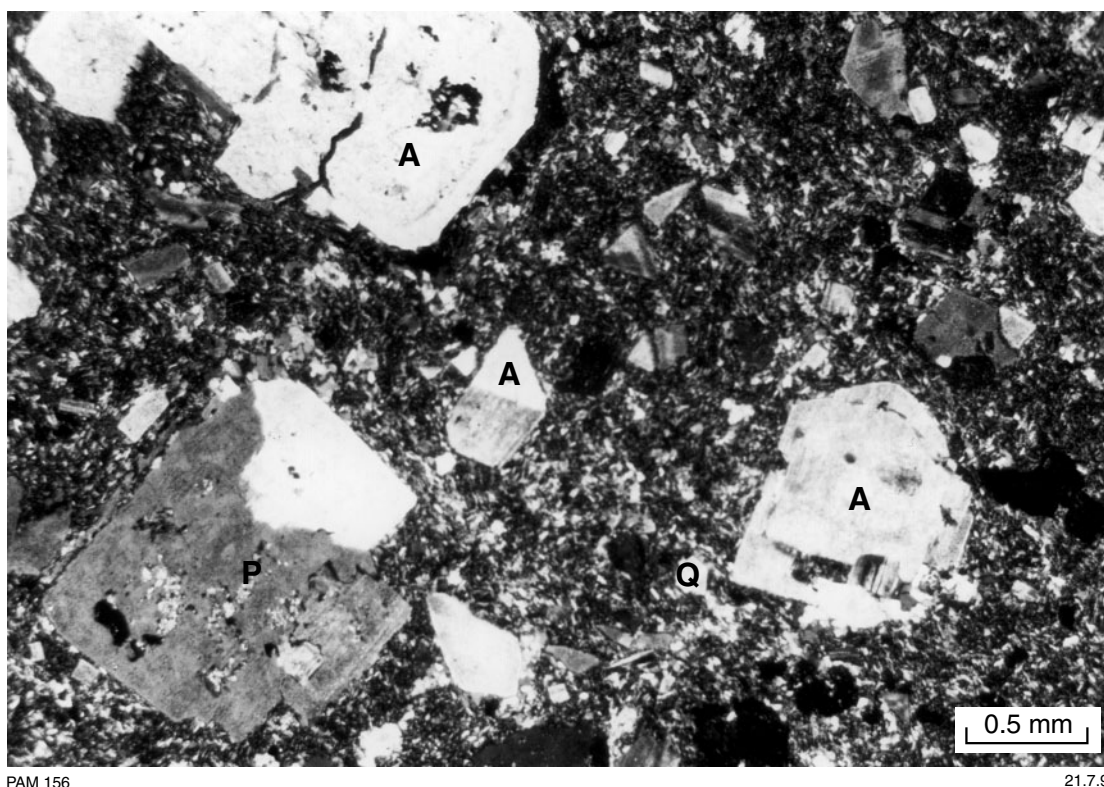


Figure 22. Black Flag Group dacite from Gibson-Honman Rock. A — alkali feldspar, P — plagioclase, Q — quartz. Sample GSWA 114498; AMG (3136) 497867; plane polarized light

## The Black Flag Group in the Kambalda–Mandilla–Widgiemooltha area

### Morgans Island

Cohesive felsic lava, breccia, and volcanoclastic sandstone and siltstone of the Black Flag Group outcrop on the western side of Lake Lefroy at Morgans Island (Fig. 23). Lithologically, the succession resembles felsic volcanic rocks encountered in drillcore at Lakewood, south of Kalgoorlie–Boulder. Sedimentary structures in the upper part of the succession at Morgans Island indicate that the succession youngs to the west. The geology of the Morgans Island area (Fig. 24) is discussed by Griffin (1990) and Brauns (1991). A sketch of the felsic volcanic stratigraphy is shown in Figure 25. At the bottom of the succession, rhyolite lava forms an elongate northerly trending outcrop at Lake Lefroy at point 1 (Fig. 24). The rock is structureless and buff-coloured, with scattered phenocrysts of feldspar and subordinate quartz in an originally glassy groundmass. The minimum thickness is 200 m and the rock lacks any internal subdivision.

On the small headland at points 5 and 6 (Fig. 24) oligomictic breccia has subangular dacite clasts lithologically identical to cohesive lava (Fig. 26). The breccia is clast supported, with individual clasts up to 40 cm in diameter. At locality 6 the dacite is more cohesive. Lithologically similar breccias at locality 4 show

pseudojigsaw-fit texture (Fig. 27). Weakly foliated breccias outcrop at localities 2 and 3.

In thin section, cohesive lava is porphyritic (Fig. 28) with euhedral phenocrysts of plagioclase (optically oligoclase; up to 2.5 mm long) that are weakly resorbed and sericitized. Quartz phenocrysts (up to 4.5 mm long) are locally embayed and rounded, and show weak undulose extinction. These phenocrysts and scattered disseminated aggregates of biotite flakes (some ghosts after ?amphibole) are set in a groundmass of weakly granoblastic quartz and feldspar with wispy muscovite.

Sample GSWA 114200 is a porphyritic rhyolite clast from a breccia on the western shore of Lake Lefroy. It is weakly foliated with euhedral to subhedral unzoned plagioclase phenocrysts (up to 1 mm long) that are optically albite–oligoclase. The groundmass has cryptocrystalline quartz and feldspar, and scattered biotite, chlorite, and opaque oxide. Unlike the lava, the rock lacks quartz phenocrysts and the groundmass shows relict perlitic texture.

Between breccia clasts the matrix is strongly foliated and iron stained (e.g. GSWA 109084). Scattered elongate subhedral to euhedral albitic plagioclase (up to 2 mm long) are set in a granoblastic matrix of quartz and feldspar with scattered muscovite. Crude bedding is preserved as grain size changes. Sample GSWA 109085 is petrographically similar, but contains rare rock fragments more than 7 mm

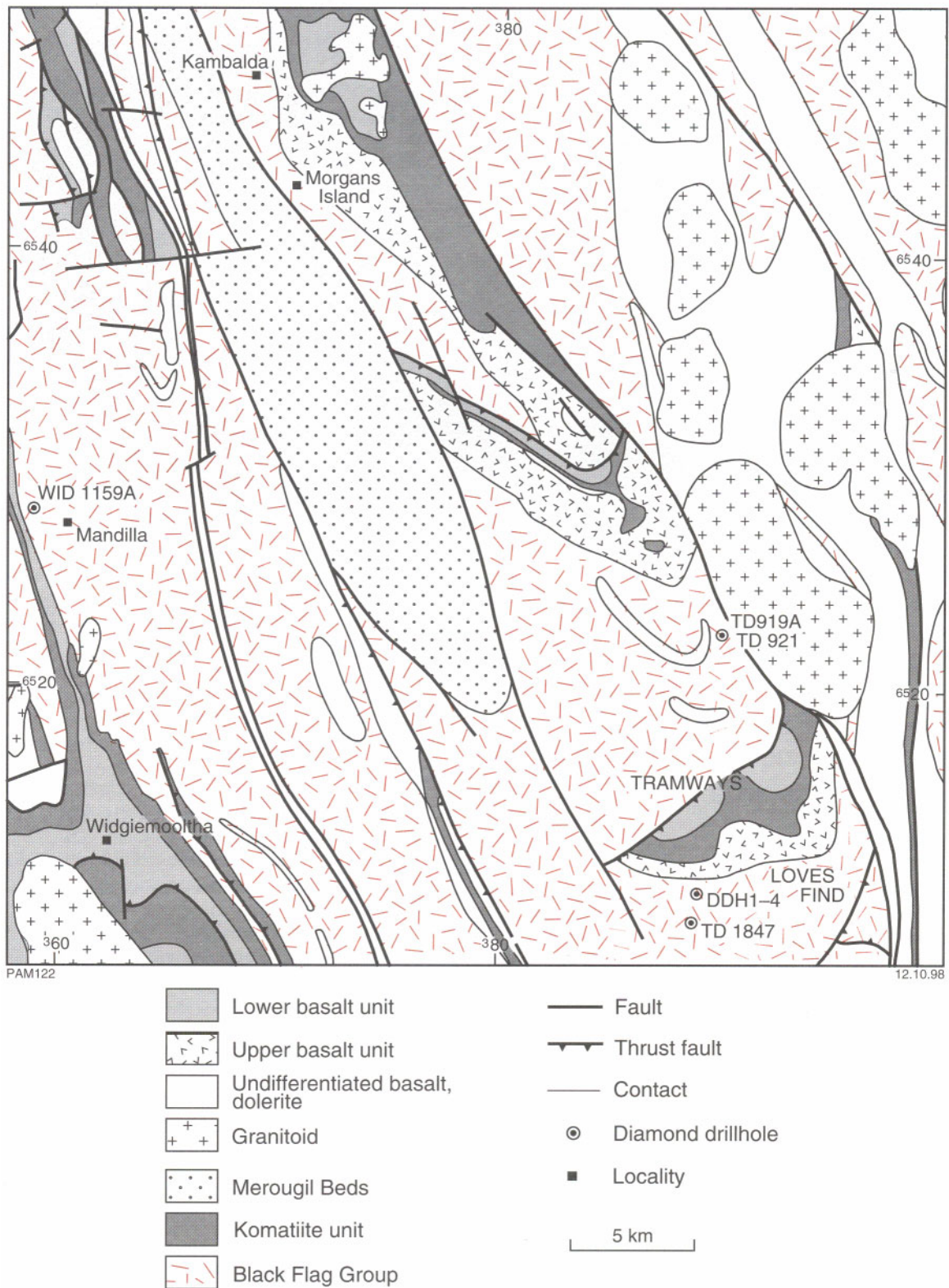
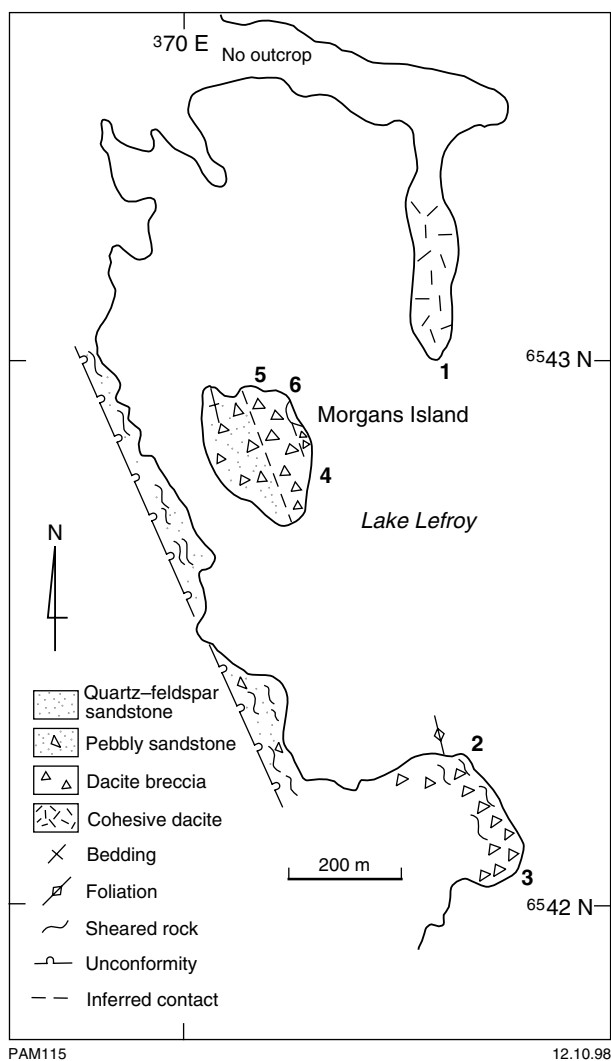


Figure 23. Simplified Archaean geology of the Kambalda–Widgiemooltha area (after Swager et al., 1990)



**Figure 24. Geological sketch map of Morgans Island (after Brauns, 1991). Numbers refer to localities discussed in the text**

long of iron-stained granoblastic quartz and feldspar. Bedding is shown by alternating 3–4 mm-thick micaceous and quartzofeldspathic bands.

### Interpretation

The lithology and spatial relationship of lava and oligomictic breccia at Morgans Island are similar to that at Lakewood. At Morgans Island cohesive lava could represent a subaqueous lava lobe bordered by in situ breccia, the latter resulting from the quenching of lava by contact with water. Following extrusion and brecciation, spalled-off lava fragments accumulated as mass-flow breccias adjacent to lobes. Finer grained spalled-off components represent sand- to silt-grade quench fragmentation of the lobe. Breccias are interbedded with volcanoclastic sandstones dominated by felsic volcanic debris with a minor mafic component. These represent turbidity current deposits of reworked lobe-derived detritus.

### Mandilla area

Felsic igneous rocks form low, lithologically homogeneous outcrops west and south of Kambalda in the Mandilla area. The rocks are dacitic in composition. Boulderly outcrops of grey, plagioclase-porphyrific felsic igneous rock (AMG (3135) 590339 on the YILMIA 1:100 000 map sheet; Fig. 23) contain numerous inclusions of pink feldspar porphyry (Swager et al., 1990). In thin section (GSWA 114401) the rock is recrystallized and inhomogeneous. Aggregates of granoblastic feldspar, quartz, and biotite up to 7 mm in diameter are set in a groundmass of quartz, feldspar, biotite, and subordinate chlorite and muscovite. Less common single crystals of subhedral plagioclase (up to 5 mm long) are cloudy and variably sericitized, and some are replaced by feldspar and biotite. Sample GSWA 114402 contains partly resorbed and sericitized alkali feldspar crystals, up to 5 mm long, showing cross-hatched twinning. Subordinate quartz grains (less than 2 mm long) are weakly embayed.

Low hills about 1.2 km west of the Coolgardie–Widgiemooltha road at Mandilla (Fig. 23; AMG 593277) are composed of coarse-grained, porphyritic felsic rock with pink alkali feldspar crystals and subordinate plagioclase. Lithologically, this unit appears similar to the previously described porphyry fragments (AMG 590339). In thin section (GSWA 114404) the rock is strongly porphyritic, comprising rounded and locally aggregated perthitic alkali feldspar (up to 2 mm long) with less common albitic plagioclase, embayed quartz (less than 1 mm long), and scattered muscovite flakes. The groundmass has granoblastic quartz, feldspar, minor amounts of biotite, and scattered opaque oxide.

### Interpretation

Felsic igneous rocks at both locations are similar to extrusive felsic rocks at Morgans Island and Gibson-Honman Rock. They are coarser grained and interpreted as high-level, intrusive equivalents of lava lobes. Lithologically similar inclusions represent either fragments of pre-existing felsic igneous rocks or cognate inclusions, possibly ripped from margins of the body during intrusion.

### Diamond drillcore from the Kambalda area

Diamond drillcore through the Black Flag Group near Tramways and Loves Find have been examined (Fig. 23), in addition to drillcore from one hole south of Loves Find (DHD421). Although their stratigraphic position within the Black Flag Group is unknown, these drillholes give additional information on the variety of rock types in the Black Flag Group. Some of the core are unusual in that they contain a high proportion of mafic volcanic rocks.

All lithologies in drillcore from TD 1847 are strongly recrystallized and foliated, with pervasive secondary biotite and calcite, and locally developed quartz veins, galena, pyrite, and hematite. The core includes polymictic breccias and basalt flows. The breccias have both open and

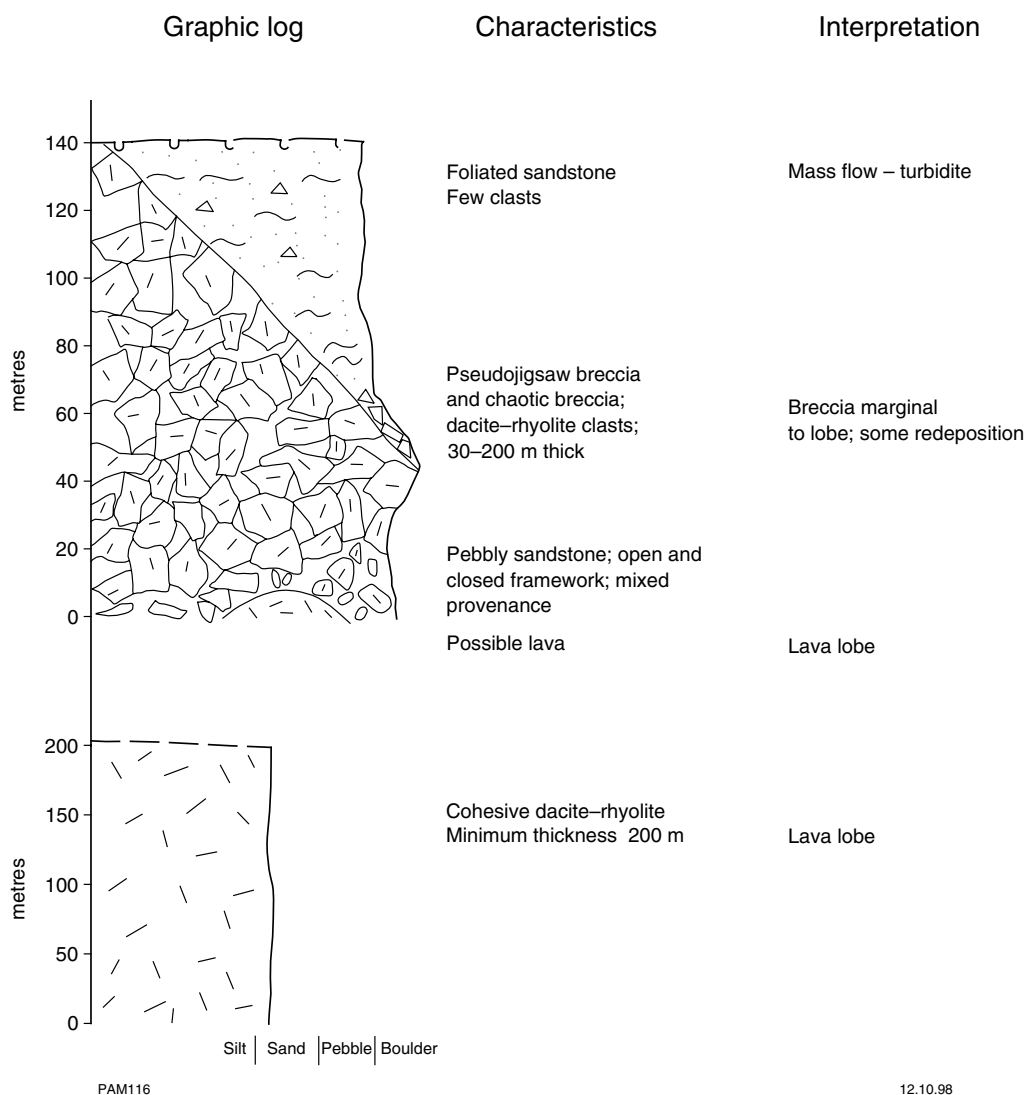


Figure 25. Interpreted stratigraphy at Morgans Island

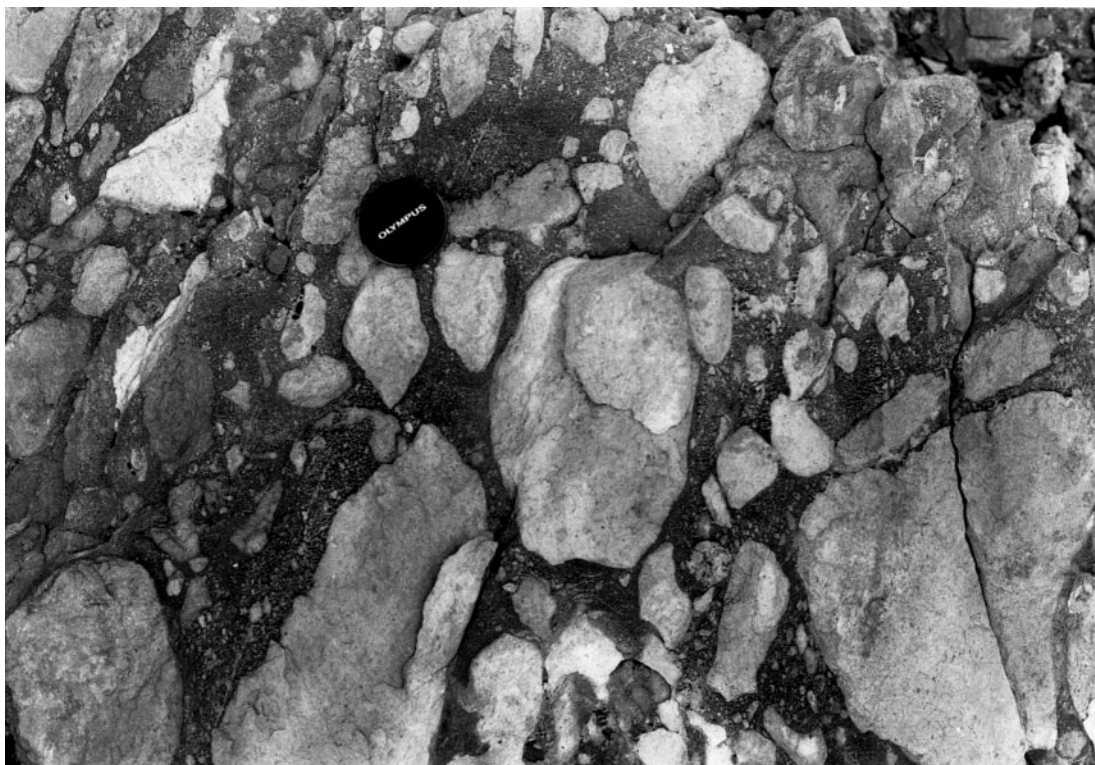
closed framework, with clasts up to 10 cm in diameter of subangular to rounded amygdaloidal basalt and less common felsic volcanic rocks. Interbedded with these breccias are 1–2 m-thick pillow lava units that contain thin interbeds of epidotized sedimentary rock. In thin section, pillow lava is strongly recrystallized and carbonated, comprising feldspar, minor amounts of quartz, biotite, and green amphibole. The rock is weakly porphyritic, with ragged microphenocrysts of feldspar in a weakly granoblastic felsic groundmass with scattered biotite, opaque oxide, amphibole, and secondary calcite. Amygdales (up to 4 mm in diameter) are subrounded and composed of fine-grained granoblastic feldspar, minor amounts of quartz, amphibole, and biotite. They appear to be more felsic than the host.

Diamond drillcore from DHD421 is also recrystallized, and contains variably vesicular and amygdaloidal basalts (some of which are pillowed) and basalt breccia. Polymictic breccias have angular to subrounded clasts of felsic and mafic volcanic rocks. The lower 15% of the

hole is fragmental basalt, overlain by amygdaloidal pillow lava, then breccia. There are intrusions of felsic porphyry throughout the core.

In thin section, basalt (e.g. GSWA 114481) is fine grained, non-porphyritic, strongly recrystallized, and carbonated. Relict feldspar phenocrysts (0.5 mm long) are now granoblastic quartz in a groundmass of weakly granoblastic feldspar and amorphous chlorite. Vesicles are preserved as cavities infilled with quartz. The rock contains secondary sphene and calcite.

About 40 km south of Kambalda at Loves Find, quartzfeldspathic schists, locally developed pyritic and carbonaceous shale, and 3–4 m-thick units of closed- and open-framework breccias form rubbly outcrops (Fig. 23). North of Loves Find, graded and cross-bedded felsic sandstones outcrop on the lake shore, striking at 345° and dipping 45°W. Lithologies comprise pebbly sandstone, sandstone, and shale with coarse-grained sandstone beds up to 2 m thick containing rip-up shale clasts. Shale units



PAM 157

21.7.98

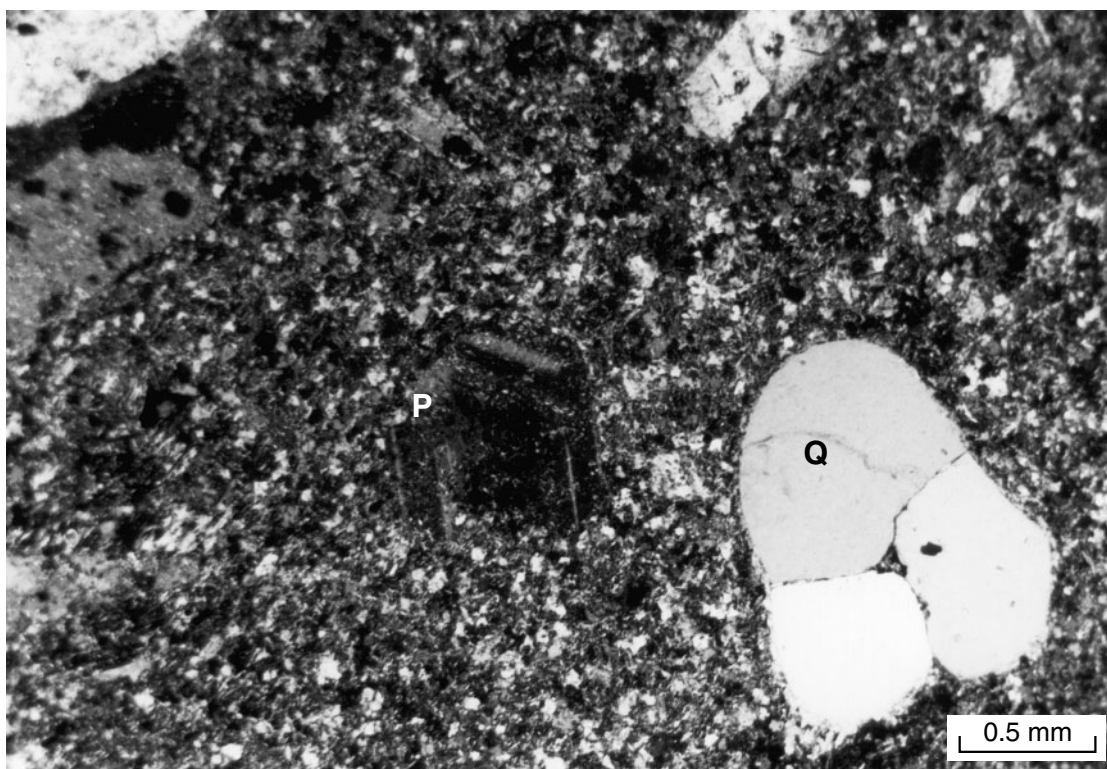
**Figure 26. Oligomictic breccia in Black Flag Group at locality 5 (Fig. 24), Morgans Island. Lens cap is 54 mm in diameter**



PAM 125

21.7.98

**Figure 27. Pseudojigsaw-fit oligomictic breccia in Black Flag Group at locality 4 (Fig. 24), Morgans Island. Lens cap is 54 mm in diameter**



PAM 158

21.7.98

**Figure 28.** Rhyolite lava in Black Flag Group at locality 1 (Fig. 24), Morgans Island. Q — quartz, P — plagioclase. Groundmass has quartz, feldspar, biotite flakes, and opaque oxides. Sample GSWA 109087; AMG (3235) 704431; plane polarized light

range from 20 to 40 cm in thickness. The outcrop changes rapidly along strike to felsic schists.

Four diamond drillholes through the Loves Find succession (Fig. 29) contain lithic breccia, sandstone, and shale. Normal and less common reverse grading throughout all four holes (with localized cross-bedding in DDH3), the polymictic nature of breccias, and the lack of any clearly defined primary volcanic features are consistent with redeposition.

Closed- and open-framework breccias consist of angular, fine-grained felsic volcanic clasts and a more coarsely porphyritic variety. The fine-grained clasts form about 90% of the clast population, reaching a maximum of 6 cm in diameter (c.f. 13 cm clast in DDH3 at 108 m). In parts of the core they are flattened parallel to the regional foliation (e.g. DDH1, 32 m), whereas coarsely porphyritic clasts are not flattened. The latter are compositionally similar to the fine-grained clasts in terms of phenocryst type and groundmass composition. Breccias are crystal rich (with much more feldspar than quartz), although some parts are lithic rich (e.g. DDH2 at 105 m) and size graded.

Breccia units either grade into sandstone (e.g. DDH3 from 89 to 102 m) or are in sharp contact with each other. Sandstone units are poorly bedded, feldspathic, crystal rich, and lithologically similar to the matrix of breccias. Drillhole DDH2 has a series of internally graded,

amalgamated sandstone beds from 45 to 51 m depth. Finer grained sandstones (e.g. DDH2 from 127 to 134 m) have scattered garnet porphyroblasts. Sandstone grades locally into shale (e.g. DDH1 at 87 m).

Crystal-rich, buff-coloured, fine-grained sandstone units have sharp contacts with volcanoclastic units. The upper contacts are undulose and eroded in some instances. They rarely exceed 20 cm in thickness (e.g. DDH4 at 116.5 m and 115.8 m), and from 93.5 to 100.5 m in drillhole DDH4 they are present as a rhythmic series.

In thin section all samples examined are recrystallized and some are foliated. Sandstones are poorly sorted (e.g. GSWA 114410 in DDH3 at 118.3 m), consisting of feldspar, with alkali feldspar greater than plagioclase (albite), and rock fragments in a matrix of granoblastic quartz, feldspar, and biotite flakes. The feldspar is subhedral to euhedral, partly sericitized, cloudy, weakly zoned, and up to 6 mm long. Rock fragments are less common, consisting of granoblastic feldspar, subordinate quartz, and biotite flakes hosting microphenocrysts of alkali feldspar and minor amounts of plagioclase. Sample GSWA 114424 contains elongate micaceous fragments.

Sample GSWA 114415 (DDH3 at 75 m) contains cloudy, euhedral, and locally broken grains of alkali feldspar and subordinate plagioclase, up to 6 mm long, in a weakly granoblastic quartzofeldspathic matrix. About 5% of the rock consists of intergrown alkali feldspar, plagioclase, and muscovite, up to 4 mm in diameter.

In drillhole DDH3 at 111 m, elongate fine-grained rock fragments are set in a felsic matrix. The rock is strongly foliated with partly disaggregated alkali feldspar crystals up to 6 mm long set in a fine-grained matrix of granular sericite, feldspar, and minor amounts of quartz, with secondary biotite flakes and calcite. Rock fragments are preserved as truncated bands of quartz and feldspar with biotite flakes.

Garnet-bearing sandstone (GSWA 114425 in DDH3 at 120.1 m) contains anhedral pink garnet up to 4 mm in diameter with inclusions of quartz and feldspar. The matrix is a mixture of granoblastic quartz and feldspar with abundant green biotite and recrystallized feldspar laths up to 2 mm long, and scattered pyrite cubes.

The crystal-rich, buff-coloured, fine-grained sandstone units are relatively fresh and only weakly foliated in thin section. Sample GSWA 114420 (at 48.9 m in DDH3) contains about 40% crystals, comprising 70% alkali feldspar and 30% plagioclase, that are cloudy, weakly zoned, euhedral, and sometimes broken. Rounded fragments of granoblastic quartz are probably remnants of rock fragments. The matrix is quartzofeldspathic and fine grained, with scattered muscovite and some calcite patches. Sample GSWA 114422 (at 100.2 m in DDH4) is petrographically similar, with feldspar grains up to 4 mm long. Rock fragments comprise less than 10 volume %.

### Interpretation

Amygdaloidal basalt, similar to basalt in drillcore from Foster and Democrat, is present as conglomerate clasts in the upper parts of the Black Flag Group, west of White Flag Lake. Drillcore from LED 10, south of Kalgoorlie–Boulder, also contains amygdaloidal basalt flow units.

Sandstone and breccia in drillcore from Loves Find are lithologically similar to volcanoclastic rocks in drillcore from the Lakewood area of Kalgoorlie. In all four diamond drillholes examined there is no evidence of primary volcanic fragmentation or deposition. Breccias contain two clast types, the most common of which is a fine-grained, porphyritic felsic volcanic rock. More strongly porphyritic clasts are less common. Both clast types have a similar mineralogy and may be textural variants of the same magma type. Breccias and sandstones range from massive ungraded units through to normal and less common reverse-graded units. Cross-bedded units are rare. These sedimentary structures are consistent with rapid deposition by mass-flow and turbidity currents. Fine-grained, crystal-rich units throughout the core represent the fine-grained fraction elutriated from the deposit, which has settled out of the water column during still periods.

In a regional study of the Black Flag Group, Brauns (1991) argued that the breccias at Loves Find resulted from mass flow of autobrecciated debris from a flow front. Finer grained, more-distal equivalents of these deposits resulted from turbidity current flow. Results of this study cannot confirm this as no cohesive lava facies have been identified, although the limited range in clast type and the sedimentary processes are similar to those associated with lava-lobe wastage at Kalgoorlie.

## Felsic volcanism in the northern Eastern Goldfields and Kanowna areas

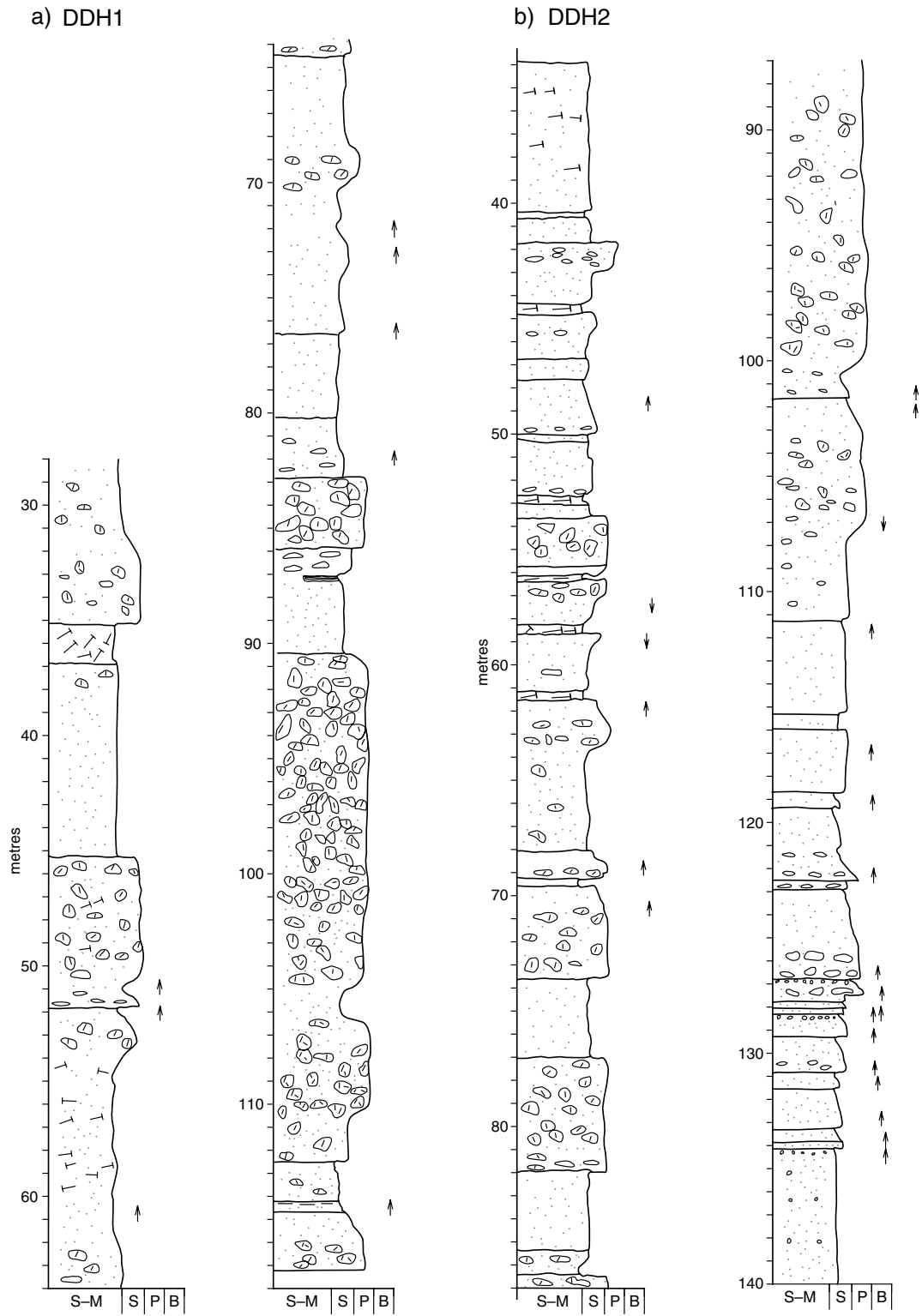
Hallberg et al. (1993) argued on the basis of eruption style and geochemistry that felsic volcanic rocks exposed south of Leonora, in the northern Eastern Goldfields region (Fig. 1), form part of an elongate belt extending south to the Kanowna district, east of Kalgoorlie, even though the Kanowna succession has been treated as part of the Black Flag Group (Taylor, 1984). The felsic volcanic association south of Leonora is treated here, together with the Kanowna succession, as part of the Gindalbie Terrane (Swager, 1995; Witt et al., 1996).

### Northern Eastern Goldfields region

Although there are several well-exposed felsic volcanic centres in the northern Eastern Goldfields region (Fig. 1; Hallberg, 1985, 1986) the stratigraphic and structural complexity of this area has meant that the relationships of these centres to each other and to the Kalgoorlie Terrane are presently unclear (Witt, 1993a; Rattenbury, 1993). One suite of felsic volcanic rocks forms part of a 350 km-long, rhyolite-dominated belt extending from Teutonic Bore southward to Kanowna (Hallberg et al., 1993), and part of this belt is discussed below. Witt (1993a) discussed two volcanic centres forming part of this belt south of Leonora. The two centres were originally termed the Melita rhyolite centre and Jeedamya porphyry pluton respectively by Hallberg (1985), and were renamed the Melita Rhyolite and the Jeedamya Rhyodacite by Witt (1993a), whose terminology is adopted here. The Melita Rhyolite is arguably the best preserved felsic eruption centre in the Eastern Goldfields region. Much of the following description is taken from Witt (1993a).

The Melita Rhyolite comprises rhyolitic ash, lapilli tuff, pyroclastic breccia, and minor amounts of dacite flows. Felsic rocks are interleaved with basalt and basaltic andesite, and dominated by vitric fragments with subordinate crystals and few lithic fragments. These poorly sorted, massive deposits are attributed to pyroclastic flows resulting from a Plinian-style eruption. The associated well-bedded, fine-grained ash deposits (some with accretionary lapilli) represent airfall deposits, some of which have been subaqueously reworked. Based on the degree of sorting, clast size, bed thickness, and proportions of sedimentary to volcanic rock, Witt (1993a) suggested that the vent system is located in the north-eastern corner of the MELITA 1:100 000 map sheet. Witt (1993a) calculated that a total of 900 km<sup>3</sup> of rhyolitic material was erupted, based on an estimated north-south extent of 70 km and a stratigraphic thickness of 700 m.

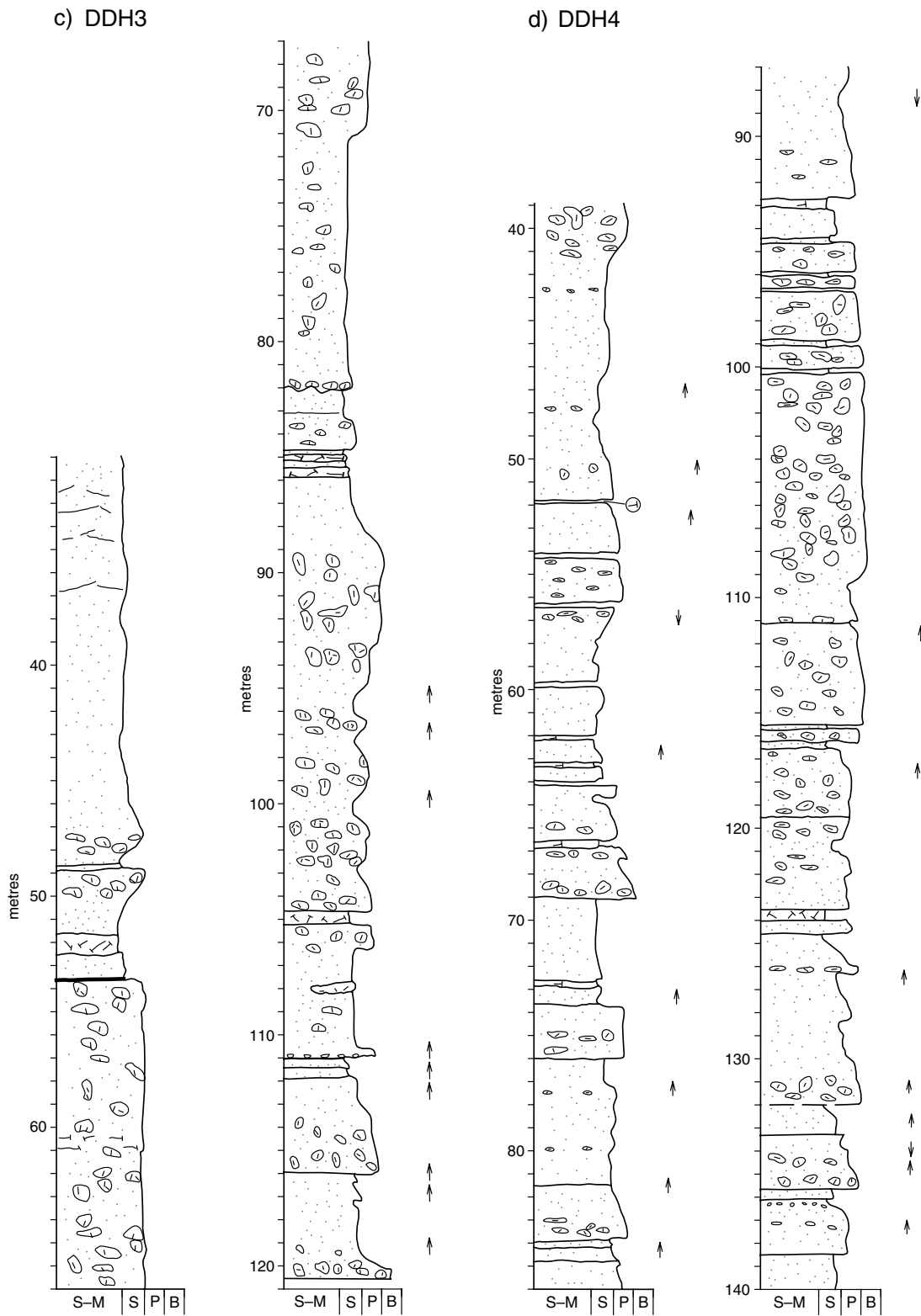
The Jeedamya Rhyodacite, south of the Melita volcanic centre, is less well exposed. According to Witt (1993a) it consists of rhyolitic to rhyodacitic pyroclastic rocks, related epiclastic rocks, minor amounts



PAM118

12.10.98

**Figure 29. This page and opposite: Graphic log of diamond drillholes in the Black Flag Group at Loves Find: a) DDH1; b) DDH2; c) DDH3; and d) DDH4. See Figure 9 for legend**



of felsic porphyry, basalt, and dolerite. Hallberg (1985) maintained that many of these felsic rocks were intrusive, but Witt (1993a) recorded widespread metre-scale compositional and textural banding (bedding) and fragmental textures.

## Kanowna area

The greenstone geology of the Kanowna area (Taylor, 1984; Swager et al., 1990; Ahmat, 1995a,b) is stratigraphically and structurally complex, with coeval mafic, ultramafic, and felsic volcanic activity and synvolcanic uplift, erosion, and hydrothermal activity. There are several areas where felsic volcanic rocks form continuous or semi-continuous outcrops. Available U–Pb Sensitive High-Resolution Ion Microprobe (SHRIMP) ages (Table 3) indicate that at least some parts of the Kanowna succession are coeval with the Black Flag Group (Nelson, 1995).

## Perkolilli

A 1500 m-thick succession of coarse-grained felsic fragmental rocks outcrops over 5 km<sup>2</sup> at Perkolilli, 6 km southeast of Kanowna (Fig. 30; Taylor, 1984; Swager et al., 1990). Two facies associations are recognized. The most common is a poorly sorted breccia occupying about 95% of the outcrop area. Less common is a better sorted breccia that is locally bedded (Fig. 31). Both form part of

Taylor's (1984) ignimbritic conglomerate – rhyolite wacke association. Taylor (1984) estimated that individual breccia units were about 20 m thick.

The poorly sorted breccia association is clast supported, consisting of angular to subangular (locally rounded) clasts in a coarse-grained matrix. The clasts reach a maximum diameter of 1 m, but most are 10 to 40 cm in diameter. According to Taylor (1984), about 99% of the clasts are rhyolite; the remainder consists of amygdaloidal and variolitic basalt, grey banded chert, dacite, and komatiite.

Rhyolite clasts are usually black, glassy, and conchoidally fractured. They have scattered quartz phenocrysts (about 5 volume %) up to 2 mm long. Some clasts are flow banded on a millimetre to centimetre scale, and less glassy clasts contain quartz and feldspar phenocrysts. The matrix has centimetre-scale angular grains that are compositionally similar to the clasts. In thin section the groundmass of most rhyolite clasts is devitrified, and preserved as either fine-grained cryptocrystalline quartz or, less commonly, as spherules (Fig. 32). Scattered phenocrysts of embayed quartz 1–2 mm in diameter are accompanied by less common cloudy, euhedral, albitic plagioclase (less than 1 mm in diameter). Flow-banded varieties are weakly porphyritic, with cloudy, rounded phenocrysts of alkali feldspar (less than 2 volume %) set in a groundmass of millimetre-scale alternations of cryptocrystalline quartz, with accessory zircon. The coarse-grained breccia has both open- and closed-framework matrix and consists of felsic

**Table 3. Chronology of intermediate and felsic volcanic rocks from parts of the Eastern Goldfields region**

<i>Location</i>	<i>Age (Ma)<sup>(a)</sup></i>	<i>Data source</i>	<i>Method</i>
<b>Northern Eastern Goldfields region</b>			
Mount Geramatong, Leonora	2735 ± 10	1, 2	C
Pig Well, Leonora	2697 ± 3	1, 2	C
Teutonic Bore, Leonora area	2699 ± 10	1, 2	C
Royal Arthur Mine, Leonora	2692 ± 4	5	SH
Carpet Snake Soak, Jeedamya	2681 ± 4	6	SH
<b>Kalgoorlie Terrane (Black Flag Group)</b>			
Nelsons Fleet	2681 ± 5	5	SH
Kalgoorlie	2676 ± 4	3	SH
Mount Kirk, Norseman	2689 ± 7	4	SH
Ora Banda (Pipeline Andesite)	2704 ± 8	1, 2	C
Black Rabbit Dam	2658 ± 6	5	SH
Ghost Rocks	2691 ± 6	5	SH
Four Mile Hill	2613 ± 11	5	SH
Ballarat – Last Chance	2708 ± 7	6	SH
<b>Gindalbie Terrane</b>			
Wild Dog Dam	2708 ± 4	5	SH
Bulong	2704 ± 4	5	SH
Perkolilli	2675 ± 3	5	SH
Maggies Dam	2681 ± 5	5	SH
Kanowna (tuff)	2698 ± 4	2	C
Bulong Anticline	2672 ± 13	5	SH
Reidy Swamp	2682 ± 3	5	SH

**NOTES:** (a) Error of 95% confidence limit  
 Method: C = conventional mass spectrometry  
 SH = Sensitive High-Resolution Ion Microprobe (SHRIMP)

**SOURCES:** 1. Pidgeon (1986) 4. Campbell and Hill (1988)  
 2. Pidgeon and Wilde (1989, 1990) 5. Nelson (1995)  
 3. Claoué-Long (1990) 6. Nelson (1996)

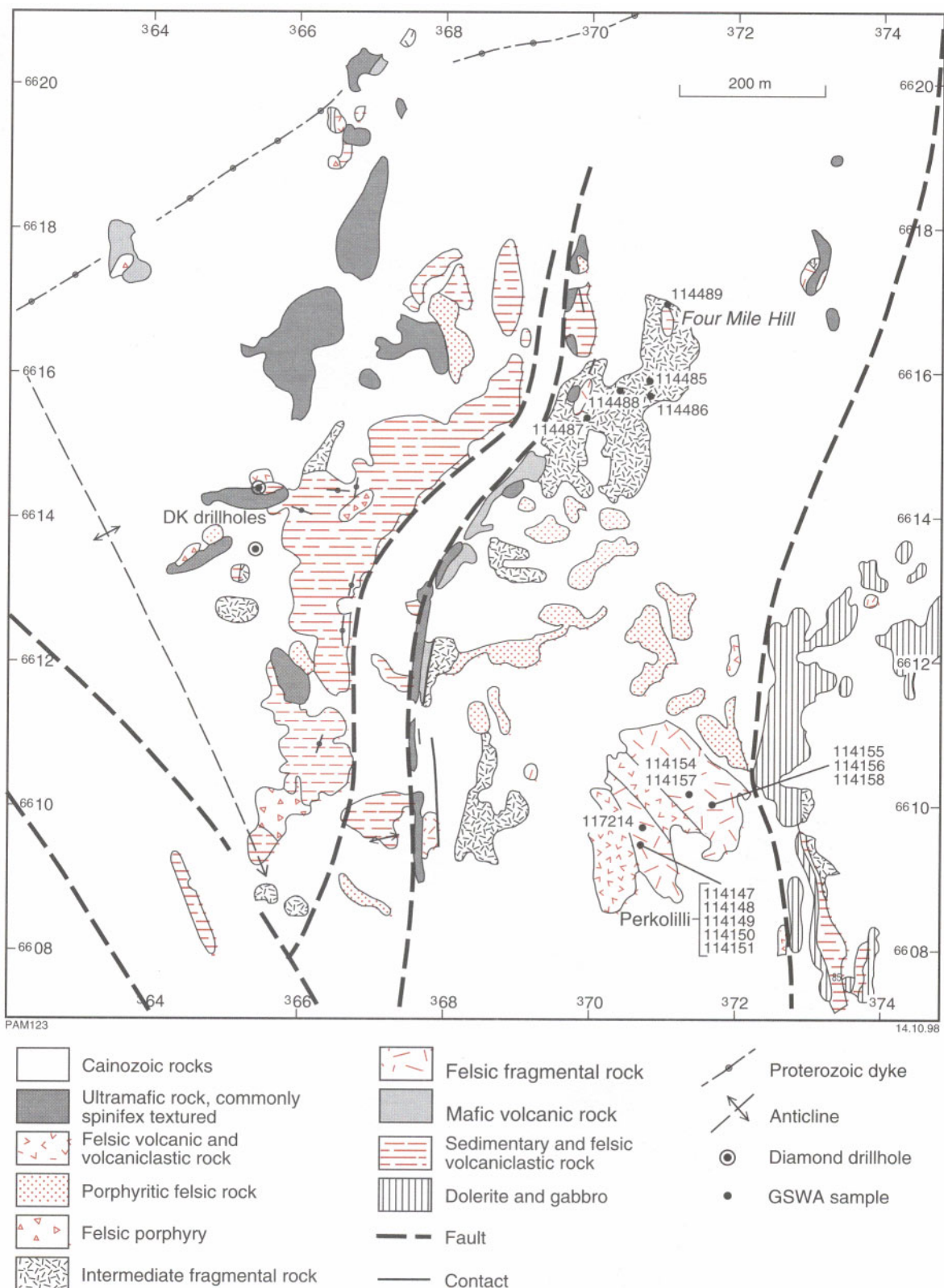
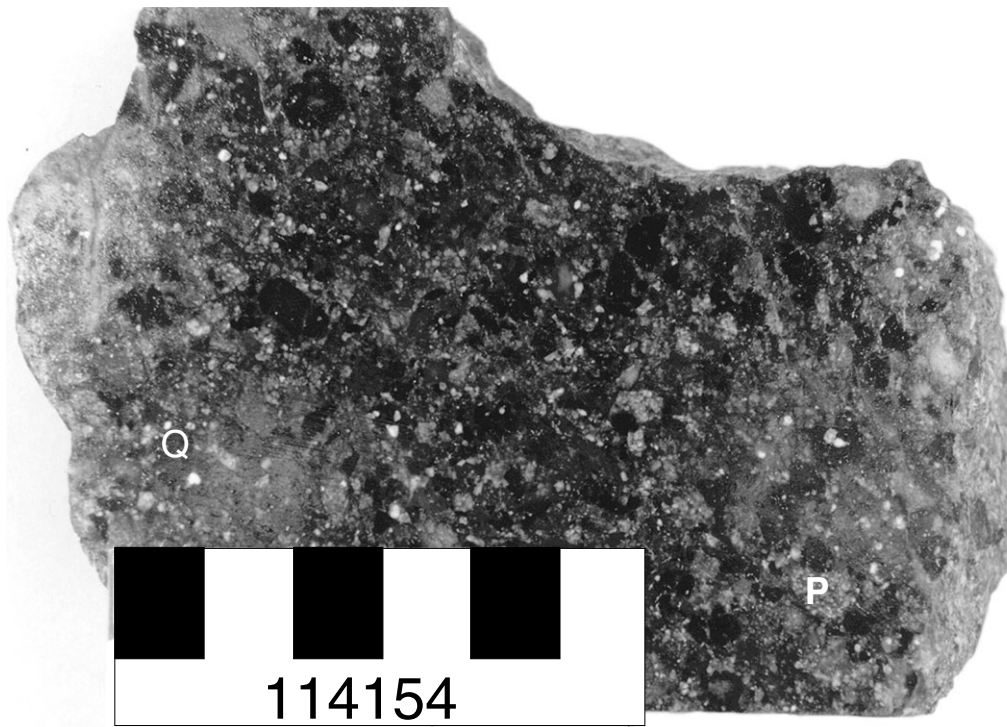


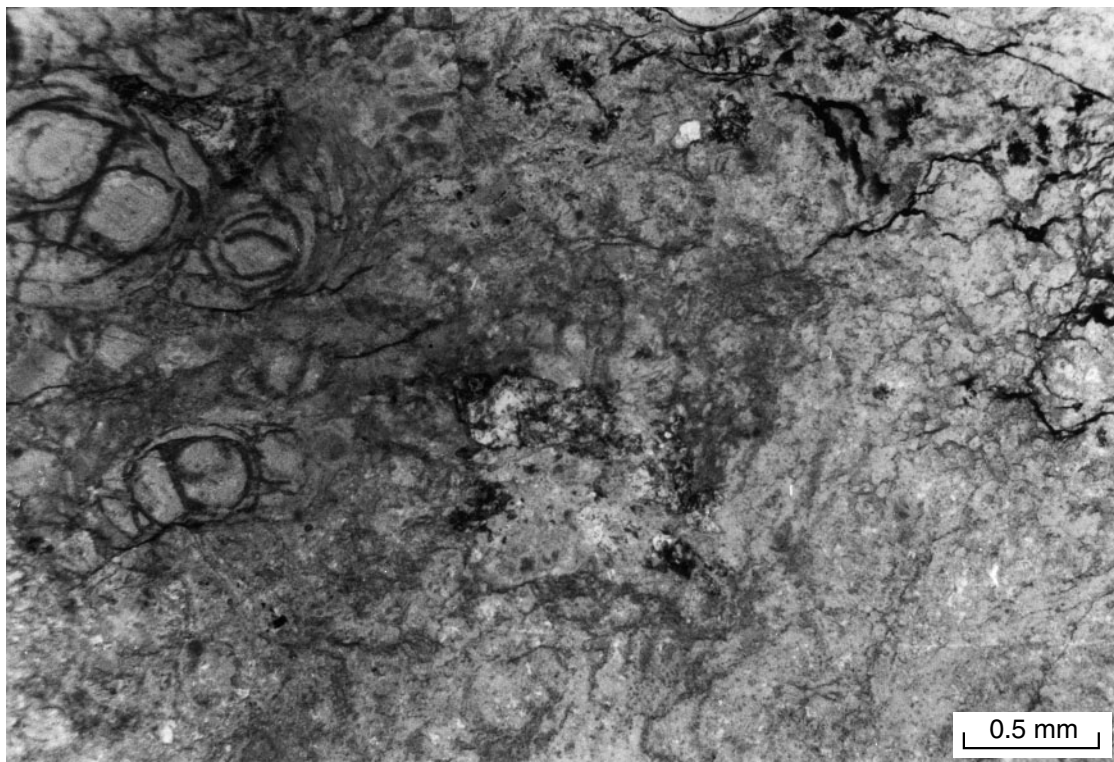
Figure 30. Simplified geological map of the Kanowna area (after Ahmat, 1995a), showing the sample locations at Perkolilli and Four Mile Hill, and the DK diamond drillholes



PAM 159

13.10.98

**Figure 31.** Moderately well sorted felsic fragmental unit at Perkolilli. Dark fragments are glassy rhyolite. Q — quartz grain, P — porphyritic rock fragment; GSWA 114154; AMG (3236) 712100



PAM 160

21.7.98

**Figure 32.** Glassy, spherulitic matrix to rhyolite clast in breccia unit from Perkolilli. Sample GSWA 114145; AMG (3236) 712100; plane polarized light

volcanic rock fragments (compositionally similar to clasts), less common more-basic rock fragments, and single crystals in a variably devitrified glassy groundmass. Angular rhyolite rock fragments are more than 2 cm in diameter. Some are flow banded with weakly developed eutaxitic texture (GSWA 114158 and 114157; Figs 33 and 34). Other fragments are perlitic or cryptocrystalline, whereas less siliceous examples consist of a glassy groundmass with phenocrysts of sericitized feldspar. Discrete quartz grains comprise up to 30% of the rock. They are embayed and locally broken. Less common are cloudy broken grains of albitic plagioclase (up to 1 mm long).

The better sorted breccia association forms crudely bedded lenticular units up to 100 m long and 30 m thick, although most units are closer to 1 m thick. They are in sharp contact with the coarse breccia facies and have a similar clast composition, but a smaller clast size. Bedding is on a scale of 2 to 10 cm, and one fine-grained unit has locally developed graded bedding and low-angle cross-beds. In thin section, a visual mode of fine-grained breccia is 20% crystals (comprising 60% quartz and 40% feldspar), 70% rock fragments, and 10% matrix. Clasts are less than 1 mm in diameter. Quartz and feldspar grains are angular and broken, and the latter are cloudy and subhedral. Rock fragments are cusped and usually clast supported. Most are composed of cryptocrystalline quartz, although a few are perlitic. The matrix comprises cryptocrystalline quartz with accessory zircon. Sample GSWA 117214 (from the cross-bedded unit at

AMG (3236) 708093) consists of thinly bedded (up to 10 mm in thin section) quartzose sandstone bands of angular quartz grains ranging from less than 0.5 mm to 1 mm in diameter. Less common are subangular, locally cusped clasts of granoblastic quartz with subordinate sericitized alkali feldspar grains less than 1 mm long. The matrix consists of cryptocrystalline quartz with relict devitrification texture, and minor amounts of sericite.

### Interpretation

Williams (1970) described the Perkolilli felsic fragmental unit as a primary volcanic deposit, whereas Taylor (1984) believed the succession had been redeposited. Taylor (1984) based this argument on the absence of glass shards, favouring instead subaerial erosion of ignimbrite or rhyolite domes and flows by steep-gradient streams, depositing the resultant debris in an adjacent graben.

In this study there is some evidence to indicate that the Perkolilli felsic fragmental unit resulted from fragmentation and deposition in a hot state, that is, a pyroclastic flow. The clast population shows a limited compositional range and is dominated by non-vesiculated, locally flow-banded rhyolite. Clasts are angular to subangular and poorly sorted, ranging from more than 1 m in diameter to a few centimetres. The matrix is compositionally similar to the clasts. It lacks a fine ash component and contains scattered broken feldspar

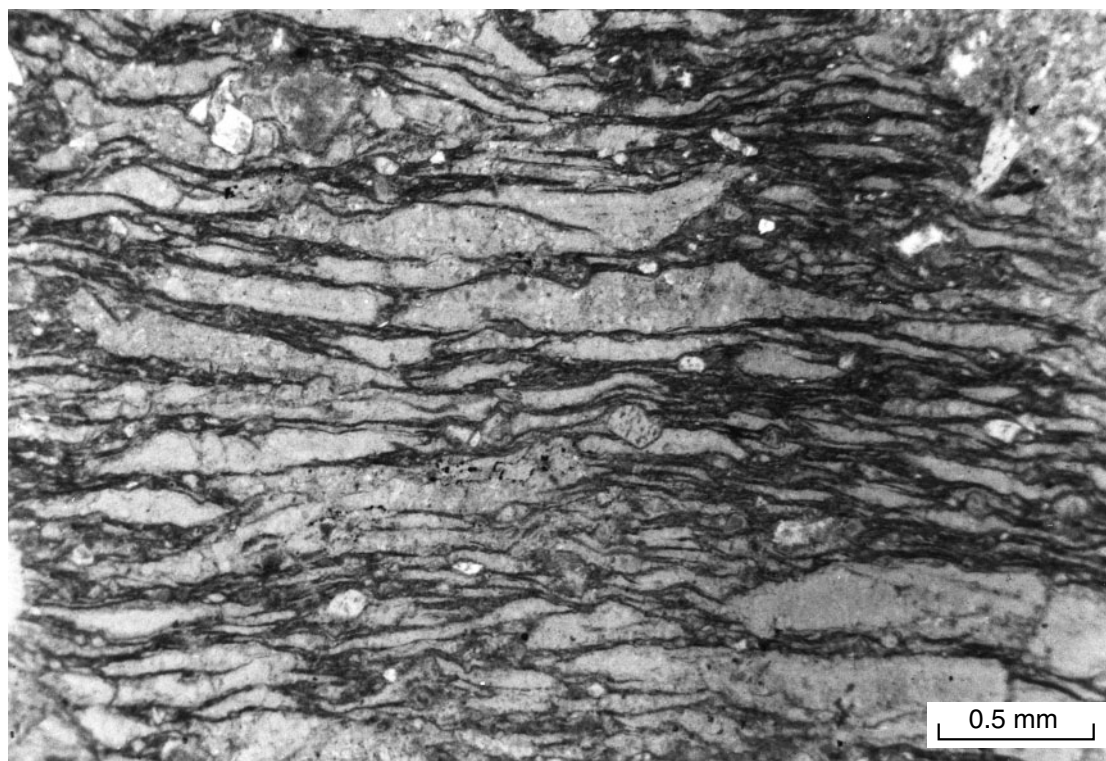
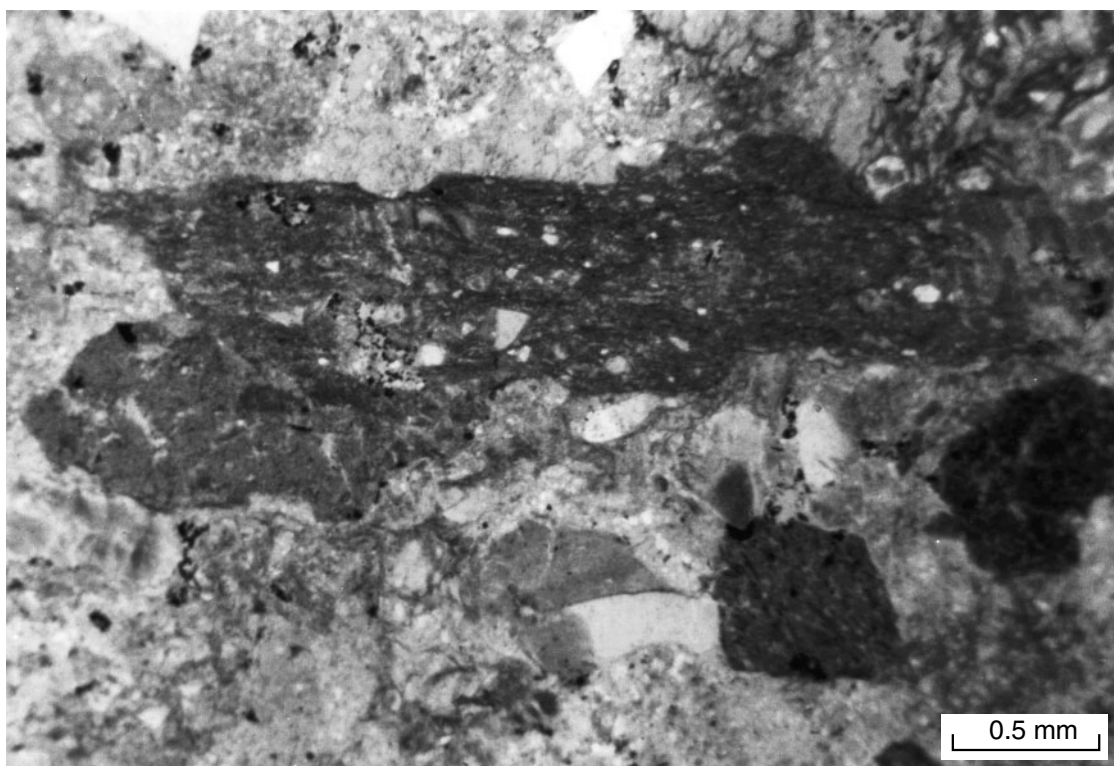


Figure 33. Eutaxitic texture developed in sample GSWA 114158 from Perkolilli; AMG (3236) 713094; plane polarized light



**Figure 34. Eutaxitic texture developed in clast from Perkolilli. Sample GSWA 114158; AMG (3236) 713094; plane polarized light**

and quartz crystals in addition to lithic clasts. Breccias are both clast and matrix supported. Rare thinly bedded or graded units comprise angular, broken grains of resorbed quartz and cusped, originally glassy fragments set in a partly devitrified groundmass. In thin section (Fig. 33) there is clear evidence of welding, indicating a hot state of emplacement. Breccia units are about 100 m long and 30 m wide, and the total volume of the deposit is probably less than 1 km<sup>3</sup>.

The Perkolilli deposit resembles small-volume pyroclastic flows (*nueés ardentes* or block and ash flows), such as those described from St Kitts by Wright et al. (1980), Smith and Roobol (1982), and Roobol et al. (1987). On St Kitts, block and ash flows consist of lithic breccias with angular to subangular lithic fragments (commonly 25 to 50 cm long, but up to 3 m long) showing both clast and matrix support and fines depletion. Individual flows are 20 m thick and 150 m wide. These block and ash flows are attributed to gravitational collapse or explosion of a lava flow or dome. The resultant block and ash flow is usually small and travels a limited distance from the vent (e.g. 1903 pyroclastic flow on Mount Pelée was 0.1 km<sup>3</sup>, flowing 8 km from the vent; Smith and Roobol, 1982). The flows comprise non-vesiculated angular blocks and can show normal, reverse, or no grading. Smith and Roobol (1982) noted that some parts of block and ash flows lack a coarse component and are instead characterized by crystal and vitric components showing unidirectional bedforms (e.g. cross-stratification).

Such deposits could represent lateral blasts (ground surge) prior to pyroclastic flow. As the flow is gravity controlled and has an appreciable gas component (Smith and Roobol, 1982), it is possible that the accompanying turbulence would elutriate any fine (ash) fraction, including glass shards. This could explain the lack of glass shards in the Perkolilli deposit. As a consequence of high initial temperature, changes can occur in the block and ash flow after deposition. These include compaction, welding, recrystallization, devitrification, and chemical alteration. According to Smith and Roobol (1982), the degree of welding is a function of the lithostatic pressure (i.e. thickness of the unit), composition of the residual volatiles, and the physical properties of the glass.

### Four Mile Hill

Outcrops of weakly schistose felsic rocks with local intercalations of ultramafic and chemical sedimentary rocks are found at Four Mile Hill (Fig. 30), 20 km northeast of Kalgoorlie (Ahmat, 1995a). Felsic rocks comprise sandstones, conglomerates, and breccias, some of which show graded bedding and load structures. Less common lithologies include porphyritic felsic igneous rocks and tourmalinite beds (Taylor, 1984). The succession strikes roughly north-south and is folded on a regional scale, so that facing directions from sedimentary structures are misleading. Graded bedding in felsic sandstone

associated with tourmalinite indicates an easterly facing direction, but volcanoclastic sandstone (AMG 695150) strikes at 035° and youngs to the west. Here the sandstone is underlain by poorly sorted breccia containing clasts with weakly developed flow banding. A conglomerate unit (AMG 711161) contains angular clasts up to 30 cm long of fine-grained volcanic rock. About 10% of the clasts are dacites. Sandstones are fine to medium grained, locally pebbly, crystal rich, and dominated by angular quartz grains.

In thin section, sandstones (e.g. GSWA 114489 at AMG 710169) are moderately well sorted and dominated by angular quartz grains up to 2 mm long. Subordinate feldspar is subangular, albitic, cloudy, less than 2 mm long, and accompanied by scattered fine-grained quartzofeldspathic rock fragments. A visual mode of clasts is 70% quartz, 15% feldspar, and 15% rock fragments. The matrix is fine grained, quartzose, and networked by sericite. The rock shows weak grain support.

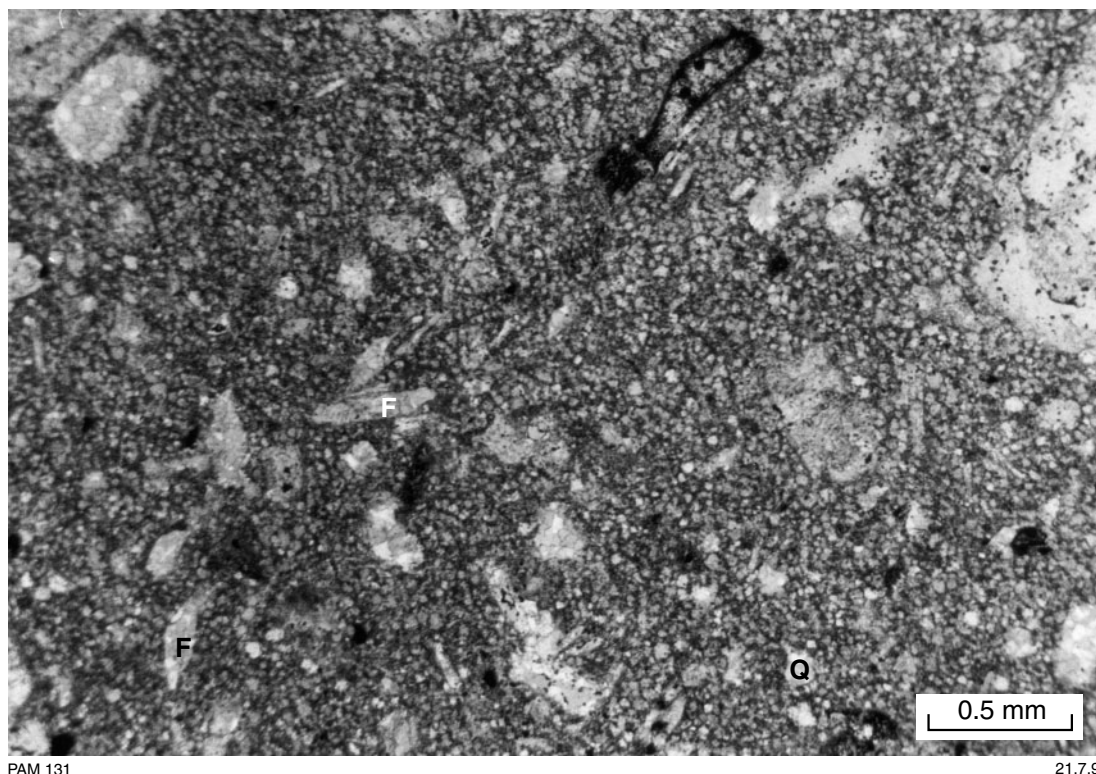
Tourmalinites comprise thinly bedded to laminated assemblages of fine-grained felsic sandstone and black tourmaline. The sandstones show well-developed size grading. In thin section (GSWA 114485, AMG 709160), laminae comprise tourmaline and quartz–feldspar-rich bands, although there are gradations between the two types. Felsic bands range from 1 mm to 2–3 cm in thickness and clasts are dominated by angular to rounded quartz grains usually less than 1 mm long. Some are weakly embayed and feldspar grains are absent. Smaller

clasts comprise wispy to bladed, bluish-green to pale-yellow tourmaline. The matrix is a weakly cryptocrystalline mass of quartz with minor amounts of feldspar and wispy muscovite. Tourmaline-rich bands are crowded with blocky to bladed, bluish-green to pale-yellow tourmaline (less than 0.5 mm long), and less common angular quartz grains. The matrix is cryptocrystalline and felsic.

A coarsely porphyritic rock (GSWA 114488, AMG 703159) contains quartz and feldspar phenocrysts in a devitrified glassy groundmass. The rock shows weakly developed columnar jointing. Quartz phenocrysts, up to 3 mm long, are locally embayed and feldspar phenocrysts are less common, cloudy, partly resorbed, and originally euhedral. Scattered fragments consist of granoblastic quartz aggregates. The groundmass is weakly recrystallized glass with signs of devitrification (Fig. 35).

Rhyolite lava (GSWA 114486, AMG 709159) contains embayed and rounded quartz phenocrysts up to 2 mm long set in a fine-grained recrystallized groundmass of quartz and mica. Equant voids (some filled with quartz and sericite) are possibly after alkali feldspar, and scattered amygdales are infilled with quartz.

Although sericitized, a fragmentary rock (GSWA 114487, AMG 698153) lacks crystals or rock fragments, but contains shard-like clasts up to 3 mm long. The matrix is cryptocrystalline quartz and abundant sericite.



PAM 131

21.7.98

Figure 35. Quartz (Q) and feldspar (F) phenocrysts in a partly devitrified groundmass in rhyolite at Four Mile Hill, Kanowna. Sample GSWA 114488; AMG (3236) 703159; plane polarized light

## **Interpretation**

The stratigraphic succession at Four Mile Hill comprises quartz-dominated, redeposited, felsic volcanic rocks with subordinate volcanic flows and chemical sedimentary rocks. The redeposited rocks comprise current-bedded sandstones, unbedded and poorly sorted conglomerates and breccias, and reworked crystal and vitric tuffs.

Cohesive lava units are difficult to identify in outcrop, but some are columnar jointed and others show devitrification textures in thin section. The dominance of quartz over feldspar phenocrysts indicates a rhyolitic composition.

Tourmalinites outcrop as thinly bedded and laminated units in successions of quartzose sandstones. Davidson (1988) maintained that stratabound tourmalinite deposits formed in a sedimentary evaporitic environment, probably during diagenesis. The original boron was of hydrothermal origin. Porada and Behr (1988) described a 1 m-thick stratabound tourmalinite horizon stretching over 20 km in Late Proterozoic alkali lake deposits in Namibia. They suggested that the tourmalinite resulted from either replacement of a pre-existing borate layer in the lake or the incursion of boron-rich fluids, possibly of hydrothermal origin.

## **Diamond drilling near Kanowna**

Diamond drillcore from four holes (prefaced 'DK') near Kanowna (Figs 8 and 30) contain intercalated basalt, komatiite, shale, and felsic volcanoclastic rocks. Felsic volcanoclastic rocks are siltstones, sandstones, and conglomerates. Pebbly sandstones contain a variety of clasts, including siltstone (locally pyritic), mafic and felsic volcanic rocks, porphyritic felsic rocks, less common ultramafic volcanic rocks, and quartz grains. Typical clast proportions are 60% siltstone, 30% felsic volcanic rocks, 5% mafic and ultramafic volcanic rocks, and 5% other rock types. Fragments are up to 4 cm long. Most sandstone units are poorly sorted, but some show normal size grading. Clasts are dominantly of felsic volcanic rocks, of which two types can be distinguished based on the ratio of quartz:feldspar phenocrysts. The more common type has feldspar with subordinate quartz phenocrysts, whereas the other has about 80% feldspar and 20% quartz phenocrysts.

In thin section the sandstones are volcanoclastic. Sample GSWA 111963 (at 83 m in DK14) contains quartz grains up to 1 mm long that are angular, locally cusped, or broken. Less common are fragments of recrystallized quartz; a 1 cm-diameter fragment is fine grained and possibly glassy. The matrix has sericite flakes, calcite, quartz, and disseminated ?manganese or ?carbonaceous material. Sample GSWA 111954 (at 59.4 m in DK8) is texturally similar, but has a higher proportion of feldspar (80%) than quartz (5%). Rock fragments (15%) are of felsic volcanic rocks, some of which are flow-banded rhyolite. The groundmass is largely fine-grained chlorite and quartz with accessory clinozoisite.

Breccia at 49.6 m in drillhole DK8 (GSWA 111958) is texturally well preserved, with quartz, feldspar, and rock fragments in a fine-grained, possibly devitrified groundmass. Clast proportions are 40% plagioclase, 40% quartz, and 20% rock fragments. The clasts are up to 3 mm long. Quartz is subangular and embayed, whereas feldspar is cloudy, unzoned, euhedral albite showing weak resorption and signs of breakage. Rock fragments consist of cryptocrystalline and weakly granoblastic quartz and feldspar. The groundmass is cryptocrystalline quartz and feldspar, with relict perlitic texture outlined by mica and calcite alteration. Rare mafic rock fragments are now fine-grained chlorite and plagioclase aggregates.

## **Interpretation**

The wide variety of clast types, their angularity, and the poor sorting of sedimentary rocks indicate erosion of a wide variety of igneous rock types. Clasts in sandstones and conglomerates include a variety of felsic volcanic rock types, ranging from those with quartz greater than feldspar (rhyolite) to those with quartz less than feldspar (dacite). Some clasts were originally glassy, whereas others are holocrystalline. The range in composition and texture suggests erosion of extrusive and high-level intrusive rhyolite and dacite.

## **Gordon mining centre**

About 2 km south of the Gordon mining centre, felsic rocks are interbedded with komatiite, tholeiitic basalt, dolerite, carbonated mafic and ultramafic volcanic rocks, and banded iron-formation (Ahmat, 1995b; Fig. 36). Way-up indicators show that the succession youngs to the east. Although some of the basalts are pillowed, the felsic rocks contain few features that unequivocally belie their origin. The felsic rocks are typically homogeneous, massive, porphyritic (feldspar and quartz) units with locally developed planar features that could be either relict bedding or flow banding.

In thin section felsic rocks show signs of secondary alteration, although textures in some rocks are well preserved. Partly disaggregated quartz bipyramids in GSWA 114195 are up to 1 mm long. They are set in a fine-grained groundmass now comprised of minute quartz crystals, sericite, and wispy chlorite. Relict devitrification texture is seen in plane-polarized light. The rock contains a few ovoid features that are possibly amygdalae.

## **Interpretation**

The Gordon succession has interleaved mafic, ultramafic, and felsic rocks, the latter dominated by rhyolites with subordinate dacite. Although mafic pillow lava is consistent with subaqueous eruption, felsic rocks offer few features to indicate their origin; however, petrographic examination indicates that some are flow banded and probably extrusive. Along with the Mount Shea area, Gordon is one of the few areas in the Kalgoorlie-Kanowna region where there is local-scale interleaving of mafic and felsic volcanic rocks.

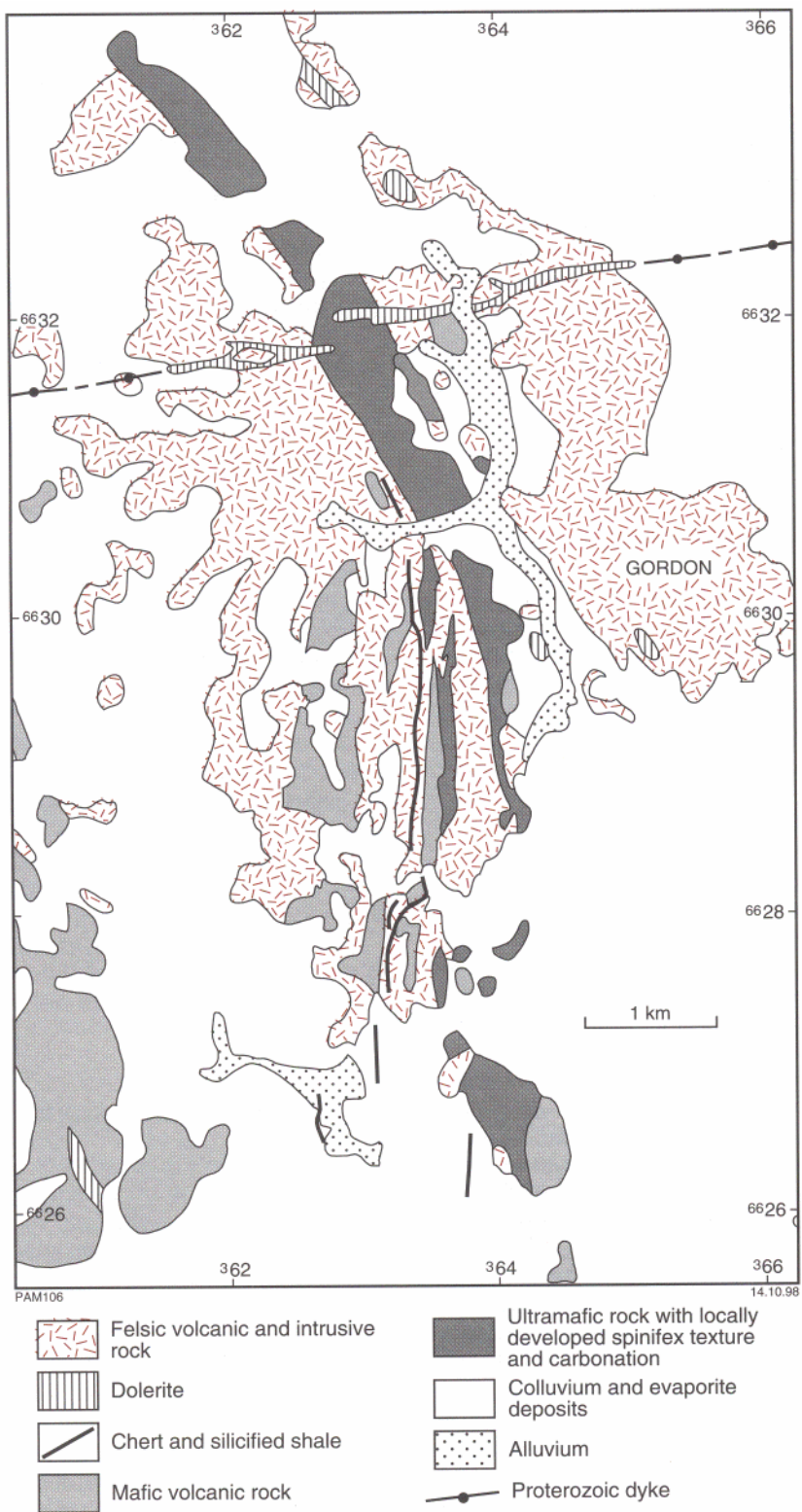


Figure 36 Simplified geology near the Gordon mining centre (after Ahmat, 1995b)

## Geochronology of felsic volcanic rocks

Until recently the absolute age of greenstones in the Eastern Goldfields region was poorly understood, as two commonly used isotope systems (Rb–Sr and Sm–Nd) proved insufficiently robust to preserve the cooling age of igneous rocks (Claoué-Long et al., 1984; Chauvel et al., 1985). More-reliable chronology is now available from U–Pb dating of zircon crystals, especially by the SHRIMP. A compilation of currently available zircon ages relevant to this study is presented in Table 3. Because there are few data, defining age relations within and between greenstone belts must await the systematic dating of mafic and felsic parts of greenstone successions. Furthermore, the interpretation of available zircon ages is hampered by poor stratigraphic control for some samples and the difficulty in comparing ages determined by conventional U–Pb mass spectrometry versus SHRIMP dating.

### Kalgoorlie and Kanowna areas

A date of  $2676 \pm 4$  Ma for a felsic volcanic rock at Kalgoorlie has been reported by Claoué-Long (1990). This is the same age, within analytical error, as a date of  $2681 \pm 5$  Ma from a felsic porphyry at Nelsons Fleet in the Parker Domain (Nelson, 1995). Similar ages of  $2689 \pm 7$  Ma and  $2691 \pm 6$  Ma have been reported for felsic volcanic rocks from Mount Kirk, near Norseman (Campbell and Hill, 1988), and Ghost Rocks (Nelson, 1995) respectively. An age of  $2658 \pm 6$  Ma for a felsic igneous rock from the lower part of the Kalgoorlie Terrane succession at Black Rabbit Dam (Nelson, 1995) is notably younger than these ages, but field relations indicate that this unit could be a later stage intrusion. A porphyry sample at Four Mile Hill has a very young age of  $2613 \pm 11$  Ma, which could relate to a significantly younger period of felsic volcanic activity. A date of  $2708 \pm 7$  Ma for a felsic volcanic rock interleaved with komatiite in the Kanowna area at Ballarat – Last Chance indicates a period of coeval felsic and ultramafic volcanism (Nelson, 1996). This age is similar to that of  $2704 \pm 8$  Ma for the Pipeline Andesite at Ora Banda (Pidgeon, 1986; Pidgeon and Wilde, 1989, 1990), although the latter is a conventional U–Pb age.

The age of the Pipeline Andesite is similar to another conventional U–Pb zircon age ( $2698 \pm 4$  Ma) for tuff from near Kanowna, although this locality is part of Hallberg et al.'s (1993) strike extension of Leonora felsic rocks (i.e. part of the Gindalbie Terrane) rather than part of the Black Flag Group. Nelson (1995) recorded an age of  $2675 \pm 3$  Ma for felsic fragmental rocks from Perkolilli near the tuff locality of Pidgeon (1986) and Pidgeon and Wilde (1989). Dacite breccia from Maggie's Dam ( $2681 \pm 5$  Ma), meta-andesite breccia from Bulong Anticline ( $2672 \pm 13$  Ma), and felsic tuff from Reidy Swamp ( $2682 \pm 3$  Ma) are similar in age to the Perkolilli SHRIMP age. Older ages, similar to those of komatiite volcanism in the Kalgoorlie Terrane, have been recorded from felsic volcanic rocks elsewhere in the Gindalbie Terrane (Wild Dog Dam:  $2709 \pm 4$  Ma; Bulong:

$2704 \pm 4$  Ma). These ages equate to an older period of felsic volcanism, similar to the conventional U–Pb age of andesite from Ora Banda.

### Leonora area

Felsic volcanic rocks with ages similar to the older phase of felsic volcanism in the Kalgoorlie and Gindalbie Terranes have been reported from the Leonora area (northern Eastern Goldfields) at Pig Well, Teutonic Bore, and Royal Arthur Mine (Table 3). The sample from Mount Geramatong ( $2735 \pm 10$  Ma) is notably older than all other dated samples. Dacite from Jeedamya ( $2681 \pm 4$  Ma) is younger than these samples and has similar ages to SHRIMP dates for the younger phases of felsic volcanism in the Gindalbie and Kalgoorlie Terranes.

## Physical volcanology of felsic volcanic rocks

### Black Flag Group

Over the 110 km strike length of the Black Flag Group examined in this study, two broad lithological associations showing distinctive styles of eruption can be identified. The most common association is subaqueous dacite and rhyolite lava and associated breccia, volcanoclastic sandstone, and carbonaceous shale. The second association is less common and comprises andesite-dominated subaerial lava and subaqueously reworked pyroclastic rocks, volcanoclastic conglomerates, and breccias. These two associations correspond to the Spargoville Formation and overlying White Flag Formation of Hunter (1993), but evidence from this study indicates that andesite-dominated volcanic rocks of the second association are not confined to any one stratigraphic level.

### Dacite–rhyolite association

The most complete dacite–rhyolite succession is found in diamond drillcore from Lakewood (from SE drilling), where flow-banded dacite and rhyolite lava have been erupted as subaqueous lava lobes. Lobe margins are marked by a decrease in the amount of flow banding, finer grain size, lower crystal content (i.e. less porphyritic), and the development of jigsaw breccia. The intensity of brecciation gradually increases towards the lobe edge, culminating in jigsaw texture. Similar textural relations have been described in both Archaean and modern subaqueous lobes and breccia by de Rosen Spence et al. (1980), Pichler (1965), Yamagishi (1991), and Cas (1992). In the Black Flag Group most lobes are less than 10 m thick, although some reach 30 m and one exceeds 80 m. Using Pichler's (1965) illustration of a subaqueous lava lobe (Fig. 18), the more than 80 m intersection in drillhole SE3 may represent the central lava conduit with smaller lobes representing buds from the central feeder. Considering the composition of the lava, lobes were probably viscous and had a low length:width ratio.

Morgans Island in the Kambalda district is one of the few surface exposures of a subaqueous lava lobe – breccia association. However, unlike drillcore sections, the lobe has a minimum thickness of 200 m and may be more than 300 m thick. Gibson-Honman Rock and felsic igneous rocks in the Mandilla–Widgiemooltha area are compositionally similar to lobes at Lakewood or Morgans Island, although they are coarser grained and some contain accidentally incorporated fragments of other felsic rocks. They are interpreted as hypabyssal intrusive equivalents of lava lobes or, in the case of Gibson-Honman Rock, a lobe that has been extruded possibly like a crystal mush.

Volcaniclastic rocks spatially associated with lava lobes consist of breccias and sandstone–shale interbeds. In thick sections (e.g. in parts of Lakewood drillcore) jigsaw-textured breccias on the margins of lava lobes are in contact with massive, poorly sorted successions of dacite and rhyolite breccias, whose clasts are compositionally similar to jigsaw breccia. These give way to crudely bedded breccias and eventually to massive or locally graded sandstone units. Thus sorting improves, grain size decreases, and bedding becomes better developed, presumably with increased distance from the lava lobe. The spatial association of breccia and sandstone to lava lobes and the compositional similarity of clasts and lava suggest that lava fragments spalled from lava lobes and accumulated as gravity-controlled mass-flow deposits adjacent to lava lobes. Shale fragments represent rip-up clasts from the substrate. Mass-flow and turbidity current deposits represented by crudely bedded breccias and sandstones were deposited further from the lobe, and interbedded sandstone and shale units represent even more distal deposits. Background sedimentation is represented by fine-grained laminated carbonaceous shale, probably deposited in quiet water conditions. Golding and Walter (1979) argued that evaporite minerals in shale from drillcore at Lakewood imply shallow-water deposition. Apart from this control there is no other evidence for determining water depth during lava extrusion.

The mineralogy of the dacite–rhyolite association in the Black Flag Group is quartzofeldspathic, with quartz usually subordinate to feldspar as dacite predominates over rhyolite. Two clast types predominate in breccias and sandstones. The first comprises a weakly porphyritic, fine-grained, felsic volcanic rock. Clasts are usually angular and at Loves Find they are flattened, although this could in part be tectonic. These clasts are lithologically similar to lava from Lakewood or Morgans Island. Less common is a subangular to angular, more coarsely porphyritic variety resembling felsic rocks at Mandilla and Widgiemooltha. Based on the lithological similarity of clasts to known outcrops it is reasonable to assume that the finer grained variety results from degradation of lava, whereas the coarser grained type represents degradation of high-level intrusions or lobes extruded as a crystal mush.

### Andesite-dominated association

Compared to the dacite–rhyolite association, the andesite-dominated association is of limited extent and is well

developed at only two locations: White Flag Lake and Mount Shea. At White Flag Lake this association overlies the dacite–rhyolite association and is in turn overlain by the Kurrawang Beds, and is thus at the top of the Black Flag Group. The andesite-dominated association consists of columnar-jointed lava, reworked, crystal-rich pyroclastic rocks, and volcaniclastic conglomerates. The conglomerate contains either metre-scale clasts of locally amygdaloidal andesite or dacite, or angular submetre-scale dacite or rhyolite clasts (compositionally similar to the dacite–rhyolite association). Columnar jointing is consistent with subaerial eruption, yet adjacent crystal-rich sandstones are graded and cross-bedded, so the succession was probably deposited in shallow-water to subaerial conditions. These volcaniclastic sandstones are mainly composed of euhedral amphibole and alkali feldspar crystals (compositionally similar to lava), reaching 50 volume %. As modern volcanic rocks seldom have more than 30% phenocrysts (van der Molen and Paterson, 1979) these rocks must have undergone syn- or post-eruptive crystal enrichment processes. Cas and Wright (1987) discussed the crystal enrichment of crystal-rich pyroclastic ash by initial sorting in the eruption column followed by reworking of the ash deposit in water. This could conceivably occur by either redeposition from land to water or the settling of ash through the water column followed by reworking. Amygdaloidal volcanic clasts in a nearby conglomerate also have phenocrysts of amphibole and feldspar. They are interpreted as the products of lava-flow degradation. More-felsic clasts may result from reworking of felsic volcanic lava flows of the dacite–rhyolite association.

The andesite-dominated association at White Flag Lake indicates coeval subaerial and subaqueous eruption of crystal-rich pyroclastic ash and compositionally similar cohesive lava. Conglomerates containing lithologically similar clasts and clasts of the dacite–rhyolite association indicate contemporaneous uplift and erosion.

Volcanic and volcaniclastic rocks compositionally similar to those at White Flag Lake outcrop with mafic and ultramafic volcanic rocks at Mount Shea, south of Kalgoorlie–Boulder. Textural evidence indicates that some of these intermediate rocks were forcibly intruded into more-basic rocks as a crystal mush, although clear interleaving of intermediate and mafic volcanic rocks is only observed at the top of the succession.

The isolated occurrence of intermediate rocks low in the stratigraphic succession at Mount Shea suggests that this type of volcanic activity is not stratigraphically controlled. The Mount Shea succession is interpreted as a locally developed, high-level intrusive to extrusive, intermediate rock-dominated magmatic episode, coeval with the waning stages of mafic volcanic activity.

Basaltic to intermediate rocks in drillcore from Kalgoorlie–Boulder (LED10), Foster (TD 1847), and Democrat (DHD421) are compositionally similar to conglomerate clasts at White Flag Lake, but the stratigraphic positions of these drillholes are not certain. Basalt in LED10 coexists with felsic volcaniclastic rocks, and it is likely that mafic volcanism occurred at isolated and

small eruptive centres contemporaneous with felsic volcanic activity.

## The Kanowna and northern Eastern Goldfields areas

Characteristics of felsic volcanism at Melita, Jeedamyia, and Kanowna, and of the Black Flag Group are summarized in Table 4. This shows the markedly different style of eruption and eruption products at these three localities compared with the Black Flag Group.

The volcanology of felsic rocks at Melita has been discussed by Hallberg (1985, 1986) and Witt (1993a). At Melita, a rhyolite-dominated succession mainly consists of crystal and vitric tuffs with subordinate lithic deposits. These are interleaved with mafic and intermediate rocks, some of which have been subaqueously erupted (Witt, 1993a).

Rhyolitic to rhyodacitic pyroclastic rocks, along with epiclastic deposits, make up the Jeedamyia Rhyodacite. Witt (1993a) interpreted these rocks as distal eruption deposits, but could not confirm that they came from the same centre as the Melita Rhyolite. The stratigraphic position of these rocks is still contentious and must await the outcome of U–Pb zircon dating.

Hallberg et al. (1993) maintained that the felsic volcanic rocks at Kanowna were a strike extension of felsic volcanic associations in the Melita area and north to Teutonic Bore. This is consistent with the occurrence of explosively erupted rhyolitic rocks at Kanowna (e.g. at Perkolilli), which is in marked contrast to the eruption of less siliceous magma as lava and less common tuff in the Black Flag Group. However, there is evidence that felsic volcanic and volcanoclastic rocks in the Kanowna area are

characterized by a range of eruption styles and association with mafic and ultramafic volcanic rocks (e.g. at the Gordon mining centre). The compositional diversity of eruption products, active tectonism, probably synvolcanic uplift, and erosion are shown by the polymictic and poorly sorted nature of volcanoclastic rocks and the complex stratigraphic and structural relationships (Taylor, 1984; Swager et al., 1990). Volcanic deposits include small-volume block and ash flows, columnar-jointed lava flows, and vitric and crystal tuffs that have undergone various degrees of reworking. Hydrothermal activity is indicated by tourmalinite deposits and the growth of stromatolites in sinter pools (Grey, 1981). The mineralogy of felsic igneous rocks and felsic volcanic clasts in volcanoclastic rocks includes both more quartz than feldspar and less quartz than feldspar, although a rhyolitic composition (i.e. more quartz than feldspar) is more common.

## Geochemistry of felsic volcanic rocks

Despite their significant outcrop area, published geochemical data for felsic volcanic rocks are available for only a few areas of the Eastern Goldfields region (Hallberg, 1985, 1986; Hallberg and Giles, 1986), and most of the available data deal with volcanic centres from the northern Eastern Goldfields region. The available data are dominated by major element analyses, with little data on trace elements. One aim of this study has been to produce a precise and accurate set of major, trace, and rare-earth element (REE) data for felsic volcanic rocks of the Black Flag Group and the Kanowna district, as well as the Melita Rhyolite and Jeedamyia Rhyodacite. These data are used to assess the chemical variations within and between these felsic volcanic rock associations, and to comment on their petrogenesis.

**Table 4. Volcanological characteristics of the Black Flag Group and felsic volcanic rocks from the Melita, Jeedamyia, and Kanowna areas**

<i>Characteristics</i>	<i>Black Flag Group</i>	<i>Melita–Jeedamyia–Kanowna rocks</i>
Rock type	Dacite–rhyolite, dacite dominant; locally developed andesite; rare basalt	Dacite–rhyolite, rhyolite dominant; basalt at Melita–Jeedamyia and Gordon mining centre
Type of volcanic products	Subaqueous lava lobes and hypabyssal intrusive equivalents. Redeposited breccias derived from wastage of lobes. Redeposited ?ash. Subaerial andesite flows and degraded products. Redeposited crystal tuffs. Mafic pillow lava	Scoria and ash deposits and rare felsic flows plus redeposited equivalents. Basalt lava (Melita–Jeedamyia). Felsic lava flows, redeposited felsic volcanic rocks, chemical sediments, heterolithic sandstones (Kanowna). Block and ash flows (Perkolilli)
Clast types	Crystals: quartz < feldspar; quartzofeldspathic rock fragments	Crystals: quartz > feldspar; quartz-dominated rock fragments. Ultramafic, basaltic fragments locally
Type of volcanic activity	Largely subaqueous (locally subaerial) lava extrusion; coeval pyroclastic activity?	Largely subaerial (locally subaqueous). Synvolcanic tectonism and uplift. Rhyolite cone facies at Melita–Jeedamyia
Environment	Shallow water, locally emergent. Possible rift	Active rift. Synvolcanic uplift and tectonism. Coeval volcanism and erosion

SOURCE: Melita data is from Witt (1993a)

Following thin section examination, 73 samples were analysed for major and trace elements by x-ray fluorescence spectrometry (XRF). Thirty-three of these samples were further analysed for minor trace elements and REE by inductively coupled plasma mass spectrometry (ICP-MS). All analyses were carried out at the Chemistry Centre of Western Australia. Sample preparation, machine conditions, precision, and accuracy for XRF analysis have been discussed by Morris et al. (1991). The complete dataset is presented in the Appendix. Sixteen major and trace element analyses of the Melita Rhyolite from Hallberg (1986) are also included in the discussion.

## Alteration and element mobility

Felsic volcanic rocks are susceptible to synvolcanic alteration (Roobol et al., 1987). Greenstones of the Eastern Goldfields region are variably metamorphosed to the extent that the mineralogy is totally metamorphic, even though the igneous textures of the samples analysed are well preserved in areas of low strain. Considering these factors, it is important to assess the extent of element mobility in order to assess the within- and between-suite chemistry. This is a contentious issue (Marsh, 1991; Wood et al., 1976), and there is no consensus on which elements remain immobile during weathering or metamorphism. Commonly, however, elements with a high charge or ionic radius (high field strength or HFS elements) are considered to be less mobile than the low field strength (LFS) elements, which have a low charge or ionic radius (Saunders et al., 1980). In a study of mafic and ultramafic volcanic rocks of the Eastern Goldfields, Morris (1993) argued that the extent of element mobility should be determined on a case-by-case basis, and showed that tholeiitic basalts from Norseman maintained coherent element trends and patterns that were little modified from the igneous precursor, despite being metamorphosed to greenschist–amphibolite facies. In this study of felsic volcanic rocks, the HFS elements Zr, Hf, Ti, P, Nb, and Ta, and the rare-earth elements La–Lu and Y show coherent trends and patterns, which accords with their relative immobility (Saunders et al., 1980; Wood et al., 1976). However, even elements such as Sr (usually taken as mobile under conditions of metamorphism or alteration) show some coherent behaviour with HFS elements, indicating limited mobility. Other elements (e.g. Si, Al, and Mg) also show some degree of coherency, but elements such as Ba, Rb, K, and Na show notable scatter.

## Major- and trace-element variations

The variations of several major element oxides and trace elements with SiO<sub>2</sub> are shown in Figure 37. The SiO<sub>2</sub> divisions of basalt, andesite, dacite, and rhyolite (Fig. 37a) are from Gill (1981). Apart from a basalt (GSWA 114492 from drillhole LED 10, Boulder) and a rhyolite (GSWA 114174 from the eastern side of White Flag Lake), samples from the Black Flag Group form a continuum from andesite (at about 57 wt% SiO<sub>2</sub>) through to rhyolite (at about 73 wt% SiO<sub>2</sub>). In contrast, samples from Melita

form a bimodal distribution, with one group having between 50 and 60 wt% SiO<sub>2</sub>, and the other group between about 68 and 83 wt% SiO<sub>2</sub>. Analyses from Jeedamya show a similar spread, but the gap between 53 and 63 wt% SiO<sub>2</sub> is wider than for samples from Melita. Samples from Perkolilli are some of the most SiO<sub>2</sub>-rich rhyolites analysed in this study, plotting near 80 wt% SiO<sub>2</sub>.

Among the major element oxides, CaO (Fig. 37b) and TiO<sub>2</sub> (Fig. 37c) have smooth trends of decreasing concentration with increasing SiO<sub>2</sub>, but Black Flag Group andesites are slightly decoupled from dacites in terms of TiO<sub>2</sub>. The MgO values also show a broad decrease with increasing SiO<sub>2</sub> (Fig. 37d), but there is some scatter among basalts. For rhyolites, Al<sub>2</sub>O<sub>3</sub> is negatively correlated with SiO<sub>2</sub> (Fig. 37a), and Black Flag Group dacites show a sharp decrease in Al<sub>2</sub>O<sub>3</sub> with little change in SiO<sub>2</sub>. They are also slightly decoupled from andesites. Basalts and basaltic andesites from the Black Flag Group at Kalgoorlie and Kambalda have a wide range in Al<sub>2</sub>O<sub>3</sub> content with little variation in SiO<sub>2</sub>. Felsic volcanic rocks from Melita and Jeedamya plot with Black Flag Group rocks, and mafic volcanic rocks from Melita show some scatter in major element composition (c.f. Black Flag Group mafic rocks), but a weak positive correlation with SiO<sub>2</sub>.

The Cr distribution is similar to MgO (Fig. 37e). Black Flag Group basalts show a wide range in Cr and two basalts are depleted in Cr relative to andesites. With increasing SiO<sub>2</sub>, V shows a smooth decrease (Fig. 37f). Most samples have less than 40 ppm Y (Fig. 37j) and less than 15 ppm Nb (Fig. 37i), except Melita dacites and rhyolites, which have a wide range of Y and Nb concentrations over a limited SiO<sub>2</sub> interval. Most of these samples are enriched in these elements relative to Black Flag Group rocks with the same SiO<sub>2</sub> contents. For most samples Zr shows a weak positive correlation with SiO<sub>2</sub>, although Melita rhyolites commonly have higher Zr at any given SiO<sub>2</sub> content (Fig. 37g). At most SiO<sub>2</sub> levels Black Flag Group rocks have higher Sr than samples from either Melita or Jeedamya (Fig. 37h). Perkolilli rhyolites have low concentrations of Sr, Zr, and the compatible elements Cr and V, but similar concentrations of Nb and Y to Black Flag Group felsic rocks.

## Rare-earth element chemistry

Chondrite-normalized REE patterns are shown in Figure 38. Black Flag Group dacites and rhyolites from Lakewood show little variation (Fig. 38a). The REE patterns are steep and (La/Yb)<sub>CN</sub> average 33 with La<sub>CN</sub> of about 100 ('CN' denotes that La and Yb have been divided by their chondritic values; Boynton, 1984). The patterns flatten from Dy to Lu, and there is no Eu anomaly. The remaining dacite and rhyolite samples from the Black Flag Group (Fig. 38b) have fundamentally similar patterns, but a wider range in REE content. Rhyolite from Gibson-Honman Rock (GSWA 114500) and Loves Find (GSWA 114424) have higher LREE and middle REE contents, whereas GSWA 117206 from White Flag Lake and GSWA 111995 from Morgans Island are more HREE depleted. Rhyolite sample GSWA 111995 has a slight positive Eu anomaly.

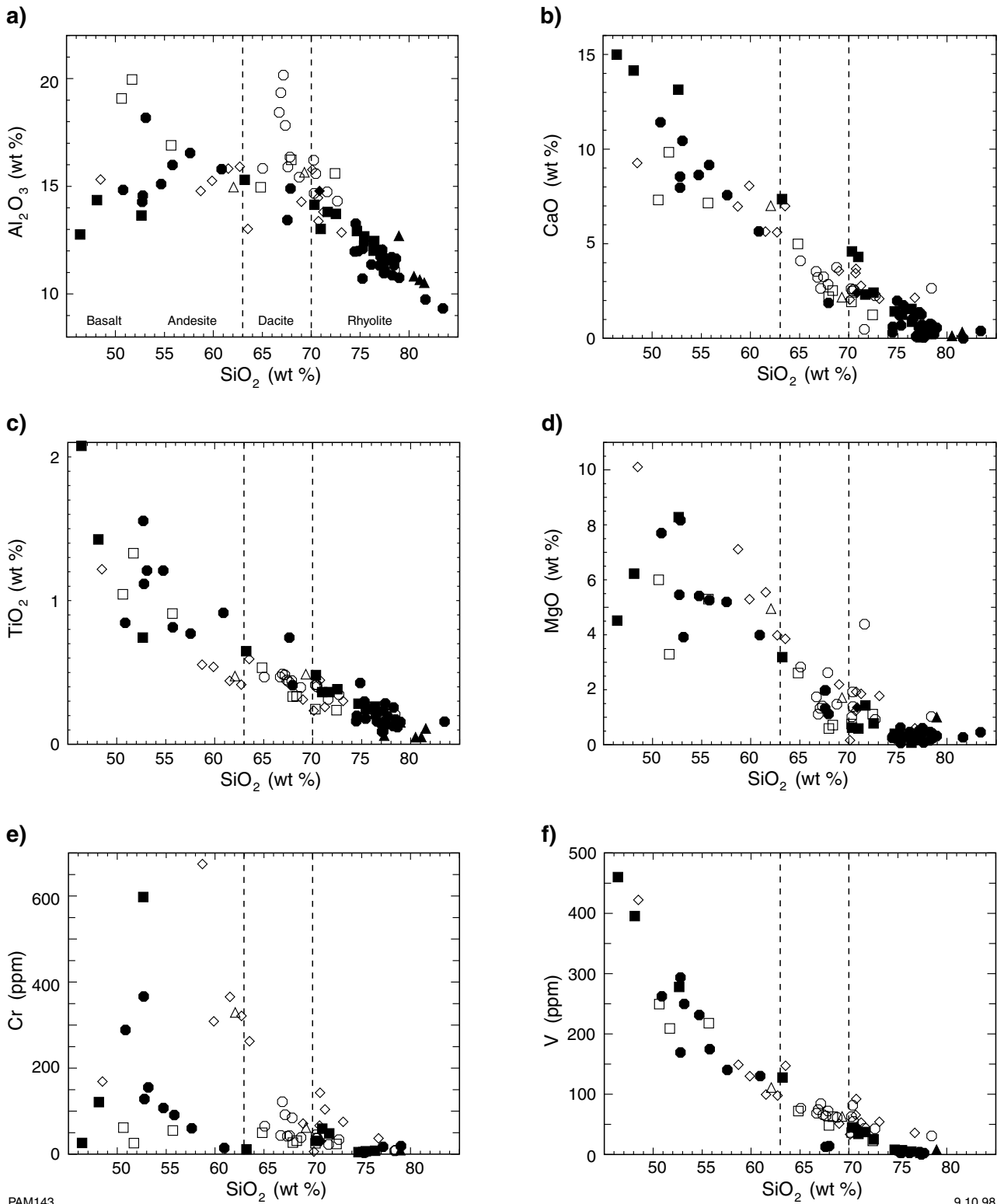
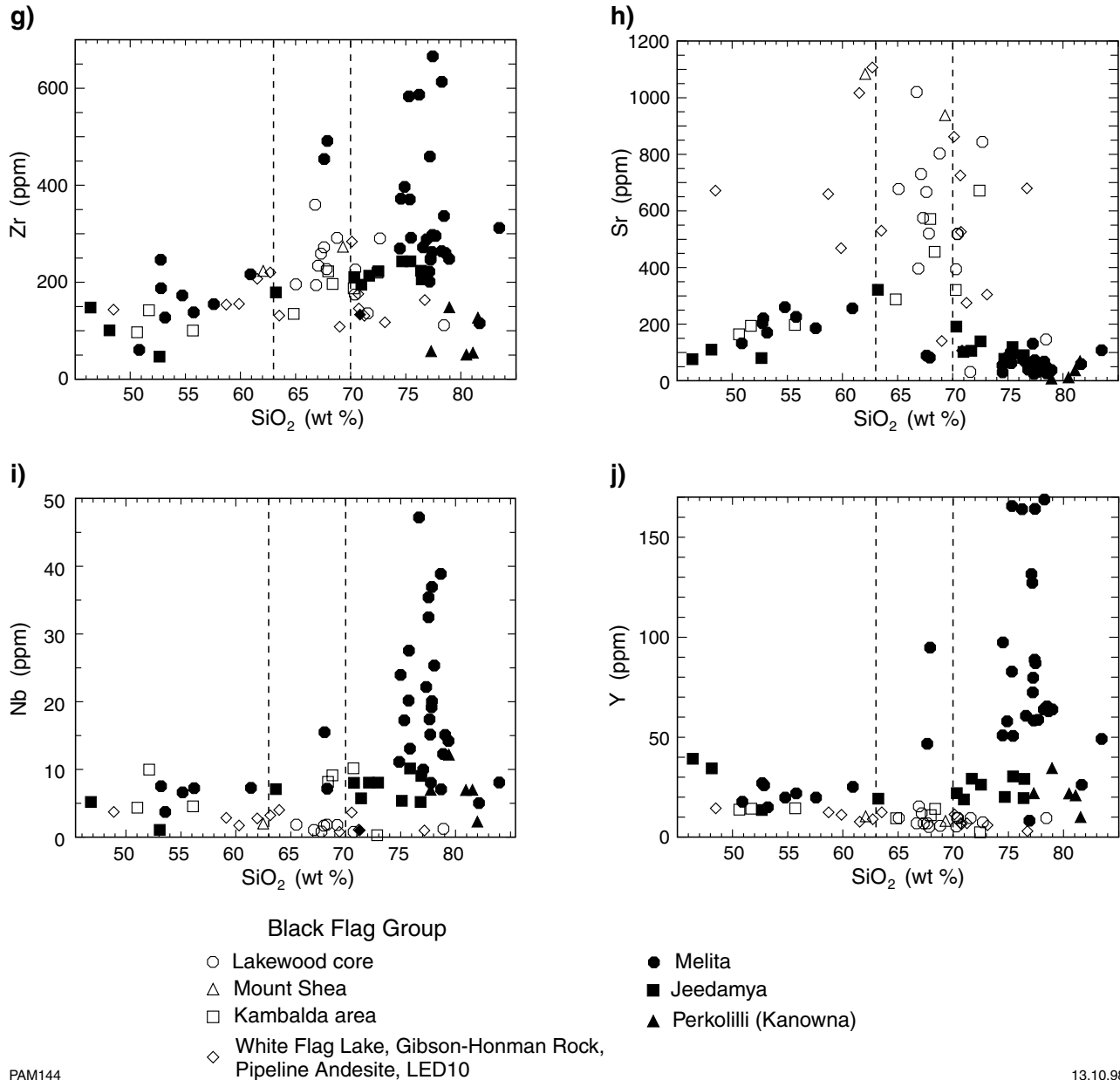


Figure 37. This page and opposite: Harker variation diagrams for mafic, intermediate, and felsic rocks from Melita, Jeedamya, Kanowna, and the Black Flag Group. Data are normalized to 100% on an anhydrous basis (see Appendix)



PAM144

13.10.98

Black Flag Group andesites from the White Flag Lake and Mount Shea areas (Fig. 38c) have similar LREE contents to Black Flag Group dacite and rhyolite. They also lack Eu anomalies, and the REE patterns flatten from Dy to Lu. However, the andesites are more enriched in HREE (8 to 10 times chondrite) compared to dacites and rhyolites (mostly 4 to 8 times chondrite). In contrast, Black Flag Group basalt and andesite (GSWA 114481) from Kalgoorlie drillcore and the Kambalda area have flatter and more variable REE patterns. Three of the four Black Flag Group basalts are weakly LREE enriched ( $(La/Yb)_{CN} = 3$  to 6) with La at about 30 times chondrite levels. The remaining sample (GSWA 114479; drillcore, Foster) is more LREE enriched ( $La_{CN}$  about 50), but has similar HREE contents to other basalts. Sample GSWA 114483 has a pronounced positive Eu anomaly.

Jeedamyia and Melita rhyolites have fundamentally similar REE patterns (Fig. 38d), but different REE

contents. Rhyolites from Melita (GSWA 110234 and 110240) have higher REE contents than rhyolites from Jeedamyia, particularly in terms of HREE. Melita REE patterns are slightly flatter than those from Jeedamyia ( $(La/Yb)_{CN}$  of about 4 compared to Jeedamyia  $(La/Yb)_{CN}$  of about 7–8), but all samples have well developed negative Eu anomalies ( $Eu/Eu^* = 0.4$  to 0.7). Rhyolite from Perkolilli (GSWA 114149) has similar LREE and middle REE contents to samples from Jeedamyia, but is HREE depleted ( $(La/Yb)_{CN} = 18$ ) and has a weaker negative Eu anomaly.

REE patterns for mafic rocks from Melita and Jeedamyia are highly variable (Fig. 38e), and are broadly comparable to mafic volcanic rocks of the Black Flag Group. Samples GSWA 110236 and 110238 from Melita are weakly LREE enriched, with  $La_{CN}$  of about 30. The other Melita sample (GSWA 110243) has a higher LREE content ( $La_{CN}$  of about 100). Mafic samples GSWA

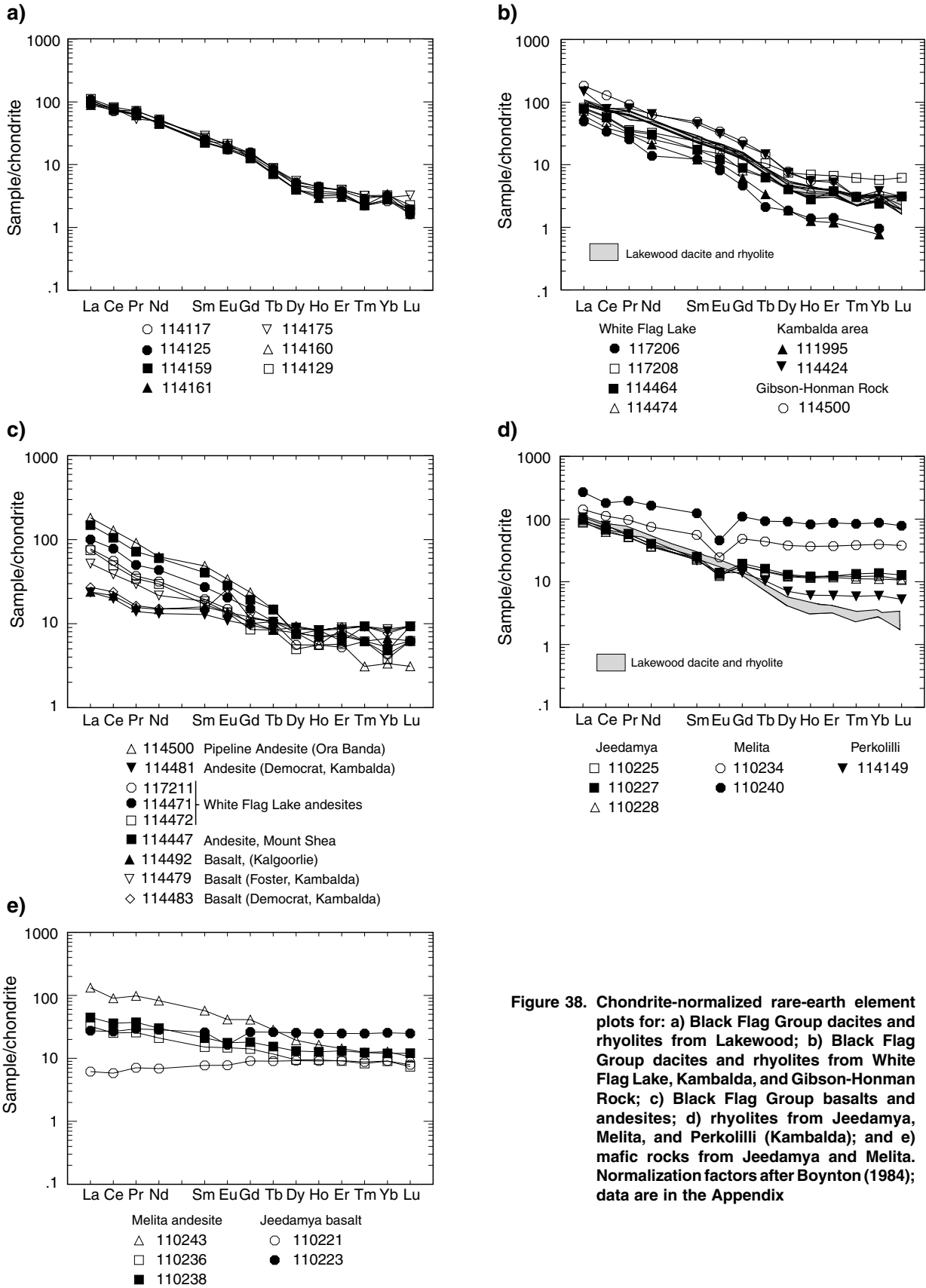


**Figure 38. Chondrite-normalized rare-earth element plots for: a) Black Flag Group dacites and rhyolites from Lakewood; b) Black Flag Group dacites and rhyolites from White Flag Lake, Kambalda, and Gibson-Honman Rock; c) Black Flag Group basalts and andesites; d) rhyolites from Jeedamya, Melita, and Perkolilli (Kambalda); and e) mafic rocks from Jeedamya and Melita. Normalization factors after Boynton (1984); data are in the Appendix**

110221 and GSWA 110223 from Jeedamya have different REE contents, but similar flat to slightly LREE depleted patterns. Sample GSWA 110223 has a negative Eu anomaly ( $\text{Eu}/\text{Eu}^* = 0.65$ ).

## Discussion

Dacites and rhyolites of the Black Flag Group and andesites from the White Flag Lake and Mount Shea areas have similar chemical characteristics. They have common trends on  $\text{V}-\text{SiO}_2$ ,  $\text{CaO}-\text{SiO}_2$ , and  $\text{TiO}_2-\text{SiO}_2$  plots (Figs. 37f,b,c), but for some elements there is slight decoupling between andesite and dacite. All these samples have similar, steep REE patterns with no Eu anomalies, but andesites are more HREE enriched than dacites and rhyolites. In contrast, basalts from the Black Flag Group and one andesite in drillcore from Kalgoorlie and Kambalda do not plot on the same trends as Black Flag Group andesites, dacites, and rhyolites. Furthermore, three of these four mafic rocks have flat REE patterns. The remaining sample (GSWA 114179) has similar HREE contents to other basalts, but is more LREE enriched.

Basalts show a wide range in concentrations of some elements (e.g. Mg and Cr), and some incompatible elements (e.g. Cr) are lower in some basalts than in andesites. The differences in chemistry of mafic rocks in drillcore from Kalgoorlie and Kambalda, and intermediate rocks from elsewhere in the Black Flag Group are also shown in terms of  $\text{Zr}/\text{Nb}$  versus  $\text{SiO}_2$  (Fig. 39). For such mafic and intermediate rocks the bulk distribution coefficients ( $D$ ) for Zr and Nb will be low and similar for fractionating minerals (Peck and Smith, 1989), so the  $\text{Zr}/\text{Nb}$  ratio should be unchanged regardless of the degree of fractionation or partial melting. Black Flag Group andesites from White Flag Lake and Mount Shea have  $\text{Zr}/\text{Nb} > 50$ , whereas Black Flag Group basalts in

drillcore have  $\text{Zr}/\text{Nb} < 50$ , similar to mafic volcanic rocks from lower in the greenstone succession (Morris et al., 1991).

On the basis of chemistry and mineralogy, volcanic rocks from the Black Flag Group can be divided into two groups. One group consists of andesites, dacites, and rhyolites from Lakewood, Mount Shea, White Flag Lake, Pipeline Andesite (Ora Banda), some samples from the Kambalda region, and drillcore from Loves Find. The other group consists of basalts in drillcore from Kalgoorlie and the remaining samples from the Kambalda district.

Felsic volcanic rocks from Melita and Jeedamya have similar trends (but commonly plot at higher  $\text{SiO}_2$  levels) to felsic rocks from the Black Flag Group for several major and trace elements, such as  $\text{TiO}_2$ ,  $\text{MgO}$ ,  $\text{Al}_2\text{O}_3$ ,  $\text{CaO}$ ,  $\text{Cr}$ , and  $\text{V}$ . However, felsic volcanic rocks from Melita have higher Y, Nb, and Zr, but lower Sr than felsic volcanic rocks with similar  $\text{SiO}_2$  from the Black Flag Group. Felsic volcanic rocks from Melita, Jeedamya, and Perkolilli have fundamentally similar REE patterns. Although LREE concentrations are similar, rhyolite samples from Melita have flat patterns with pronounced negative Eu anomalies. Samples from Jeedamya and Perkolilli are more HREE depleted than those from Melita, and have weaker negative Eu anomalies.

Selected major, trace, and REE data for felsic volcanic rocks with similar  $\text{SiO}_2$  from Melita and Jeedamya are shown on a MORB-normalized spider diagram (Fig. 40). This figure shows that Melita and Jeedamya rhyolites are depleted in Sr, P, Ti, and Cr, and enriched in Th, Ta, Nb, Y, and Yb compared to SE drillcore from the Black Flag Group. Some of these differences could be attributed to fractionation of minerals with high mineral/melt partition coefficients for some elements (e.g. Cr and Ti by separation of iron oxides; P by separation of apatite; and zircon separation accounting for HREE and Zr depletions). In the case of the Perkolilli rhyolites, Zr, Nb and HREE depletion by removal of such accessory phases is consistent with the presence of zircon in thin section. However, as felsic volcanic rocks with similar  $\text{SiO}_2$  from Melita, Jeedamya, and the Black Flag Group have fundamentally different REE patterns and divergent contents of incompatible elements like Zr and Nb, it is unlikely that they are related by either fractional crystallization or contamination of a common magma, or derived by partial melting of the same source.

Mafic and intermediate volcanic rocks at Melita and Jeedamya show a wide variation in chemistry over a narrow  $\text{SiO}_2$  range. This chemical diversity (shown in the scatter on bivariate plots), the diversity in REE patterns, depletion in some compatible elements relative to rocks with higher  $\text{SiO}_2$ , and the few volcanic rocks of intermediate composition mean that mafic rocks are unlikely to be unfractionated precursors to more-felsic volcanic rocks.

As andesites from White Flag Lake and Mount Shea have chemical characteristics similar to dacites and rhyolites from the Black Flag Group, they could be either parental to dacites and rhyolites, or andesites, dacites, and

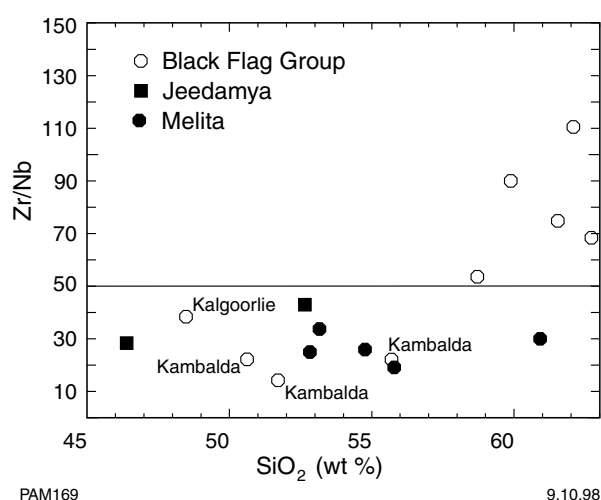


**Figure 39.**  $\text{Zr}/\text{Nb}$  versus  $\text{SiO}_2$  (wt%) for mafic and intermediate rocks from Melita, Jeedamya, and the Black Flag Group. The line at  $\text{Zr}/\text{Nb} = 50$  roughly divides Black Flag Group andesites ( $>50$ ) from other mafic rocks ( $<50$ )

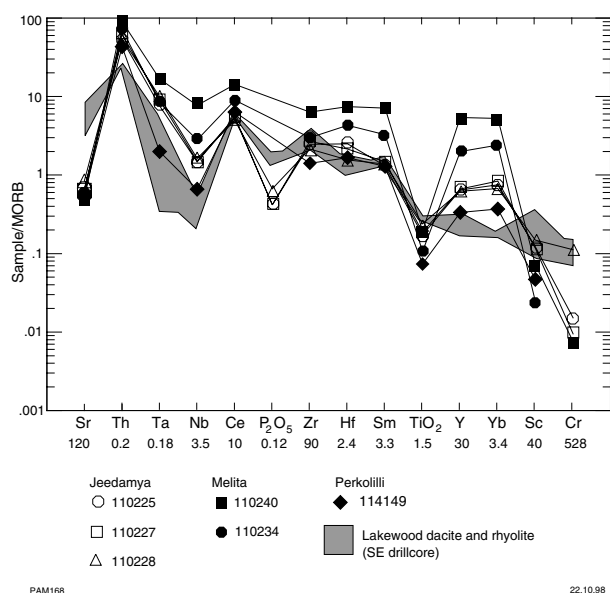


**Figure 40. MORB-normalized spider diagram for felsic volcanic rocks from Melita and Jeedamyia. Values for the SE drillcore (Black Flag Group at Lakewood) are shown for comparison. Normalizing values after Sun and McDonough (1989)**

rhyolites could be derived from the same source, which was melted under different conditions. This is further examined in **Petrogenesis**.

## Petrogenesis

### Derivation of Black Flag Group dacites and rhyolites by fractional crystallization of andesite

In order to investigate whether dacites and rhyolites of the Black Flag Group result from the fractional crystallization of andesite, two independent modelling approaches have been used. The first determines the amount and type of likely fractionating phases between parental andesite and daughter dacite by least-squares approximation using major element oxides (Bryan et al., 1969; Morris, 1984). The second approach involves estimating the concentration of selected trace elements and REE in dacite by Rayleigh fractionation modelling using likely types and proportions of fractionating phases (determined from thin section), and published mineral/melt distribution coefficients.

For both approaches, average Black Flag Group andesite and average Lakewood dacite have been used as the parent and daughter compositions respectively. Based on thin section examination of andesites, the most likely fractionating phases are amphibole and feldspar. As compositions of these phases in andesite have not been determined, published analyses (Cox et al., 1979) have been used (Table 5).

**Table 5. Mineral compositions used in least-squares modelling of fractional crystallization of the Black Flag Group**

	<i>Amphibole</i>	<i>Plagioclase (1)</i>	<i>Plagioclase (2)</i>	<i>Alkali feldspar</i>
SiO <sub>2</sub>	45.73	63.77	49.28	67.2
TiO <sub>2</sub>	1.48	—	—	—
Al <sub>2</sub> O <sub>3</sub>	11.39	22.55	32.28	18.33
FeO <sup>(a)</sup>	16.43	0.3	0.24	0.83
MnO	0.32	—	—	—
MgO	10.58	0.25	—	—
CaO	12.31	3.24	15.45	0.15
Na <sub>2</sub> O	0.99	9.84	2.58	6.44
K <sub>2</sub> O	0.77	0.05	0.17	7.04

**NOTES:** (a) All Fe as FeO

**SOURCE:** Cox et al. (1979)

The results of five least-squares models are summarized in Table 6. The difference between the observed and estimated liquid compositions is shown by the sum of squared residuals, or  $\Sigma R^2$ . Despite using various mineral combinations (including two feldspar compositions), in all cases  $\Sigma R^2$  is more than 3, which is unacceptably high. Thus, least-squares modelling using observed phenocryst minerals is not consistent with fractionation of andesite to produce dacite. The acceptability of models is in part determined by the agreement of Na<sub>2</sub>O and K<sub>2</sub>O, and both oxides are important in amphibole and feldspar. However, as discussed previously, it is possible that both Na<sub>2</sub>O and K<sub>2</sub>O were mobilized during alteration.

The second modelling approach (Rayleigh fractionation) avoids the problem of Na<sub>2</sub>O and K<sub>2</sub>O mobility. In this approach, the concentrations of several trace elements and REE in dacite are estimated by removal of amphibole and feldspar in the proportions that they are present in andesite (about 60:40). The amount of fractionation is estimated by assuming that the Yb depletion of dacite relative to andesite is controlled by fractionation. As mineral/melt distribution coefficients for Yb/amphibole (8.4) is greater than that for Yb/plagioclase (0.049; Table 7), the HREE depletion of dacites is largely controlled by the separation of amphibole. Using this

**Table 6. Summary of least-squares modelling results for fractional crystallization of the Black Flag Group**

<i>Model</i>	<i>Amphibole</i>	<i>Plagioclase</i>	<i>Alkali feldspar</i>	$\Sigma R^2$
1	x			4.842
2 <sup>#(a)</sup>		x		34.263
3 <sup>(a)</sup>	x	x		3.418
4 <sup>(b)</sup>	x	x		4.391
5 <sup>#</sup>	x		x	4.701

**NOTES:**  $\Sigma R^2$  = sum of squared residuals  
 #: Model has negative mineral component (i.e. phase added rather than lost)  
 (a) Model uses plagioclase (1)  
 (b) Model uses plagioclase (2)  
 x: Phase is used in model

**Table 7. Mineral/melt distribution coefficients for fractionation modelling of the Black Flag Group**

Element	Plagioclase	Amphibole
Rb	0.04	0.014
Ba	0.2	0.4
K	0.2	1
Th	0.05	0.05
Nb	0.01	0.8
La	0.4	0.74
Ce	0.27	1.52
Sr	4.4	0.022
Nd	0.21	4.26
Sm	0.13	7.77
Zr	0.1	0.45
Ti	0.04	1.5
Yb	0.049	8.4
Y	0.055	12

SOURCES: Cox et al. (1979)  
Le Marchand et al. (1987)  
Martin (1987)  
Peck and Smith (1989)

approach, 10% crystallization is required. Figure 41 summarizes the results of modelling, with concentrations normalized to average Black Flag Group andesite. It is clear from this diagram that although fractionation can explain the Th, La, Ce, Ti, Y, and Yb contents of dacite, it is inconsistent with the concentrations of the remaining elements, especially Nb and the other REEs.

Several other lines of evidence do not favour fractional crystallization. Firstly, andesite is slightly decoupled from dacite on some bivariate plots, and secondly, andesite is volumetrically less abundant than dacite and rhyolite. Taken in conjunction with modelling results, it is unlikely that the chemistry of dacites from the Black Flag Group can be accounted for by fractionation of andesite magma using observed liquidus phases.

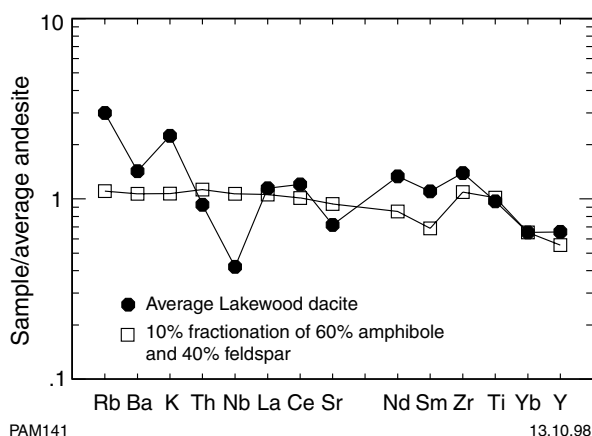


**Figure 41. Average dacite (SE drillcore, Lakewood) and results of andesite fractionation (10% fractionation of 60% amphibole and 40% plagioclase) normalized to average Black Flag Group andesite**

## Derivation of Black Flag Group andesite and dacite by partial melting of the same source

Although fractional crystallization is discounted as the controlling mechanism for the transition from intermediate to felsic volcanic rocks for the Black Flag Group, the common chemical characteristics of these rocks and their close spatial proximity argue for some genetic relationship. One possibility is that they were derived from the same source, which melted under different conditions. As there are fundamental differences in the chemistry of felsic rocks with similar  $\text{SiO}_2$  contents from the Black Flag Group, and Melita and Jeedamyia, felsic rocks of these two magma associations could not have been derived by partial melting of the same source.

Some chemical characteristics of dacites from the Black Flag Group and rhyolites from Melita and Jeedamyia are summarized in Table 8. Also shown are data for Archaean high-Al trondhjemite-tonalite-dacite (TTD) from Drummond and Defant (1990). Black Flag Group andesites (from the White Flag Lake and Mount Shea areas), dacites, and rhyolites strongly resemble high-Al TTD (e.g. high Sr, low Y — hence high Sr/Y, steep REE patterns depleted in HREE, and REE patterns with no negative Eu anomaly or a small positive anomaly). Defant and Drummond (1990) introduced the term 'adakite' to describe Cenozoic arc magmas with high-Al TTD chemistry, and separated them from 'normal' basalt andesite-dacite-rhyolite associations in terms of Sr/Y versus Y. On Figure 42 intermediate and felsic volcanic rocks from the Black Flag Group plot at high Sr/Y and low Y in the high-Al TTD field, separate from Melita and Jeedamyia rhyolites, which plot in the 'normal' (i.e. island arc) field.

## A review of relevant petrogenetic models

Defant et al. (1991) reviewed three possible mechanisms for the origin of high-Al TTD:

- direct partial melting of the mantle;
- fractional crystallization of basalt;
- partial melting of altered mid-ocean ridge basalt (MORB) transformed to amphibole-quartz eclogite.

Direct partial melting of the mantle usually results in low-volume partial melts, such as boninites and basaltic andesites, that are not as siliceous as TTD. Fractionation of these melts results in high Y and low Sr/Y, which is different to high-Al TTD.

Fractional crystallization is an important process in generating arc volcanic rocks (e.g. in the northeastern Japan arc; Sakuyama and Nesbitt, 1986), and can account for the basalt-andesite-dacite-rhyolite continuum (i.e. extrusive equivalent of gabbro-diorite-tonalite-trondhjemite). However, in many TTD occurrences, intermediate rocks are either rare or absent. Furthermore,

**Table 8. Selected characteristics of high-Al trondhjemite–tonalite–dacite, average SE dacite (from Lakewood), Jeedamyia rhyolite, and Melita rhyolite**

	<i>High-Al TTD</i> <sup>(a)</sup>	<i>SE dacite</i> (n=7)	<i>Jeedamyia</i> <i>rhyolite</i>	<i>Melita</i> <i>rhyolite</i>
Al <sub>2</sub> O <sub>3</sub> (wt%)	≥15	16	12.5	11.4
Sr (ppm)	300 to >2000	635	86	58
Y (ppm)	<15	6	19	90
LREE	enriched	enriched	enriched	enriched
HREE	depleted	depleted	not depleted	not depleted
Eu anomaly	none or positive	none	negative	negative
K <sub>2</sub> O/Na <sub>2</sub> O	commonly <1	0.55	1.1	2.5

**NOTES:** TTD: trondhjemite–tonalite–dacite  
SE: Southend drilling  
n: number of samples  
LREE: light rare-earth elements  
HREE: heavy rare-earth elements

**SOURCE:** (a) Drummond and Defant (1990)

according to Spulber and Rutherford (1983), up to 90% fractionation of tholeiitic magma would be required to produce a trondhjemite residual. Such extensive fractional crystallization is likely to involve plagioclase at some stage, which is inconsistent with the high Sr contents of TTD and the lack of a negative Eu anomaly. Assimilation of crustal material by a mafic melt followed by fractional crystallization (i.e. assimilation/fractional crystallization or AFC; DePaolo, 1981) would result in TTD, but this process is limited by the amount of heat available for efficient assimilation, and would

probably also promote fractionation of feldspar at some stage.

Defant and Drummond (1990) and Defant et al. (1991) have argued that the trace element characteristics of adakites can be produced by partial melting of a mid-ocean ridge basalt (MORB) with 15% sediment added (to simulate melting of the downgoing plate), leaving a hornblende eclogite residual. The retention of hornblende and garnet in the source results in a magma with low HREE, Y (hence high Sr/Y and (La/Yb)<sub>CN</sub>), Nb, and Ti, typical of high-Al TTD and adakites. As plagioclase is consumed during melting, the magma has high Sr and no negative Eu anomaly. Although there is general agreement that a mafic protolith is the most likely source for adakites (Wyllie et al., 1995), there are some problems. Sen and Dunn (1994), for example, pointed out that the high Sr contents of adakites are not consistent with the melting of altered MORB with about 200 ppm Sr.

Martin (1987) summarized chemical data for Archaean and post-Archaean granitic rocks, and found that most Archaean granitoids have trondhjemite–tonalite–granodiorite (TTG, the intrusive equivalents of TTD) characteristics, such as K<sub>2</sub>O/Na<sub>2</sub>O < 0.5, high (La/Yb)<sub>CN</sub>, and low (Yb)<sub>CN</sub>. Post-Archaean granitoids have higher K<sub>2</sub>O/Na<sub>2</sub>O, flatter REE patterns, and higher HREE contents. Martin (1987) suggested a two-stage process to explain this, involving firstly, the formation of mafic crust by partial melting of the mantle and secondly, transformation of this crust into garnet-bearing amphibolite, which is then melted. The retention of garnet and amphibole in the source produces low-Yb magmas (Archaean TTG), whereas the high Yb of post-Archaean granitoids reflects the absence of garnet or hornblende in the source.

As adakites are usually found at convergent margins where young (hence hot) crust is being subducted at a shallow angle (Defant and Drummond, 1990; Drummond and Defant, 1990; Morris, 1995) direct observations of the alteration, metamorphism, and melting of the downgoing plate can seldom be made. One exception is amphibolite-facies schists of Catalina Island, southern

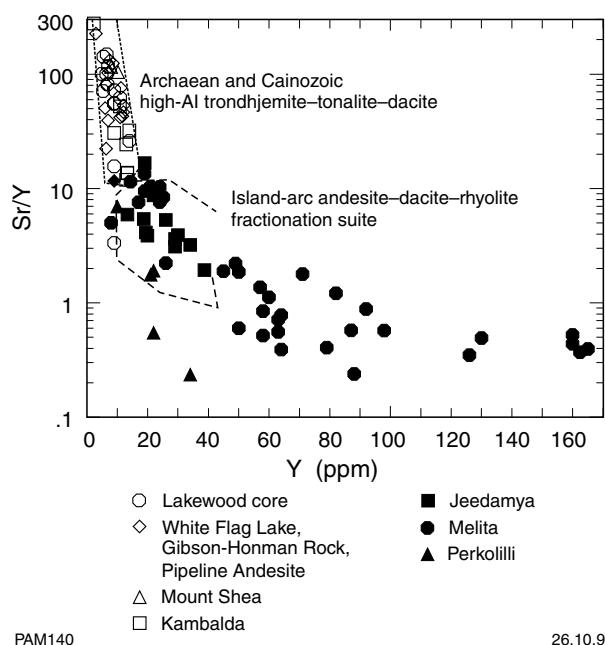


**Figure 42. Sr/Y versus Y (ppm) for felsic and intermediate rocks of the Black Flag Group and felsic rocks from Melita, Jeedamyia, and Kanowna. The fields of Archaean and Cenozoic high-Al TTD and island-arc andesite–dacite–rhyolite after Drummond and Defant (1990)**

California, which are the metamorphosed remnants of a subduction complex (Sorensen, 1988; Sorensen and Barton, 1987). These rocks are variably amphibolitized, ranging from nearly anhydrous garnet–clinopyroxene–hornblende eclogites to hydrated garnet–hornblende (–zoisite) amphibolites. Partial melts of these schists are preserved as leucocratic zones and pegmatite dykes of trondhjemitic composition. Sorensen (1988) and Sorensen and Barton (1987) interpreted the metasomatism of these rocks and the melt phases as representing fluid and melt transferred from a subducting slab into the overlying mantle wedge. The residual mineralogy is garnet–hornblende(–clinopyroxene–plagioclase–quartz). Based on mineral assemblages, metamorphic reactions, garnet–clinopyroxene geothermometry, fluid inclusion studies, and melting relationships in granite systems, Sorensen and Barton (1987) and Sorensen (1988) maintained that metamorphism and melting occurred at pressures of 8 to 11 kbar and temperatures of 640 to 750°C, with high water activity.

There have been several studies of experimental melting of mafic compositions. Beard and Lofgren (1989) melted arc basalts and andesites metamorphosed to greenschist and amphibolite facies at temperatures between 850 and 1000°C and pressures between 1 and 3 kbar. Under closed-system conditions (i.e. dehydration melting, with only structurally bound water available), the resulting felsic liquid was accompanied by 40 to 60 volume % plagioclase-rich restite, with a composition of plagioclase–clinopyroxene–orthopyroxene–magnetite(–ilmenite–apatite) at both 1 and 3 kbar pressure. For open-system melting (i.e. added water), the felsic melt was accompanied by amphibole-bearing restite with a composition of amphibole–clinopyroxene–magnetite (–plagioclase–ilmenite–apatite). Modal plagioclase reached a maximum of 50 volume % and decreased with increasing melt proportion and temperature. Regardless of the starting composition (i.e. andesite or basalt), the composition of the resulting liquid was largely determined by the amount of water available. At 3 kbar, water-saturated melts were enriched in Al and depleted in Fe and K with respect to closed-system melts. One kilobar water-saturated melts were intermediate in composition in comparison to closed-system and 3 kbar water-saturated melts. All closed-system melts were of similar composition, regardless of starting composition.

Rushmer (1991) described dehydration melting of amphibolite at 8 kbar pressure, and argued that the amount of melting is related to the quartz:feldspar ratio and the availability of volatiles. Rapp et al. (1991) examined the vapour-absent melting of four amphibolite compositions at pressures of 8, 16, 22, and 32 kbar. Amphibole and plagioclase were residual phases at 8 kbar, but garnet was not a residual phase. Garnet and amphibole were residual at 16 kbar. Partial melting ranged from 10 to 30%, but at low degrees of partial melting the liquids were granitic (versus trondhjemitic). Rapp et al. (1991) used the results of experimental work on amphibolite melting (i.e. modal abundances and type of residual phases and the degree of melting) and published mineral/melt distribution coefficients to estimate the REE patterns of liquids. In experimental runs with residual garnet, the REE patterns

were steep (i.e. HREE depleted), but at low degrees of partial melting where garnet was not a residual phase, the granitic liquids had flat REE patterns.

## Petrogenetic models for felsic volcanic rocks in the Eastern Goldfields region

Taking into account the chemistry of andesites, dacites, and rhyolites of the Black Flag Group and the results of experimental work on producing compositionally similar rocks, there is strong evidence to suggest that these rocks resulted from melting of a mafic protolith. Although in many documented cases of modern adakites the amphibolite source is taken as the subducting plate (Defant and Drummond, 1990; Drummond and Defant, 1990; Morris, 1995), in areas of thickened continental crust, melting of mafic material at the base of the crust has been proposed (e.g. in Chile by Atherton and Petford, 1993). Wyllie et al. (1995) argued that on experimental grounds, tonalite is a possible parent material for high-Al TTD.

Rhyolite from Melita has higher Y and HREE than Black Flag Group rocks, which is inconsistent with residual garnet and amphibole. In addition, the high  $K_2O/Na_2O$  ratios of felsic rocks in the Leonora region indicate melting of a more felsic protolith, and as felsic rocks from Melita, Jeedamyia, and Perkolilli have low  $Al_2O_3$  and Sr, and negative Eu anomalies, plagioclase was probably a residual phase. Possible source compositions would be lower crustal material, such as granodiorite or tonalite. Experimental melting of lower crustal compositions (Piwinski, 1968, 1973; Huang and Wyllie, 1986; Rutter and Wyllie, 1988; Skjerlie and Johnson, 1992) under hydrous conditions has shown that plagioclase enters the melt at an early stage, while garnet and hornblende are residual. However, under anhydrous conditions, garnet and hornblende are consumed early and plagioclase is residual, producing liquids with elevated HREE and Y, low Sr, and negative Eu anomalies.

Possible source compositions for the Black Flag Group and felsic volcanic rocks from Melita and Jeedamyia have been evaluated by computer modelling of partial melting. Variables used in the modelling have been constrained by observations from natural and experimental studies discussed above. Modelling involved estimating the type and proportion of residual mineral phases and the degree of partial melting by least-squares approximation to produce average Black Flag Group andesite, average Lakewood dacite, and average Jeedamyia rhyodacite. The latter is taken as representative of the felsic volcanic rocks from the Leonora district. In this study, acceptable models are those that firstly, use realistic types and proportions of residual phases, and secondly, have  $\Sigma R^2$  less than 1 (where  $\Sigma R^2$  is the sum of squared deviations between observed and calculated parent composition). These models have been further tested by estimating the REE content of the daughter liquid and comparing it with observed values (Shaw, 1970). Source compositions evaluated were a tholeiitic basalt (Martin, 1987), an I-type granite (Chappell and White, 1992), and a tonalite

Table 9. Compositions of daughter liquids (analyses 1–3), parent liquids (analyses 4–6), and minerals used in modelling of partial melting

	Daughter liquids			Parent liquids			Minerals								
	1	2	3	4	5	6	7	8	9	10	11	12	13	14	15
	<b>Percentage</b>														
SiO <sub>2</sub>	61.1	68.13	74.09	51.39	69.13	59.62	46.46	54.69	40.04	–	50.94	58.07	–	37.93	–
TiO <sub>2</sub>	0.48	0.44	0.3	1.32	0.46	0.8	0.91	–	0.08	50	0.41	0.04	–	3.2	–
Al <sub>2</sub> O <sub>3</sub>	15.54	16.69	12.66	14.63	14.73	18.47	7.88	28.58	21.93	–	2.02	0.95	–	14.9	–
MgO*	11.28	4.67	2.76	19.65	5.63	8.43	29.84	0.41	29.34	50	22.63	40.71	1.82	35.22	–
CaO	6.09	3.15	2.42	10.16	3.84	6	12.7	10.4	8.62	–	23.8	0.23	55.09	0.17	–
Na <sub>2</sub> O	4.21	4.34	3.12	2.48	3	3.86	1.59	5.67	–	–	0.12	–	–	0.15	–
K <sub>2</sub> O	1.13	2.4	4.59	0.37	3.1	2.22	0.61	0.25	–	–	0.08	–	–	8.42	–
P <sub>2</sub> O <sub>5</sub>	0.17	0.18	0.06	–	0.11	0.3	–	–	–	–	–	–	43.09	–	–
	<b>Parts per million</b>														
La	26.17	29.54	28.17	8.99	–	–	–	–	–	–	–	–	–	–	0.31
Ce	49.43	58.73	52.7	21.82	–	–	–	–	–	–	–	–	–	–	0.808
Nd	20.97	27.52	22.42	13.8	–	–	–	–	–	–	–	–	–	–	0.6
Sm	4.13	4.49	4.58	3.51	–	–	–	–	–	–	–	–	–	–	0.195
Eu	1.20	1.35	0.94	1.25	–	–	–	–	–	–	–	–	–	–	0.0735
Gd	2.90	3.45	4.75	4.01	–	–	–	–	–	–	–	–	–	–	0.259
Tb	0.47	0.36	0.71	0.66	–	–	–	–	–	–	–	–	–	–	0.0474
Dy	1.97	1.38	4.00	4.03	–	–	–	–	–	–	–	–	–	–	0.322
Er	1.47	0.71	2.53	2.27	–	–	–	–	–	–	–	–	–	–	0.21
Yb	0.93	0.6	2.57	2.16	–	–	–	–	–	–	–	–	–	–	0.209

**NOTES:**

1. Average of three Black Flag Group andesites
  2. Average of six Black Flag Group dacites from SE drillcore
  3. Average of three Jeedamya rhyolites
  4. Tholeiitic basalt (Martin, 1987)
  5. Average I-type granite (Chappell and White, 1992)
- MgO\* = FeO + Fe<sub>2</sub>O<sub>3</sub> + MnO + MgO (Martin, 1987)

6. Tonalite 101 (Huang and Wyllie, 1986)
7. Hornblende
8. Plagioclase
9. Garnet
10. Ilmenite

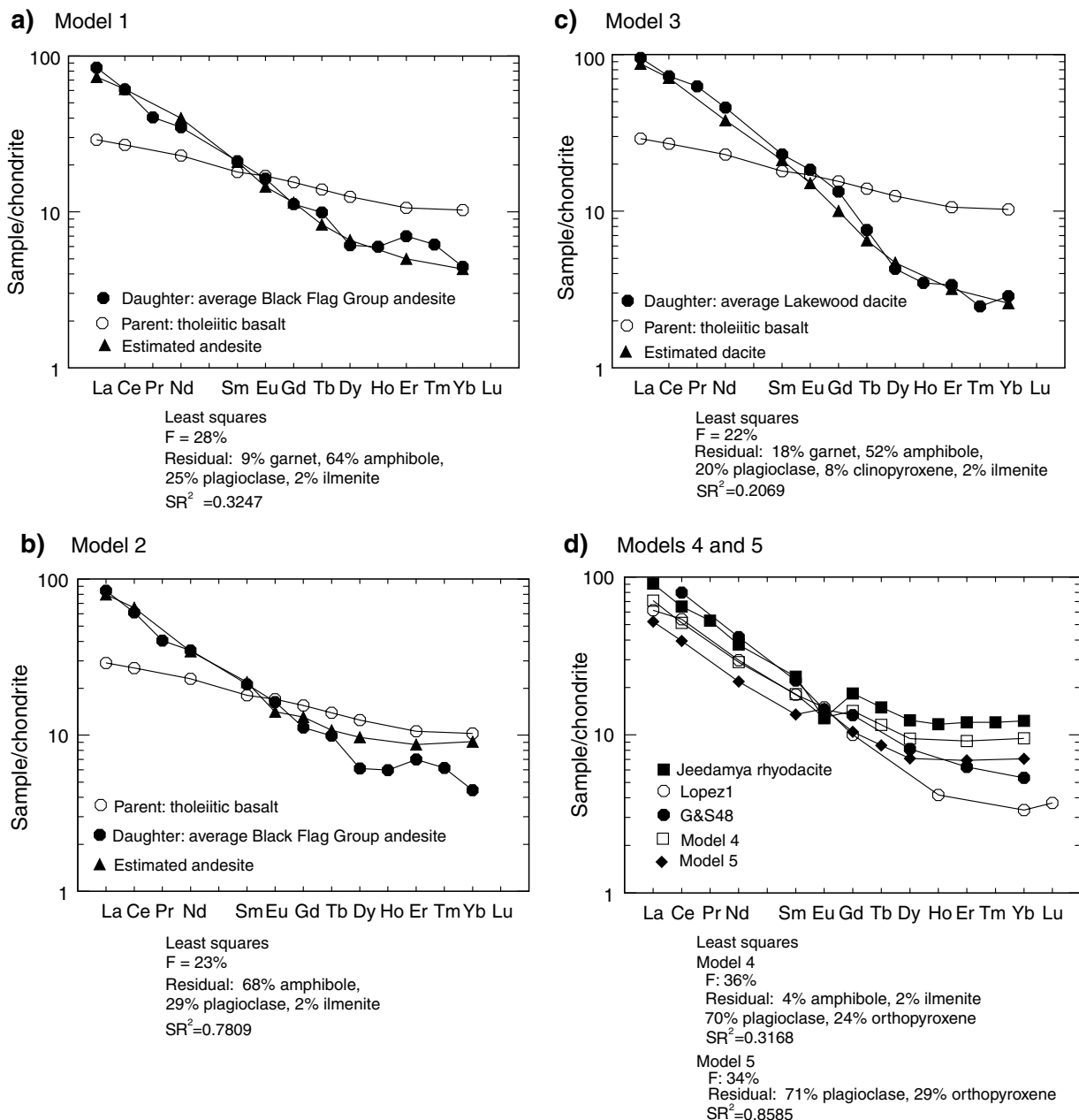
11. Clinopyroxene
12. Orthopyroxene (7–12 from Martin, 1987)
13. Apatite (Deer et al., 1966)
14. Biotite (Cox et al., 1979)
15. Chondrite-normalization factors from Boynton (1984)

(Piwinski, 1968; Huang and Wyllie, 1986). These source compositions, daughter liquid compositions, residual mineral compositions, and mineral/melt distribution coefficients are summarized in Table 9.

Model parameters and results for the Black Flag Group are shown in Figure 43. Two least-squares models for melting of a tholeiitic basalt to produce a Black Flag Group andesite have acceptably low  $\Sigma R^2$  (Fig. 43, models 1 and 2). Both models involve similar degrees of partial melting (28 and 23%), but model 1 has residual garnet in addition to hornblende and plagioclase. Model 1 gives excellent agreement between observed and

estimated REE concentrations, but the calculated HREE concentrations for model 2 are higher than those observed. Thus, residual garnet is required to account for the HREE depletion of Black Flag Group andesites, and can also account for the depletion in Y.

One least-squares model has acceptably low  $\Sigma R^2$  (0.2069) for production of Black Flag Group dacite by melting of tholeiitic basalt (Fig. 43, model 3). The model involves 22% partial melting with a residual mineralogy of hornblende, garnet, plagioclase, clinopyroxene, and ilmenite. There is excellent agreement between observed and estimated REE abundances. As there is more residual



PAM138

14.10.98

**Figure 43. Results of computer modelling for derivation of Black Flag Group andesite from tholeiitic basalt (Models 1 and 2) and SE dacite from tholeiitic basalt (Model 3). Models 4 and 5 show results of partial melting of tonalite and I-type granite respectively**

garnet in this model (18%) compared to model 1 (9%; Fig. 43), the resulting magma is correspondingly more depleted in HREE.

In all these models, the type and proportion of residual phases and degrees of partial melting are consistent with results of experimental studies on melting of amphibolite to produce high-Al TTD (Rapp et al., 1991), which suggest between 10 and 40% partial melting.

One other possible origin for Black Flag Group andesites is melting of a metasomatized mantle wedge, evidence for which comes from the relatively high compatible-element contents of Black Flag Group andesites. Compared with andesites with similar SiO<sub>2</sub> contents from elsewhere in the Eastern Goldfields region (e.g. Welcome Well and Bore Well: Hallberg, 1986; and Marda: Condie, 1982) and from most destructive plate margins (Condie, 1982; Gill, 1981), Black Flag Group andesites have high Ni (average of six Black Flag Group andesites = 153 ppm), Cr (367 ppm) and magnesium number (100Mg/(Mg + Fe<sup>2+</sup>) = 0.63). These values are in the range of primary (i.e. unfractionated) basaltic magmas according to Frey et al. (1978). Andesites with similar high incompatible-element contents that also have steep REE patterns (i.e. enriched in LREE, but depleted in HREE), high Sr, and low Y contents have been reported from Baja (California), Chile, and the Aleutians by Saunders et al. (1987) and Rogers and Saunders (1989). In all cases these rocks are erupted following ridge–trench collision, or where the rate of subduction has slowed. The chemistry of these andesites has been attributed to melting of the mantle wedge (imparting the high magnesium number, Ni, and Cr to the magma), which has been fluxed by fluids derived from the subducting plate (imparting the elevated large ion lithophile element and LREE signatures). Such a model has clear implications for the tectonic setting of the Black

Flag Group, and as discussed below, is consistent with the preferred model for the origin of dacites and rhyolites from the Black Flag Group.

In a summary of pertinent experimental work, Wyllie et al. (1995) showed that the weight of evidence clearly favoured basalt or its metamorphosed equivalent as the most likely protolith for TTD. However, they also noted that tonalite was a potential source material. The least-squares approach has been applied to the generation of Black Flag Group andesite and dacite using a tonalite composition (Table 10). However, despite using various combinations of residual phases, no least-squares model resulted in acceptably low  $\Sigma R^2$  values. In most cases, the greatest discrepancy between observed and estimated composition was for K<sub>2</sub>O. Furthermore, models with the lowest  $\Sigma R^2$  required high degrees of melting, in the order of 60%. In discussions of experimental work on adakite genesis, both Rapp et al. (1991) and Sen and Dunn (1994) noted that the K<sub>2</sub>O content of the resulting liquid is strongly influenced by the K<sub>2</sub>O content of the starting material. Thus, a potassic source material, such as tonalite, is not appropriate for the Black Flag Group, where magmas have more Na<sub>2</sub>O than K<sub>2</sub>O.

The overall chemical similarity of felsic volcanic rocks from Melita, Jeedamya, and Perkolilli was demonstrated in previous sections. To illustrate possible petrogenetic pathways for these rocks, average Jeedamya rhyodacite (Table 8) was used in computer modelling. The high K<sub>2</sub>O/Na<sub>2</sub>O ratios of felsic volcanic rocks from Melita and Jeedamya are inconsistent with melting of a mafic protolith, such as amphibolite (Beard and Lofgren, 1989). More acceptable source compositions would be lower crustal rocks. Two possible crustal compositions (an I-type granite or granodiorite of Chappell and White (1992); and a tonalite of Piwinskii (1968) and Huang and Wyllie (1986) have been evaluated in this study. In order to

**Table 10. Results of least-squares and Rayleigh fractionation modelling of two potential source compositions (I-type granite and tonalite)**

Parent Daughter Degree of melting $\Sigma R^2$	I-type granite Melita rhyolite 72% 0.2057			Tonalite Melita rhyolite 35% 0.0265		
	EF	Observed	Source	EF	Observed	Source
La	1.28	28.17	22.04	1.74	28.17	16.21
Ce	1.27	52.7	41.5	1.65	52.7	31.92
Nd	1.29	22.42	17.4	1.71	22.42	13.1
Sm	1.29	4.58	3.55	1.74	4.58	2.63
Eu	0.99	0.94	0.95	0.87	0.94	1.08
Gd	1.29	4.75	3.68	1.75	4.75	2.72
Tb	1.29	0.71	0.55	1.75	0.71	0.408
Dy	1.3	4.0	3.06	1.75	4.0	2.29
Er	1.3	2.53	1.93	1.75	2.53	1.45
Yb	1.29	2.57	1.99	1.73	2.57	1.48

**NOTES:** Residual mineralogy: I-type granite parent: 68% plagioclase, 30% orthopyroxene, 1% ilmenite, 0.2% apatite  
Tonalite parent: 70% plagioclase, 18% orthopyroxene, 9% biotite, 1% hornblende, 1% ilmenite, 1% apatite

$\Sigma R^2$  = sum of squared residuals

EF: calculated enrichment factor

Observed: rare-earth element composition of daughter liquid

Source: calculated source composition (using EF and Observed)

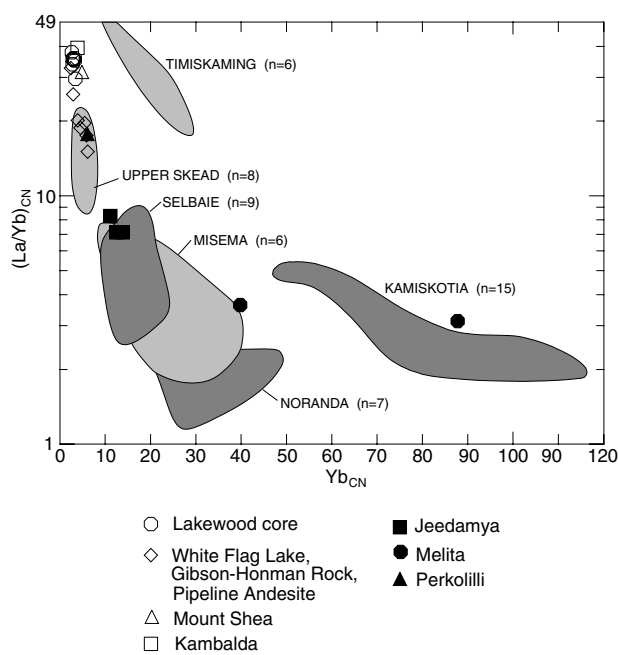
produce magmas with low  $Al_2O_3$  and Sr, negative Eu anomalies, and elevated HREE and Y contents, it is necessary that feldspar is an important part of the residual mineralogy and such phases as garnet and amphibole enter the melt. According to experimental work of Rutter and Wyllie (1988) and Skjerlie and Johnston (1992), these conditions will be met if melting occurs under anhydrous conditions. The type of residual phases for melting of both tonalite and granodiorite have been constrained by the results of experimental studies (Carroll and Wyllie, 1989; 1990) and observations of natural systems.

Least-squares modelling for the I-type granite source (Table 10) requires 72% partial melting ( $\Sigma R^2 = 0.2057$ ) with an anhydrous residual mineralogy of orthopyroxene, plagioclase, and minor amounts of ilmenite and apatite. For the tonalite source ( $\Sigma R^2 = 0.0265$ ), the degree of melting is less than that for the granite (35%), but the residual mineralogy is again dominated by plagioclase and orthopyroxene, with subordinate biotite, hornblende, ilmenite, and apatite.

For both source compositions, plagioclase is the dominant residual phase, which is consistent with magmas with low  $Al_2O_3$  and Sr and negative Eu anomalies. Furthermore, as garnet is absent from both residua, and amphibole is only present as a trace component after tonalite melting, magmas should have elevated HREE and Y contents. Thus, qualitatively, computer modelling is consistent with the chemistry of felsic volcanic rocks from Melita, Jeedamya, and Perkolilli. Despite repeated attempts, no least-squares models in which garnet was a residual phase gave acceptably low  $\Sigma R^2$  values.

As granodiorites and tonalites show a wide range in possible REE contents (Gromet and Silver, 1987; Whalen, 1985) and REE data are not available for both modelled source compositions, the REE patterns of granodiorite and tonalite have been estimated using the least-squares results and appropriate mineral/melt distribution coefficients (Peck and Smith, 1989; Frey et al., 1978). The calculated REE patterns for both sources are similar (Fig. 43, models 4 and 5), although the tonalite source has a slight positive Eu anomaly, whereas the granodiorite source has a slight negative Eu anomaly. The variable Eu anomalies could be ascribed to one of several factors. Drummond and Defant (1990) reviewed the REE characteristics of various Archaean tonalites and noted that several of them had positive Eu anomalies. They suggested that Eu anomalies could result from the variable retention of either or a combination of garnet, clinopyroxene, and hornblende in the source, accumulation or fractionation effects of plagioclase, or the oxidation state of Eu.

Tonalite and granodiorite from various tectonic settings have different REE profiles. Although Archaean tonalitic ('grey') gneisses have not been recorded in the Yilgarn Craton, they may represent unexposed crustal segments. However, they have higher Na/K and LREE/HREE ratios than the preferred tonalite source and lack a pronounced Eu anomaly (Tarney et al., 1979; Martin, 1987). Compared to the modelled source, anorogenic granitoids have higher LREE and HREE and a more pronounced negative Eu anomaly (Anderson, 1983; Rogers and Greenburg, 1990), and island-arc tonalites



PAM165

13.10.98

**Figure 44. Chondrite-normalized plot of La/Yb versus Yb for intermediate and felsic volcanic rocks of the Black Flag Group, and felsic rocks from Jeedamya, Melita, and Perkolilli. Also shown are fields of VHMS-mineralized and barren felsic volcanic rocks from the Abitibi Subprovince of Canada (Barrie et al., 1993). WFL — White Flag Lake; GHR — Gibson-Honman Rock; PA — Pipeline Andesite**

have relatively flat, unfractionated REE patterns (Whalen, 1985; Gill, 1981). Lopez-Escobar et al. (1977) presented data for andesites from Chile that are similar to the modelled source (Fig. 44). Also shown are REE patterns for continental-margin batholiths from western South and North America (Fig. 43, models 4 and 5; Atherton et al., 1979; Gromet and Silver, 1987), which show good agreement with the modelled tonalite source. Thus, the best agreement is provided by felsic rocks from convergent continental margins.

Hallberg et al.'s (1993) assertion that felsic volcanic rocks at Kanowna form part of a belt extending north through Melita and Jeedamya to Teutonic Bore is confirmed by this study (Gindalbie Terrane of Fig. 1). Although there are differences in the absolute concentrations of some elements, the Perkolilli rhyolites have similar REE patterns and show similar trace-element trends to felsic volcanic rocks from Melita and Jeedamya. Rhyolites from Perkolilli have the highest  $SiO_2$  of all felsic rocks discussed in this study, but they are depleted in Zr, Nb, Y, and HREE compared to rhyolites from Melita and Jeedamya, despite having similar LREE contents. These element depletions can be accounted for by the separation of small amounts of zircon, which has high mineral/melt partition coefficients for such elements as Zr (1000), Y (60), Yb (280), and Nb (50), but relatively low values for La (2; Peck and Smith, 1989; Henderson, 1984). Zircon fractionation is consistent with the relative abundance of zircon in thin sections of Perkolilli rhyolites.

## Summary and conclusions

Felsic volcanic rocks of the Black Flag Group and from Melita, Jeedamya, and Perkolilli comprise two regional-scale magma associations that can be distinguished in terms of REE patterns ( $(La/Yb)_{CN}$ ,  $Eu/Eu^*$ ), element ratios ( $Sr/Y$ ,  $Na_2O/K_2O$ ), and element contents ( $Y$ ,  $Nb$ ,  $HREE$ ,  $Zr$ ,  $Al_2O_3$ ). In each area there are several lines of evidence suggesting that coeval mafic and some intermediate volcanic rocks are unrelated to intermediate and felsic volcanic rocks. These are as follows:

- mafic volcanic rocks comprise only a small volume in each area;
- mafic rocks of the Black Flag Group are decoupled from intermediate or felsic volcanic rocks on some bivariate element plots;
- at Melita and Jeedamya, there are few intermediate rocks, and basic and intermediate rocks are absent at Perkolilli;
- the incompatible-element ratio  $Zr/Nb$  for mafic volcanic rocks of the Black Flag Group is  $<50$  compared to  $>50$  for andesites (values of  $<50$  are similar to those of mafic volcanic rocks from lower in the greenstone succession).

Despite lying on common element trends and having fundamentally similar REE patterns, computer modelling shows that intermediate and felsic volcanic rocks of the Black Flag Group cannot be related by fractional crystallization of observed phenocryst phases. Andesites, dacites, and rhyolites of the Black Flag Group have similar chemical characteristics to high-Al trondhjemite-tonalite-dacite and their Cenozoic analogues (adakites), which have, in many studies, been attributed to the partial melting of a mafic protolith transformed to amphibolite or eclogite (Drummond and Defant, 1990; Sen and Dunn, 1994; Wyllie et al., 1995; Morris, 1995). Computer modelling shows that average Black Flag Group andesite and dacite can be produced by roughly the same amount of partial melting (28 and 23% respectively) with more residual garnet in the source for dacite (18%) than for andesite (9%), explaining the relative depletion in HREE and Y in dacites. The types and proportions of residual phases and the degree of melting are consistent with the results of experimental work on melting of basalt to produce adakite (Rapp et al., 1991). Alternatively, the high magnesium number, Ni, and Cr of Black Flag Group andesites, coupled with elevated  $(La/Yb)_{CN}$  and high Sr contents, are consistent with melting of a metasomatized mantle source, such as the mantle wedge overlying a subducting plate.

Felsic volcanic rocks from Melita, Jeedamya, and Perkolilli have fundamentally similar REE patterns and element or oxide ratios (e.g.  $Sr/Y$ ,  $Na_2O/K_2O$ ), and are either depleted ( $Al_2O_3$ ) or enriched ( $Nb$ ,  $Zr$ ,  $Y$ , and  $HREE$ ) relative to rocks of the Black Flag Group with similar  $SiO_2$  contents. As  $K_2O/Na_2O$  is more than 1 for these rocks, a more-felsic source than the Black Flag Group is required. Least-squares modelling results for Jeedamya rhyodacite are consistent with melting of either a tonalite or granodiorite source. As plagioclase dominates the residual mineralogy, the magma should be depleted in  $Al_2O_3$  and

Sr, and have a negative Eu anomaly. However, as garnet and amphibole are consumed during melting, the magma will have relatively high HREE and Y. These predicted chemical characteristics are similar to those observed in felsic volcanic rocks from Melita and Jeedamya. Felsic volcanic rocks at Perkolilli lie on a southerly extension of these rocks and probably resulted from melting of a similar source. Relative depletion of Nb, Zr, HREE, and Y in Perkolilli rhyolites can be accounted for by the separation of small amounts of zircon. Modelled source-REE patterns for these felsic volcanic rocks are most closely approximated by volcanic and plutonic rocks at convergent continental margins, such as western South and North America.

## Locus of melting

Wyllie et al. (1995) summarized experimental work on the melting of mafic protoliths to produce TTD-like magma. As production of felsic volcanic rocks of the Black Flag Group requires residual amphibole and garnet, melting would have occurred at pressures of more than 10 kbar, corresponding to about 35 km depth. The higher content of residual garnet in the source for dacite may indicate deeper levels of melting than for andesite. Taking into account published studies on the occurrence of adakites and their experimental synthesis (Defant and Drummond, 1990; Atherton and Petford, 1993; Rapp et al., 1991; Wyllie et al., 1995) there are two contenders for the source of intermediate and felsic volcanic rocks of the Black Flag Group: melting of amphibolite at the base of the crust (i.e., underplated magmas), or melting of a subducted slab. Both possibilities are evaluated in **Interpretation of tectonic setting**.

By analogy with continental-margin settings, the Jeedamya rhyodacite resulted from melting of thickened continental crust. According to Atherton and Petford (1993), the crust beneath such areas (e.g. Chile) is 60 km thick.

## Mineralization potential

There is now general consensus that gold mineralization in the Eastern Goldfields region is epigenetic (Witt, 1993a,b; Ridley and Groves, 1993). Volcanogenic-hosted massive sulfide deposits are possible targets in felsic-dominated volcanic successions. Barrie et al. (1993) reviewed the geochemistry of felsic volcanic rocks associated with Cu–Zn mineralization in the Archaean Abitibi subprovince. They showed that barren and mineralized successions can be separated on host-rock chemistry. Mineralized successions are characterized by bimodal basalt–andesite and high-silica rhyolite with elevated HFSE contents and flat to depleted LREE patterns with negative Eu anomalies. In contrast, barren successions consist of basaltic andesite to rhyodacite with low HFSE contents and relatively higher  $(La/Yb)_{CN}$  ratios.

Some of these characteristics are summarized in Figures 44 to 46. Although there is some overlap in the fields of barren and mineralized provinces, barren

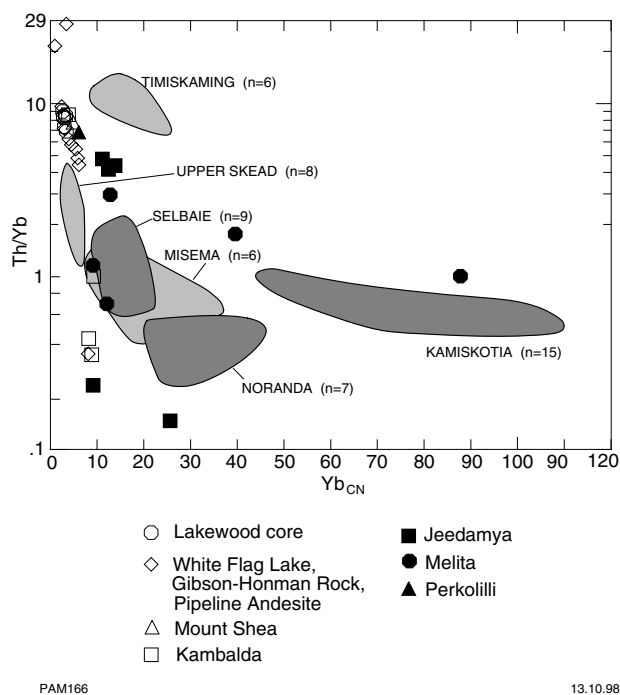


**Figure 45. Th/Yb versus chondrite-normalized Yb for intermediate and felsic volcanic rocks of the Black Flag Group, and felsic rocks from Jeedamya, Melita, and Perkolilli. Also shown are fields of VHMS-mineralized and barren felsic volcanic rocks from the Abitibi Subprovince of Canada (Barrie et al., 1993). WFL — White Flag Lake; GHR — Gibson-Honman Rock; PA — Pipeline Andesite**

provinces (Timiskaming and Upper Skead) are relatively LREE enriched (Fig. 44), relatively depleted in HREE, and have higher large ion lithophile (i.e. Th; Fig. 45) and HFS (i.e. Zr; Fig. 46) element concentrations. As such, these are useful discrimination diagrams for VHMS exploration. Data from this study are also shown on these diagrams. Analyses from the Black Flag Group largely overlap the Timiskaming and Upper Skead fields, which are barren in terms of VHMS. Although there are few data for  $(La/Yb)_{CN}$  versus  $Yb_{CN}$  and  $Th/Yb$  versus  $Yb_{CN}$ , Melita and Jeedamya data largely overlap the Selbaie, Noranda, and Kamiskotia fields (all of which are mineralized), and the barren Misema field. Figure 46 is perhaps more useful, in that both Zr and Y can be accurately measured by XRF, hence there are more data available. This diagram shows that felsic volcanic rocks from Melita and Jeedamya plot with mineralized Abitibi rocks, but Black Flag Group rocks plot with barren areas.

## Interpretation of tectonic setting

There are several lines of evidence that suggest that greenstones of the Eastern Goldfields region erupted through continental crust, even though (to date) basement rocks have not been unequivocally identified. The evidence includes the presence of zircons with >3000 Ma

U–Pb zircon ages in basalts (Compston et al., 1986), isotope and trace-element evidence that some komatiites were contaminated by continental crust (Arndt and Jenner, 1986; Barley et al., 1989), and the dominance of potassic granitoids intruding greenstones (Archibald et al., 1978; Witt and Davy, 1993). The chemistry of felsic volcanic rocks from Melita, Jeedamya, and Perkolilli and computer modelling provide further evidence for thickened sialic crust underlying the greenstone succession.

Despite broad consensus on the presence of sialic crust, there is controversy as to the tectonic setting in which greenstones of the Eastern Goldfields region were erupted. Groves and Batt (1984) and Campbell and Hill (1988) argued for intracontinental rifting, whereas Barley et al. (1989), Swager et al. (1990), and Morris and Witt (1997) favour a continental-margin setting, where the Kalgoorlie Terrane is viewed as a back-arc rift with the volcanic arc to the east. Mafic and ultramafic volcanic rocks, which make up the majority of the greenstone pile in the Kalgoorlie Terrane, were probably erupted through tectonically thinned continental crust. Barley et al. (1989) maintained that andesitic volcanic centres of the Minerie Terrane (Fig. 1) represented the proto-volcanic arc, although this arc association has not been recognized further south (Swager, 1993). Between the arc and the back-arc, rhyolitic volcanism resulted from crustal anatexis initiated by ponded mafic or ultramafic magma in the Gindalbie Terrane (Witt, 1993a). Further evidence

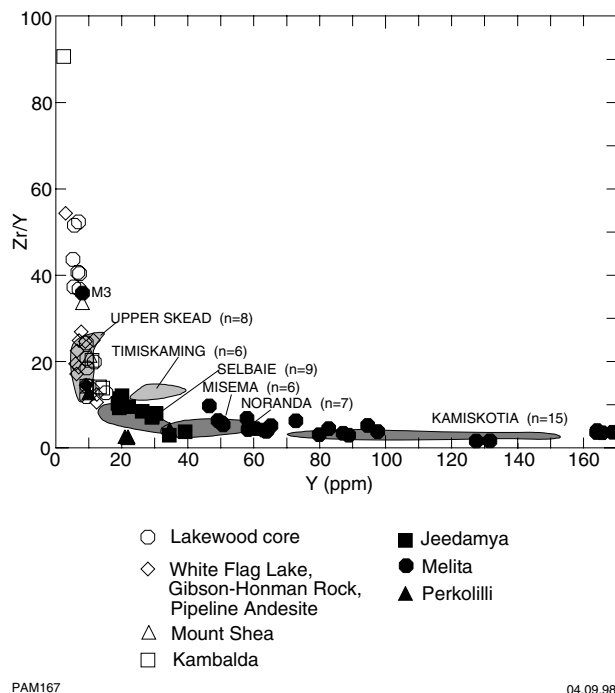
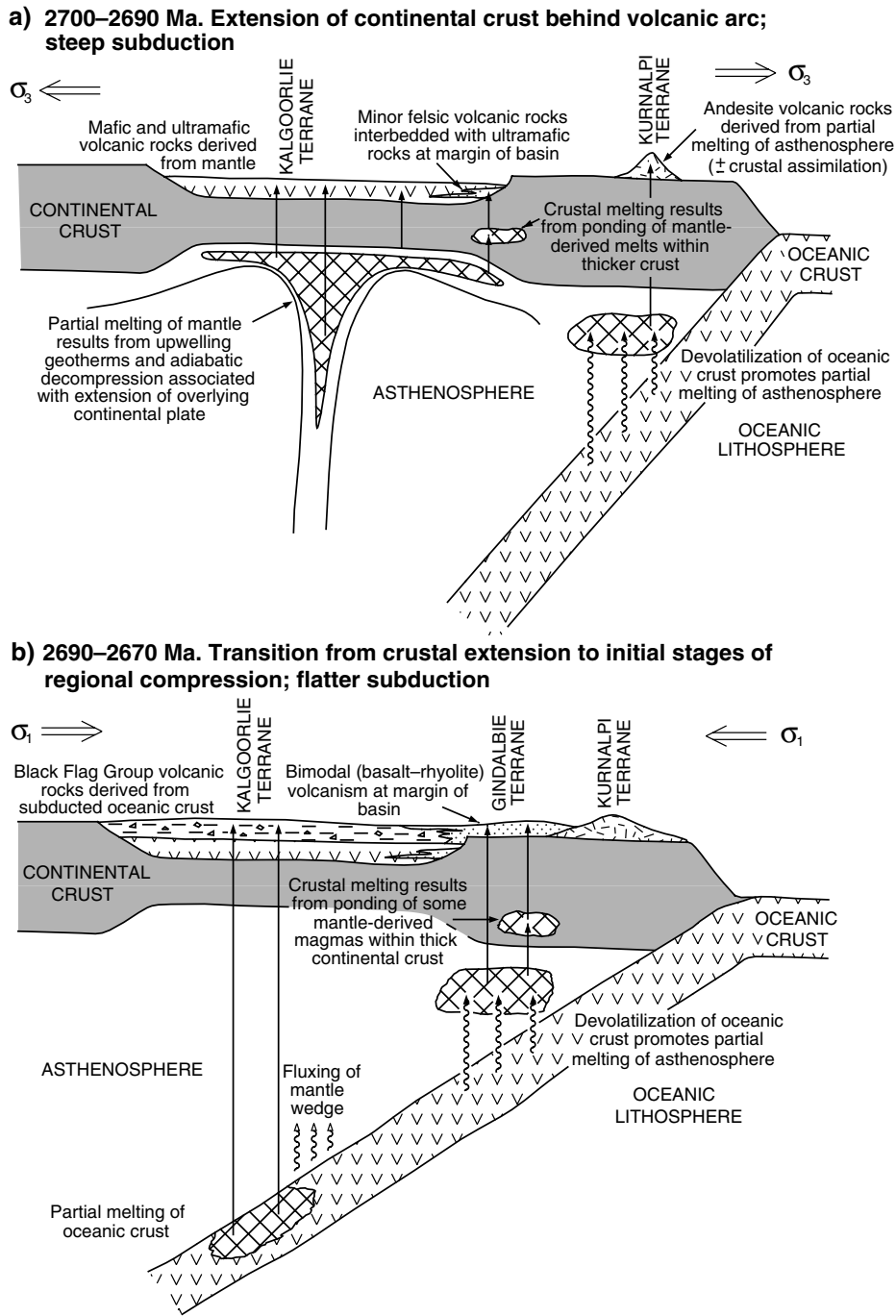


**Figure 46. Zr/Y versus Y (ppm) for intermediate and felsic volcanic rocks of the Black Flag Group, and felsic rocks from Jeedamya, Melita, and Perkolilli. Also shown are fields of VHMS-mineralized and barren felsic volcanic rocks from the Abitibi Subprovince of Canada (Barrie et al., 1993). WFL — White Flag Lake; GHR — Gibson-Honman Rock; PA — Pipeline Andesite**



PAM101

13.10.98

**Figure 47. Tectonic cartoon for the Eastern Goldfields region at two stages in the late Archaean (after Morris and Witt, 1997): a) Steep subduction of a westerly dipping plate is accompanied by extension of continental crust behind the arc. Eruption of mafic and ultramafic magmas in the Kalgoorlie Terrane, and asthenosphere melting to the east. b) Flatter subduction accompanied by compression. Melting of the downgoing plate produces felsic volcanic rocks of the Black Flag Group. Melting of the metasomatized mantle wedge could account for Black Flag Group andesites. Crustal melting to the east results in felsic volcanic rocks at Melita, Jeedamya, and Kanowna**

for a convergent margin is provided by the lack of symmetry of greenstone types and their distribution on either side of the Kalgoorlie Terrane (Swager et al., 1990).

In areas of thick continental crust, such as continental arcs, melting of the mafic underplate at the base of the crust has been proposed as one model for producing high-Al TTD magmas (Atherton and Petford, 1993). As demonstrated above, amphibolite melting to produce the andesites and dacites of the Black Flag Group is constrained to depths of about 35 km due to the presence of residual garnet; therefore, melting must have occurred at depths greater than the base of the crust. One candidate is melting of a lithospheric plate that was subducting from east to west. Further support for subduction comes from the possibility that the unusual chemistry of Black Flag Group andesites results from melting of a metasomatized mantle wedge.

Swager and Griffin (1990) and Witt (1993a) have shown that eruption of the Black Flag Group volcanic rocks roughly coincided with a change from extensional to compressional tectonics. During the extensional period, mantle-derived magma was erupted through tectonically thinned continental crust in the Kalgoorlie Terrane. Following the change to compressional tectonics, subducted oceanic crust underlying the Kalgoorlie Terrane underwent dehydration melting, producing high-Al TTD magma.

The chronology of felsic volcanic rocks from Melita, Jeedamya, and Perkolilli is not as well constrained, although Nelson (1995) reported that the felsic volcanic rocks at Perkolilli are coeval with felsic volcanism (i.e. Black Flag Group) in the Kalgoorlie Terrane. Results of this study suggest that these felsic volcanic rocks result from anatexis of crustal rocks, possibly by ponded mafic or ultramafic magma related to the waning stage of mafic-ultramafic volcanism represented by the lower parts of the greenstones in the Kalgoorlie Terrane. The tectonic model explaining petrogenesis of the two magma associations is shown in cartoon form in Figure 47.

Campbell and Hill (1988) used precise U–Pb dating in support of a two-stage model for the evolution of granite and greenstone in the Kalgoorlie–Norseman area. Basalts forming the lowest parts of the greenstone succession of the Kalgoorlie Terrane resulted from melting of the asthenospheric mantle by a rising komatiite plume. The overlying komatiite represented eruption of the plume axis. They estimated a hiatus of about 15 million years between the end of mafic and ultramafic volcanism and the initiation of felsic magmatism (i.e. Black Flag Group), which corresponded to the elapsed time for conduction of heat from the rising asthenosphere into the crust, initiating crustal anatexis. Hill et al. (1992) maintained that the bimodal nature of greenstones, the presence of komatiites, and the regional extent of the magmatic events favoured a mantle-plume model rather than subduction-related volcanism.

Barley et al. (1989) and Barley and Groves (1990) identified two tectono-stratigraphic terranes in the Norseman–Wiluna greenstone belt: an eastern tectono-stratigraphic association dominated by tholeiitic and calc-alkaline volcanic rocks (overlain by feldspathic sedimentary and associated rocks); and a western belt (corresponding to the Kalgoorlie Terrane of Swager et al., 1990) comprising tholeiitic and komatiitic volcanic rocks overlain by sedimentary and pyroclastic rocks (including the Black Flag Group), the latter derived from the eastern association. They equated the two terranes to an arc association (eastern terrane) and a back-arc association (western terrane). Cassidy et al. (1991) equated granitoids of the Norseman–Wiluna greenstone belt to the Peninsular Ranges Batholith (subduction related), but Hill et al. (1992) noted a difference in chemistry and the duration of the magmatic episodes. Significantly, the bimodal nature of volcanism in the Norseman–Wiluna greenstone belt is in marked contrast to the broad compositional range of the Peninsular Ranges Batholith.

Results of this study do not support the contention of Campbell and Hill (1988) that felsic volcanic rocks forming the upper part of the greenstone stratigraphy in the Kalgoorlie Terrane result from melting at the base of the crust, although such crustal melting is consistent with the origin of the Melita and related felsic volcanic rocks. Furthermore, the chemical and volcanological evidence discussed here indicate that the Black Flag Group volcanics were not derived from the eastern arc association of Barley et al. (1989) and Barley and Groves (1990), but were erupted in the back-arc as a result of slab melting or melting of a mantle wedge (Morris and Witt, 1997), or both. In order to explain the diversity in chemistry and spatial relationship of these two magma associations, two compositionally distinctive protoliths must be melted. A convergent-margin setting is the most viable model for this to take place.

## Acknowledgements

Access to diamond drillcore and drill logs was provided by Western Mining Corporation Exploration, Kalgoorlie Consolidated Gold Mines, and North Limited. Walter Witt (Sons of Gwalia) and Cees Swager (North Limited) are thanked for their continued interest in Eastern Goldfields geology.

## References

- AHMAT, A. L., 1995a, Kanowna, W.A. Sheet 3236: Western Australia Geological Survey, 1:100 000 Geological Series.
- AHMAT, A. L., 1995b, Gindalbie, W.A. Sheet 3237: Western Australia Geological Survey, 1:100 000 Geological Series.
- ANDERSON, J. L., 1983, Proterozoic anorogenic plutonism of North America: Geological Society of America, Memoir, v. 161, p. 133–154.
- ARCHIBALD, N. J., BETTENAY, L. F., BINNS, R. A., GROVES, D. I., and GUNTORPE, R. J., 1978, The evolution of Archaean greenstone terrains, Eastern Goldfields region, Western Australia: *Precambrian Research*, v. 6, p. 103–131.
- ARNDT, N. T., and JENNER, G. A., 1986, Crustally contaminated komatiites and basalts from Kambalda, Western Australia: *Chemical Geology*, v. 56, p. 229–255.
- ATHERTON, M. P., and PETFORD, N., 1993, Generation of sodium-rich magmas from newly underplated basaltic crust: *Nature*, v. 362, p. 144–146.
- ATHERTON, M. P., McCOURT, W. J., SANDERSON, L. M., and TAYLOR, W. P., 1979, The geochemical character of the segmented Peruvian Coastal Batholith and associated volcanics, in *Origin of Granitoid Batholiths* edited by M. P. ATHERTON and J. TARNEY: Kent, U.K., Shiva Publishing, p. 45–64.
- BARLEY, M. E., and GROVES, D. I., 1990, Deciphering the tectonic evolution of Archaean greenstone belts — the importance of contrasting histories to the distribution of mineralization in the Yilgarn Craton, Western Australia: *Precambrian Research*, v. 46, p. 3–20.
- BARLEY, M. E., EISENLOHR, B. N., GROVES, D. I., PERRING, C. S., and VEARNCOMBE, J. R., 1989, Late Archaean convergent margin tectonics and gold mineralization — a new look at the Norseman–Wiluna Belt: *Geology*, v. 17, p. 826–829.
- BARRIE, C. T., LUDDEN, J. N., and GREEN, T. H., 1993, Geochemistry of volcanic rocks associated with Cu–Zn and Ni–Cu deposits in the Abitibi Subprovince: *Economic Geology*, v. 88, p. 1341–1358.
- BEARD, J. S., and LOFGREN, G. E., 1989, Effect of water on the composition of partial melts of greenstone and amphibolite: *Science*, v. 244, p. 195–197.
- BOYNTON, W. V., 1984, Cosmochemistry of the rare earth elements — meteorite studies, in *Rare Earth Element Geochemistry (Developments in Geochemistry 2)* edited by P. HENDERSON: Amsterdam, Elsevier Publications, p. 63–114.
- BRAUNS, K. A., 1991, Palaeovolcanological and environmental setting of the Archaean Black Flag Beds, Kambalda, Western Australia: Melbourne, Monash University, Bsc (Hons) thesis (unpublished).
- BRYAN, W. B., FINGER, L. W., and CHAYES, F., 1969, Estimating proportions in petrographic mixing equations by least-squares approximation: *Science*, v. 163, p. 926–927.
- CAMPBELL, I. H., and HILL, R. I., 1988, A two-stage model for the formation of the granite–greenstone terrains of the Kalgoorlie–Norseman area, Western Australia: *Earth and Planetary Science Letters*, v. 90, p. 11–23.
- CARROLL, M. R., and WYLLIE, P. J., 1989, Experimental phase relations in the system tonalite–peridotite–H<sub>2</sub>O at 15 kb — implications for assimilation and differentiation processes near the crust–mantle boundary: *Journal of Petrology*, v. 30, p. 1351–1382.
- CARROLL, M. P., and WYLLIE, P. J., 1990, The system tonalite–H<sub>2</sub>O at 15 kbar and the genesis of calc-alkaline magmas: *American Mineralogist*, v. 75, p. 345–357.
- CAS, R. A. F., 1992, Submarine volcanism — eruption styles, products, and relevance to understanding the host-rock successions to volcanic-hosted massive sulfide deposits: *Economic Geology*, v. 87, p. 511–541.
- CAS, R. A. F., and WRIGHT, J. V., 1987, Volcanic successions, modern and ancient — a geological approach to processes, products, and successions: London, Allen and Unwin, 528p.
- CAS, R. A. F., and WRIGHT, J. V., 1991, Subaqueous pyroclastic flows and ignimbrites — an assessment: *Bulletin of Volcanology*, v. 53, p. 357–380.
- CASSIDY, K. F., BARLEY, M. E., GROVES, D. I., PERRING, C. S., and HALLBERG, J. A., 1991, An overview of the nature, distribution and inferred tectonic setting of granitoids in the Late Archaean Norseman–Wiluna Belt: *Precambrian Research*, v. 51, p. 51–83.
- CHAPPELL, B. W., and WHITE, A. J. R., 1992, I- and S-type granites in the Lachlan Fold Belt: *Transactions of the Royal Society of Edinburgh: Earth Sciences*, v. 83, p. 1–26.
- CHAUVEL, C., DUPRE, B., and JENNER, G. A., 1985, The Sm–Nd age of Kambalda volcanics is 500 Ma too old!: *Earth and Planetary Science Letters*, v. 74, p. 315–324.
- CLAOUÉ-LONG, J. C., 1990, High resolution timing constraints on the evolution of the Kalgoorlie–Kambalda mineral belt: 3<sup>rd</sup> International Archaean Symposium, Perth, W.A., 1990, Abstracts, p. 355–356.
- CLAOUÉ-LONG, J. C., THIRLWALL, M. F., and NESBITT, R. W., 1984, Revised Sm–Nd systematics of Kambalda greenstones, Western Australia: *Nature*, v. 307, p. 697–701.
- CLOUT, J. M. F., CLEGHORN, J. H., and EATON P. C., 1990, Geology of the Kalgoorlie gold field, in *Geology of the mineral deposits of Australia and Papua New Guinea, Volume 1* edited by F. E. HUGHES: Australasian Institute of Mining and Metallurgy, Monograph 14, p. 411–431.
- COMPSTON, W., WILLIAMS, I. S., CAMPBELL, I. H., and GRESHAM, J. J., 1986, Zircon xenocrysts from the Kambalda volcanics — age constraints and direct evidence for older continental crust beneath the Kambalda–Norseman greenstones: *Earth and Planetary Science Letters*, v. 76, p. 299–311.
- CONDIE, K. C., 1982, Archaean Andesites, in *Andesites*, edited by R. S. THORPE: New York, John Wiley and Sons, p. 575–590.
- COX, K. G., BELL, J. D., and PANKHURST, R. J., 1979, The interpretation of igneous rocks: London, George Allen and Unwin, 450p.
- DAVIDSON, G. J., 1988, Types of tourmaline and exploration applications in the Selwyn district: University of Tasmania,

- Proterozoic gold-copper project, Workshop manual, no. 2, p. 143-159.
- de ROSEN SPENCE, A. F., PROVOST, G., DIMROTH, E., GOCHNAUER, K., and OWEN, V., 1980, Archaean subaqueous felsic flows, Rouyn-Noranda, Quebec, Canada, and their Quaternary equivalents: *Precambrian Research*, v. 12, p. 43-77.
- DEER, W. A., HOWIE, R. A., and ZUSSMAN, J., 1966, An introduction to the rock-forming minerals: London, Longman, 528p.
- DEFANT, M. J., and DRUMMOND, M. S., 1990, Derivation of some modern arc magmas by melting of young subducted lithosphere: *Nature*, v. 347, p. 662-665.
- DEFANT, M. J., RICHERSON, P. M., De BOER, J. Z., STEWART, R. H., MAURY, R. C., BELLON, H., DRUMMOND, M. S., and FEIGENSON, M. D., 1991, Dacite genesis via both slab melting and differentiation — petrogenesis of La Yeguada Volcanic Complex, Panama: *Journal of Petrology*, v. 32, p. 1101-1142.
- DELTA GOLD N.L., 1997, Annual report to 30 June 1997: Delta Gold N.L., 79p.
- DePAOLO, D. J., 1981, Trace elements and isotopic effects of combined wallrock assimilation and fractional crystallization: *Earth and Planetary Science Letters*, v. 53, p. 189-202.
- DRUMMOND, M. S., and DEFANT, M. J., 1990, A model for trondjemite-tonalite-dacite genesis and crustal growth via slab melting — Archaean to modern comparisons: *Journal of Geophysical Research*, v. 95, p. 21503-21521.
- FISHER, R. V., 1961, Proposed classification of volcanoclastic sediments and rocks: *Geological Society of America Bulletin*, v. 72, p. 1409-1414.
- FISHER, R. V., 1966, Rocks composed of volcanic fragments and their classification: *Earth Science Reviews*, v. 1, p. 287-298.
- FREY, F. A., GREEN, D. H., and ROY, S. D., 1978, Integrated models of basalt petrogenesis — a study of quartz tholeiites to olivine melilitites from southeastern Australia utilizing geochemical and experimental petrological data: *Journal of Petrology*, v. 19, p. 463-513.
- GEMUTS, I., and THERON, A. C., 1975, The Archaean between Coolgardie and Norseman — stratigraphy and mineralization, in *Economic geology of Australia and Papua New Guinea — I. Metals* edited by C. L. KNIGHT: Australasian Institute of Mining and Metallurgy, Monograph 5, p. 66-74.
- GILL, J. B., 1981, Orogenic andesites and plate tectonics: Berlin, Springer-Verlag, 390p.
- GOLDING, L. Y., and WALTER, M. R., 1979, Evidence of evaporite minerals in the Archaean Black Flag Beds, Kalgoorlie, Western Australia: *Australia BMR, Journal of Australian Geology and Geophysics*, v. 4, p. 67-71.
- GREY, K., 1981, Small conical stromatolites from the Archaean near Kanowna, Western Australia: Western Australia Geological Survey, Annual Report 1980, p. 90-94.
- GRIFFIN, T. J., 1990, Geology of the granite-greenstone terrane of the Lake Lefroy and Cowan 1:100 000 sheets, Western Australia: Western Australia Geological Survey, Report 32, 53p.
- GROMET, L. P., and SILVER, L. T., 1987, REE variations across the Peninsular Ranges Batholith — implications for batholithic petrogenesis and crustal growth in magmatic arcs: *Journal of Petrology*, v. 28, p. 75-125.
- GROVES, D. I., and BATT, W. D., 1984, Spatial and temporal variations of Archaean metallogenic associations in terms of evolution of granitoid-greenstone terrains with particular emphasis on the Western Australian Shield, in *Archaean geochemistry* edited by A. KRONER, G. N. HANSON, and A. M. GOODWIN: Berlin, Springer-Verlag, p. 73-98.
- HALLBERG, J. A., 1985, Geology and mineral deposits of the Leonora-Laverton area, northeastern Yilgarn Block, Western Australia: Carlisle, W.A., Hesperian Press, 140p.
- HALLBERG, J. A., 1986, Archaean basin development and crustal extension in the northeastern Yilgarn Block, Western Australia: *Precambrian Research*, v. 31, p. 135-156.
- HALLBERG, J. A., and GILES, C. W., 1986, Archaean felsic volcanism in the northeastern Yilgarn Block, Western Australia: *Australian Journal of Earth Sciences*, v. 33, p. 413-427.
- HALLBERG, J. A., AHMAT, A. L., MORRIS, P. A., and WITT, W. K., 1993, An overview of felsic volcanism within the Eastern Goldfields region, Western Australia: Australian Geological Survey Organisation, Record 1993/54, p. 29-32.
- HAUSBACK, B. P., 1987, An extensive, hot, vapor-charged rhyodacite flow, Baja California, Mexico, in *The emplacement of silicic domes* edited by J. H. FINK: Geological Society of America, Special Paper, v. 22, p. 111-118.
- HENDERSON, P., 1984, General geochemical properties and abundances of the rare earth elements, in *Rare Earth Element Geochemistry* edited by P. HENDERSON: Amsterdam, Elsevier, 510p.
- HILL, R. I., CHAPPELL, B. W., and CAMPBELL, I. H., 1992, Late Archaean granites of the southeastern Yilgarn Block, Western Australia — age, geochemistry, and origin: *Transactions of the Royal Society of Edinburgh: Earth Sciences*, v. 83, p. 211-226.
- HUANG, W. L., and WYLLIE, P. J., 1986, Phase relations of gabbro-tonalite-granite-water at 15 kbar with applications to differentiation and anatexis: *American Mineralogist*, v. 71, p. 301-316.
- HUNTER, W. M., 1988, Kalgoorlie, W.A. Sheet 3136: Western Australia Geological Survey, 1:100 000 Geological Series.
- HUNTER, W. M., 1993, Geology of the granite-greenstone terrane of the Kalgoorlie and Yilmia 1:100 000 sheets, Western Australia: Western Australia Geological Survey, Report 35, 80p.
- KEATS, W., 1987, Regional geology of the Kalgoorlie-Boulder gold-mining district: Western Australia Geological Survey, Report 21, 44p.
- KRUMBEIN, W. C., 1934, Size-frequency distribution of sediments: *Journal of Sedimentary Petrology*, v. 4, p. 65-77.
- LARGE, R. R., 1992, Australian volcanic-hosted massive sulfide deposits — features, styles, and genetic models: *Economic Geology*, v. 87, p. 471-510.
- LE MAITRE, R. W., 1989, A classification of igneous rocks and glossary of terms. Recommendations of the International Union of Geological Sciences Subcommittee on the Systematics of Igneous Rocks: Oxford, Blackwell Scientific Publications, 193p.
- LE MARCHAND, F., VILLEMANT, B., and CALAS, G., 1987, Trace element distribution coefficients in alkaline series: *Geochimica et Cosmochimica Acta*, v. 51, p. 1071-1081.
- LOPEZ-ESCOBAR, L., FREY, F. A., and VERGARA, M., 1977, Andesites and high-alumina basalts from the central-south Chile high Andes — geochemical evidence bearing on their petrogenesis: *Contributions to Mineralogy and Petrology*, v. 63, p. 199-228.
- MARSH, J. S., 1991, REE fractionation and Ce anomalies in weathered Karoo dolerite: *Chemical Geology*, v. 90, p. 189-194.
- MARSTON, R. J., 1984, Nickel mineralization in Western Australia: Western Australia Geological Survey, Mineral Resources Bulletin 14, 271p.
- MARTIN, H., 1987, Petrogenesis of Archaean trondjemites, tonalites, and granodiorites from Eastern Finland — major and trace element chemistry: *Journal of Petrology*, v. 28, p. 921-953.
- MORRIS, P. A., 1984, MAGFRAC — a Basic program for least-squares approximation of fractional crystallization: *Computers and Geosciences*, v. 10, p. 437-444.

- MORRIS, P. A., 1993, Archaean mafic and ultramafic volcanic rocks, Menzies to Norseman, Western Australia: Western Australia Geological Survey, Report 36, 107p.
- MORRIS, P. A., 1995, Slab melting as an explanation of Quaternary volcanism and aseismicity in southwest Japan: *Geology*, v. 23, p. 395–398.
- MORRIS, P. A., PESCU, L., THOMAS, A., GAMBLE, J., TOVEY, E., MARSH, N., and EVERETT, R., 1991, Geochemical analyses of Archaean mafic and ultramafic volcanics, eastern Yilgarn Craton, Western Australia: Western Australia Geological Survey, Record 1991/8, 78p.
- MORRIS, P. A., and WITT, W. K., 1997, The geochemistry and tectonic setting of two contrasting Archaean felsic volcanic associations in the Eastern Goldfields region, Western Australia: *Precambrian Research*, v. 83, p. 83–107.
- NELSON, D. R., 1995, Compilation of SHRIMP U–Pb zircon geochronology data, 1994: Western Australia Geological Survey, Record 1995/3, 244p.
- NELSON, D. R., 1996, Compilation of SHRIMP U–Pb zircon geochronology data, 1995: Western Australia Geological Survey, Record 1996/5, 168p.
- O'BEIRNE, W. R., 1968, The acid porphyries and porphyroid rocks of the Kalgoorlie area: University of Western Australia, PhD thesis (unpublished).
- PECK, D. C., and SMITH, T. E., 1989, The geology and geochemistry of an Early Proterozoic volcanic-arc association at Cartwright Lake, Lynne Lake greenstone belt, northwestern Manitoba: *Canadian Journal of Earth Sciences*, v. 26, p. 716–736.
- PICHLER, H., 1965, Acid hyaloclastites: *Bulletin Volcanologique*, v. 28, p. 293–310.
- PIDGEON, R. T., 1986, The correlation of acid volcanics in the Archaean of Western Australia: Western Australian Mining and Petroleum Research Institute (WAMPRI), Report 27, 109p.
- PIDGEON, R. T., and WILDE, S. A., 1989, Geochronology of granite and granite–greenstone terrains: Western Australia, Curtin University of Technology, School of Physics and Geosciences, Report SPG 514/19, 70p.
- PIDGEON, R. T., and WILDE, S. A., 1990, The distribution of 3.0 Ga and 2.7 Ga volcanic episodes in the Yilgarn Craton of Western Australia: *Precambrian Research*, v. 48, p. 309–325.
- PIWINSKII, A. J., 1968, Experimental studies of igneous rock series, central Nevada batholith, California: *Journal of Geology*, v. 76, p. 548–570.
- PIWINSKII, A. J., 1973, Experimental studies of igneous rock series, central Nevada batholith, California, Part II: *Neue Jahrbuch für Mineralogie, Monatshefte*, v. 5, p. 193–215.
- PORADA, H., and BEHR, H. J., 1988, Setting and sedimentary facies of late Proterozoic alkali lake (playa) deposits in the southern Damara Belt of Namibia: *Sedimentary Geology*, v. 58, p. 171–194.
- RAPP, R. P., WATSON, E. B., and MILLER, C. F., 1991, Partial melting of amphibolite/eclogite and the origin of Archaean trondhjemites and tonalites: *Precambrian Research*, v. 51, p. 1–25.
- RATTENBURY, M. S., 1993, Tectonostratigraphic terranes in the northern Eastern Goldfields: Australian Geological Survey Organisation, Record 1993/54, p. 73–75.
- RIDLEY, J., and GROVES, D. I., 1993, Gold mineralization at various regional metamorphic grades: Australian Geological Survey Organisation, Record 1993/53, p. 101–134.
- ROBERTS, D. E., and ELIAS, M., 1990, Gold deposits of the Kambalda – St Ives region, in *Geology of the mineral deposits of Australia and Papua New Guinea* edited by F. E. HUGHES: Australasian Institute of Mining and Metallurgy, Monograph 14, p. 479–491.
- ROGERS, J. W., and GREENBURG, J. K., 1990, Late-orogenic, post-orogenic and anorogenic granites — distinction by major element and trace element chemistry and possible origins: *Journal of Geology*, v. 98, p. 291–309.
- ROGERS, G., and SAUNDERS, A. D., 1989, Magnesian andesites from Mexico, Chile and the Aleutian Islands — implications for magmatism associated with ridge–trench collision, in *Boninites and related rocks* edited by A. J. CRAWFORD: London, Unwin Hyman, p. 416–445.
- ROOBOL, M. J., SMITH, A. L., and WRIGHT, J. V., 1987, Lithic breccias in pyroclastic flow deposits on St Kitts, West Indies: *Bulletin of Volcanology*, v. 49, p. 694–707.
- RUSHMER, T., 1991, Partial melting of two amphibolites — contrasting experimental results under fluid-absent conditions: *Contributions to Mineralogy and Petrology*, v. 107, p. 41–59.
- RUTTER, M. J., and WYLLIE, P. J., 1988, Melting of vapor-absent tonalite at 10 kbar to simulate dehydration melting in the deep crust: *Nature*, v. 331, p. 159–160.
- SAKUYAMA, M., and NESBITT, R. W., 1986, Geochemistry of the Quaternary volcanic rocks of the northeast Japan arc: *Journal of Volcanology and Geothermal Research*, v. 29, p. 413–450.
- SAUNDERS, A. D., TARNEY, J., MARSH, N. G., and WOOD, D. A., 1980, Ophiolites as ocean crust or marginal basin — a geochemical approach, in *Ophiolites* edited by A. PANAYIOUTOU: International Ophiolite Symposium, Cyprus, 1979, Proceedings, p. 193–204.
- SAUNDERS, A. D., ROGERS, G., MARRINER, G. F., TERRELL, D. J., and VERMA, S. P., 1987, Geochemistry of Cenozoic volcanic rocks, Baja, California, Mexico — implications for the petrogenesis of post-subduction magmas: *Journal of Volcanology and Geothermal Research*, v. 32, p. 223–245.
- SEN, C., and DUNN, T., 1994, Dehydration melting of a basaltic composition amphibolite at 1.5 and 2.0 GPa — implications for the origin of adakites: *Contributions to Mineralogy and Petrology*, v. 177, p. 394–409.
- SHAW, D. M., 1970, Trace element fractionation during anatexis: *Geochimica et Cosmochimica Acta*, v. 34, p. 237–243.
- SKJERLIE, K. P., and JOHNSTON, A. D., 1992, Vapor-absent melting at 10 kbar of a biotite- and amphibole-bearing tonalite gneiss — implications for the generation of A-type granites: *Geology*, v. 20, p. 263–266.
- SMITH, A. L., and ROOBOL, M. J., 1982, Andesitic pyroclastic flows, in *Andesites* edited by R. S. THORPE: New York, John Wiley and Sons, p. 415–433.
- SORENSEN, S. S., 1988, Petrology of amphibolite-facies mafic and ultramafic rocks from the Catalina Schist, Southern California — metasomatism and migmatization in a subduction zone metamorphic setting: *Journal of Metamorphic Geology*, v. 6, p. 405–435.
- SORENSEN, S. S., and BARTON, N. D., 1987, Metasomatism and partial melting in a subduction complex — Catalina Schist, Southern California: *Geology*, v. 15, p. 115–118.
- SPULBER, S. D., and RUTHERFORD, M. J., 1983, The origin of rhyolite and plagiogranite in the oceanic crust — an experimental study: *Journal of Petrology*, v. 24, p. 1–25.
- SUN, S. S., and McDONOUGH, W. F., 1989, Chemical and isotopic systematics of oceanic basalts — implications for mantle composition and process, in *Magmatism in the Ocean Basins* edited by A. D. SAUNDERS and M. J. NORRY: Oxford, The Geological Society, Special Publication no. 42, p. 313–345.
- SWAGER, C. P., 1989, Structure of the Kalgoorlie greenstones — regional deformation history and implications for the structural

- setting of gold deposits within the Golden Mile: Western Australia Geological Survey, Report 25, Professional Papers, p. 59–84.
- SWAGER, C. P., 1993, Kurnalpi, W.A. Sheet 3336: Western Australia Geological Survey 1:100 000 Geological Series.
- SWAGER, C. P., 1995, Geology of the greenstone terranes in the Kurnalpi–Edjudina region, southeastern Yilgarn Craton: Western Australia Geological Survey, Report 47, 31p.
- SWAGER, C. P., and GRIFFIN, T. J., 1990, An early thrust duplex in the Kalgoorlie–Kambalda greenstone belt, Eastern Goldfields region, Western Australia: *Precambrian Research*, v. 48, p. 63–73.
- SWAGER, C. P., GRIFFIN, T. J., WITT, W. K., WYCHE, S., AHMAT, A. L., HUNTER, W. M., and MCGOLDRICK, P. J., 1990, Geology of the Archaean Kalgoorlie terrane — an explanatory note: Western Australia Geological Survey, Record 1990/12, 55p.
- TARNEY, J., WEAVER, B., and DRURY, S. A., 1979, Geochemistry of Archaean trondhjemitic and tonalitic gneisses from Scotland and East Greenland, *in* *Trondhjemites, dacites and related rocks edited by F. BARKER*: Amsterdam, Elsevier, 659p.
- TAYLOR, T., 1984, The paleoenvironmental and tectonic setting of the Archaean volcanogenic rocks in the Kanowna district, near Kalgoorlie, Western Australia: University of Western Australia, MSc thesis (unpublished).
- TRAVIS, G. A., WOODALL, R., and BARTRAM, G. D., 1971, The geology of the Kalgoorlie goldfield, *in* *Symposium on Archaean Rocks edited by J. E. GLOVER*: Geological Society of Australia, Special Publication 3, p. 175–190.
- van der MOLEN, I., and PATERSON, M. S., 1979, Experimental deformation of partially melted granite: *Contributions to Mineralogy and Petrology*, v. 70, p. 299–318.
- WHALEN, J. B., 1985, Geochemistry of an island-arc plutonic suite — the Uasilau – Yau Yau Intrusive Complex, New Britain, P.N.G.: *Journal of Petrology*, v. 26, p. 603–632.
- WILLIAMS, I. R., 1970, Kurnalpi, W.A. Sheet SH 51-10: Western Australia Geological Survey, 1:250 000 Geological Series.
- WILLIAMS, I. R., 1976, Regional interpretation map of the Archaean geology, southeast part of the Yilgarn Block: Western Australia Geological Survey, 1:1 000 000 scale map.
- WITT, W. K., 1993a, Melita, W.A. Sheet 3139: Western Australia Geological Survey, 1:100 000 Geological Series.
- WITT, W. K., 1993b, Gold mineralization in the Menzies–Kambalda region, Eastern Goldfields, Western Australia: Western Australia Geological Survey, Report 39, 165p.
- WITT, W. K., and DAVY, R., 1993, Pre- and post-regional folding I-type granitoid suites in the southwest Eastern Goldfields region — an Archaean syn-collisional plutonic event?: Australian Geological Survey Organisation, Record 1993/54, p. 33–37.
- WITT, W. K., MORRIS, P. A., WYCHE, S., and NELSON, D. R., 1996, The Gindalbie Terrane as a target for VMS-style mineralization in the Eastern Goldfields region of the Yilgarn Craton: Western Australia Geological Survey, Annual Review 1995–96, p. 41–47.
- WOOD, D. A., GIBSON, I. L., and THOMPSON, R. N., 1976, Elemental mobility during zeolite facies metamorphism of the Tertiary basalts of eastern Iceland: *Contributions to Mineralogy and Petrology*, v. 55, p. 241–254.
- WOODALL, R. W., 1965, Structure of the Kalgoorlie Goldfield, *in* *Geology of Australian ore deposits, 2<sup>nd</sup> edition edited by J. McANDREW*: Australasian Institute of Mining and Metallurgy; 8<sup>th</sup> Commonwealth Mining and Metallurgical Congress, Australia and New Zealand, 1965; Publications, v. 1, p. 71–79.
- WRIGHT, J. V., SMITH, A. L., SELF, S., 1980, A working terminology of pyroclastic deposits: *Journal of Volcanology and Geothermal Research*, v. 8, p. 315–336.
- WYLLIE, P. J., WOLF, M. B., and van der LAAN, S. R., 1995, Conditions for formation of tonalites and trondhjemites — magmatic sources and products, *in* *Tectonic evolution of greenstone belts edited by M. J. de WIT and L. D. ASHWAL*: Oxford University Press, p. 256–266.
- YAMAGISHI, H., 1991, Morphological features of Miocene submarine coherent lavas from the “Green Tuff” basins — examples from basaltic and andesitic rocks from the Shimokita Peninsula, northern Japan: *Bulletin of Volcanology*, v. 53, p. 173–181.



## Appendix

# Whole-rock chemistry of mafic, intermediate, and felsic volcanic rocks from parts of the Eastern Goldfields region

**NOTES:** All analyses were carried out at the Chemistry Centre of Western Australia (CCWA).

Major- and trace-element analyses were by x-ray fluorescence (XRF), except for analyses for which there are complete rare-earth element (REE) data. In these cases, Hf, Pb, Y, Sc, Nb, Th, U, Ta, and REE were analysed by inductively coupled plasma mass spectrometry (ICP-MS).

GHR: Gibson-Honman Rock

hb: hornblende

cgte: conglomerate

plag: plagioclase

qtz: quartz

fspar: feldspar

A digital version of these data (FELCHEM.CSV) is contained in the pocket.

**SOURCES:** Analytical techniques for XRF analysis are discussed in Morris et al. (1991).

For analysis of standards, 'Potts' refers to consensus values in Potts et al. (1992).

Data for Melita and Jeedamya are from Witt (1996).

## Appendix (continued)

GSWA sample	SE drillcore							
	114129	114125	114159	114117	114116	114175	114188	114161
Rock type	Glassy dacite	Flow-banded dacite	Flow-banded dacite	Flow-banded dacite	Dacite	Amygdaloidal dacite	Dacite	Porphyritic dacite
Location	Lakewood	Lakewood	Lakewood	Lakewood	Lakewood	Lakewood	Lakewood	Lakewood
Drillhole	SE3	SE3	SE3	SE3	SE3	SE7	SE7	SE7
Depth (m)	370.6	527.9	295.7	635.2	654.6	1699.0	1242.1	1541.0
Map code	3236	3236	3236	3236	3236	3236	3236	3236
Easting	358800	358800	358800	358800	358800	358961	358961	358961
Northing	6590200	6590200	6590200	6590200	6590200	6587191	6587191	6587191
	<b>Percentage</b>							
SiO <sub>2</sub>	63.7	64.6	66.0	68.1	68.3	62.2	62.9	64.3
TiO <sub>2</sub>	0.45	0.43	0.38	0.4	0.39	0.45	0.45	0.42
Al <sub>2</sub> O <sub>3</sub>	17.6	17.1	14.8	15.7	15.1	15.1	18.9	15.5
Fe <sub>2</sub> O <sub>3</sub>	0.68	0.63	1.2	0.54	0.9	1.38	0.41	0.59
FeO	2.05	2.13	1.72	1.58	2.17	2.49	1.74	2.71
MnO	–	–	–	–	–	0.05	–	0.06
MgO	1.67	1.35	1.41	0.99	1.34	2.7	1.26	2.48
CaO	3.38	3.06	3.61	2.52	2.48	3.91	2.47	2.72
Na <sub>2</sub> O	3.41	3.81	4.44	4.43	3.79	6.54	2.29	3.16
K <sub>2</sub> O	2.32	2.62	2.21	2.45	2.34	0.53	3.08	2.68
P <sub>2</sub> O <sub>5</sub>	0.19	0.17	0.16	0.16	0.17	0.23	0.2	0.16
LOI	5.39	5.09	5.05	4.17	4.2	5.01	6.06	6.25
<b>Total</b>	<b>100.84</b>	<b>100.99</b>	<b>100.98</b>	<b>101.04</b>	<b>101.18</b>	<b>100.59</b>	<b>99.76</b>	<b>101.03</b>
	<b>Parts per million</b>							
Ba	1 008	682	674	880	845	186	941	1 371
Cu	21	–	12	5	8	–	9	12
Cr	42	39	37	36	35	62	86	80
Ga	22	22	19	19	20	18	25	20
Hf	3.65	3.44	3.32	3.26	–	2.3	–	4.45
Nb	1	0.87	1.72	0.72	–	1.8	–	1.69
Ni	33	31	37	22	33	43	49	45
Pb	13.4	23.9	11.2	29.2	6	11.4	15	16.5
Rb	67	50	57	54	57	18	96	72
Sc	4.07	3.72	3.51	3.27	5	14.2	8	5.44
Sr	975	551	772	381	502	648	684	494
Ta	0.06	–	0.14	0.09	–	1	–	0.16
Th	5.36	5.54	4.72	4.76	6	4.4	6	4.55
U	–	2	2	2	2	1.1	2	–
V	66	64	59	60	53	73	79	68
Y	6.57	6.77	5.43	5.36	9	9	11	4.92
Zn	66	56	61	93	76	156	52	52
Zr	344	249	280	200	219	187	219	215
La	32.92	32.44	28.39	28.77	32	30.1	24	26.18
Ce	63.73	57.2	59.8	55.45	65	61.2	56	56.6
Pr	8.37	8.35	7.47	7.52	–	6.2	–	7.02
Nd	30.08	30.12	25.55	26.93	–	28.2	–	26
Sm	4.99	4.83	4.16	4.36	–	5.4	–	4.37
Eu	1.5	1.31	1.24	1.24	–	1.4	–	1.5
Gd	3.77	3.91	3.13	3.29	–	3.6	–	3.21
Tb	0.4	0.39	0.32	0.33	–	0.4	–	0.33
Dy	1.44	1.61	1.23	1.26	–	1.7	–	1.23
Ho	0.29	0.31	0.24	0.22	–	0.3	–	0.2
Er	0.8	0.77	0.69	0.67	–	0.8	–	0.61
Tm	0.1	0.09	0.07	0.07	–	0.1	–	0.07
Yb	0.65	0.65	0.56	0.53	–	0.6	–	0.55
Lu	0.07	0.05	0.06	0.06	–	0.1	–	0.05
(La/Yb) <sub>CN</sub>	34.15	33.65	34.18	36.60	–	33.82	–	32.09

## Appendix (continued)

GSWA sample	SE drillcore						GHR	White Flag Lake
	114160	114178	114162	114174	117203	114439	114500	114471
Rock type	Dacite lobe margin	Dacite	Weakly brecciated rhyolite	Brecciated rhyolite	Flow-banded dacite	Flow-banded dacite	Dacite lobe margin	Dolerite
Location	Lakewood	Lakewood	Lakewood	Lakewood	Lakewood	Lakewood	Gibson-Honnan Rock	SSE of Crown Dam
Drillhole	SE7	SE7	SE7	SE7	SE4	SE4		
Depth (m)	1574.6	1589.0	1541.3	1710.0	1934.0	1044.9		
Map code	3236	3236	3236	3236	3236	3236	3136	3136
Easting	358961	358961	358961	358961	358360	358360	3497	3291
Northing	6587191	6587191	6587191	6587191	6589900	6589900	65867	66142
	<b>Percentage</b>							
SiO <sub>2</sub>	64.7	67.3	70.7	75.4	61.6	68.6	68.9	57.2
TiO <sub>2</sub>	0.42	0.4	0.34	0.2	0.45	0.3	0.23	0.54
Al <sub>2</sub> O <sub>3</sub>	15.2	14	13.9	10.7	17.8	14.1	15.5	14.4
Fe <sub>2</sub> O <sub>3</sub>	0.66	0.93	0.1	0.77	0.26	0.97	0.82	2.61
FeO	2.52	1.85	1.29	1.12	2.35	3.72	0.14	3.92
MnO	0.07	0.05				0.08	0.05	0.09
MgO	1.89	1.84	0.89	0.99	1.03	4.22	0.16	6.93
CaO	2.82	2.39	2.22	2.56	2.98	0.46	2.02	6.79
Na <sub>2</sub> O	5.73	5.23	7.16	1.54	1.34	0.4	6.74	3.63
K <sub>2</sub> O	1.52	1.48	0.54	2.79	4.03	2.9	3.56	1.13
P <sub>2</sub> O <sub>5</sub>	0.15	0.15	0.14	0.07	0.23	0.08	0.13	0.19
LOI	5.41	4.81	3.65	4.13	6.57	4.36	2.09	3.07
<b>Total</b>	<b>101.09</b>	<b>100.43</b>	<b>100.93</b>	<b>100.27</b>	<b>98.64</b>	<b>100.19</b>	<b>100.34</b>	<b>100.5</b>
	<b>Parts per million</b>							
Ba	553	485	200	414	1 931	440	1 335	427
Cu	20	12	12	11	20	–	–	47
Cr	40	44	33	8	112	22	6	657
Ga	19	19	12	14	22	16	17	15
Hf	2.45	–	–	–	–	–	0.4	2.7
Nb	1.58	–	–	1.2	–	–	3.6	2.8
Ni	31	34	34	16	49	17	9	246
Pb	19.6	19	17	5	10	–	30	10.3
Rb	40	37	13	88	156	48	69	24
Sc	4.24	8	5	3	9	4	4	27.9
Sr	639	495	821	141	365	30	847	643
Ta	0.15	–	–	0.7	–	–	1.3	1.6
Th	4.69	5	6	5	8	5	20.2	6
U	–	2	–	–	2	2	2.6	0.8
V	62	78	42	30	69	41	33	145
Y	6.39	9	7	9	14	9	11.2	12.1
Zn	76	75	65	83	115	135	30	75
Zr	260	167	283	107	179	130	279	150
La	28.53	28	18	8	41	10	56.5	31.2
Ce	59.6	65	52	17	86	17	104	63.1
Pr	7.23	–	–	–	–	–	11.2	6.1
Nd	26.45	–	–	–	–	–	37.6	26.1
Sm	4.23	–	–	–	–	–	9.5	5.3
Eu	1.28	–	–	–	–	–	2.5	1.5
Gd	3.39	–	–	–	–	–	6.1	3.9
Tb	0.37	–	–	–	–	–	0.7	0.5
Dy	1.48	–	–	–	–	–	2.5	2.5
Ho	0.26	–	–	–	–	–	0.4	0.5
Er	0.72	–	–	–	–	–	1.2	1.5
Tm	0.07	–	–	–	–	–	0.1	0.2
Yb	0.68	–	–	–	–	–	0.7	1.1
Lu	0.06	–	–	–	–	–	0.1	0.2
(La/Yb) <sub>CN</sub>	28.29	–	–	–	–	–	54.42	19.12

## Appendix (continued)

GSWA sample	White Flag Lake							
	114472	117208	117211	114464	114474	114465	114461	114463
Rock type	Hb andesite clast	Andesite cgte clast	Andesite cgte tuff	Plag-hb	Felsic tuff dacite flow	Plag-hb tuff	Plag-hb tuff	Plag-hb
Location	E of White Flag Dam	W of White Flag Dam	W of White Flag Lake	SW of Georges Dam	E of White Flag Dam	N of Crown Dam	NW of Crown Dam	NW of Crown Dam
Drillhole Depth (m)								
Map code	3136	3136	3136	3136	3136	3136	3136	3136
Easting	3330	3320	3320	3283	3315	3283	3284	3285
Northing	66100	66098	66098	66168	66100	66155	66163	66163
	<b>Percentage</b>							
SiO <sub>2</sub>	59.9	60	60.3	68.6	69.8	69.9	71.2	72.8
TiO <sub>2</sub>	0.43	0.56	0.4	0.31	0.44	0.38	0.26	0.3
Al <sub>2</sub> O <sub>3</sub>	15.4	12.3	15.3	14.2	13.2	14.3	13.8	12.8
Fe <sub>2</sub> O <sub>3</sub>	2.45	2.31	2.09	0.22	1.92	1.74	1.16	1.34
FeO	2.84	3.84	3.14	2.47	1.36	1.07	1.38	1.3
MnO	0.07	0.11	0.07	–	0.05	0.06	–	–
MgO	5.4	3.64	3.83	2.18	1.9	1.22	1.85	1.77
CaO	5.49	6.6	5.39	3.54	3.62	3.41	2.78	2.08
Na <sub>2</sub> O	4.19	3.19	4.39	5.54	3.91	4.2	6.17	5.09
K <sub>2</sub> O	1.04	1.74	1.1	2.25	2.35	2.49	1.22	2.02
P <sub>2</sub> O <sub>5</sub>	0.14	0.15	0.14	0.1	0.11	0.11	0.1	0.08
LOI	2.95	4.08	2.64	1.01	1.42	1.64	1.02	1.12
<b>Total</b>	<b>100.3</b>	<b>98.52</b>	<b>98.79</b>	<b>100.42</b>	<b>100.08</b>	<b>100.52</b>	<b>100.94</b>	<b>100.7</b>
	<b>Parts per million</b>							
Ba	480	838	450	516	1 491	1 243	533	869
Cu	35	90	45	7	13	15	6	–
Cr	356	248	309	71	141	66	104	75
Ga	17	13	16	12	13	15	13	10
Hf	2.3	2.2	2.5	2.6	0.1	–	–	–
Nb	2.7	3.8	3.1	0.8	1.1	–	–	–
Ni	153	79	143	40	51	38	49	40
Pb	6.8	13.6	8.2	14.2	9.3	14	17	7
Rb	20	48	14	41	53	55	22	32
Sc	15.2	25.5	18	11.2	14.4	8	6	7
Sr	990	501	1 064	140	519	717	275	303
Ta	1.4	1	1.4	1.5	2.2	–	–	–
Th	5	5.3	5.2	4.8	4.3	5	8	4
U	0.8	1.2	0.8	1.4	1.2	–	2	–
V	97	139	94	51	91	65	53	54
Y	7.5	11.7	8.6	6.3	6.4	7	7	6
Zn	66	73	77	35	46	44	37	41
Zr	202	124	212	108	144	174	131	117
La	23.2	25.3	24.1	24.1	22.5	14	18	11
Ce	40	47.7	45.2	46.1	39.2	33	32	23
Pr	4.2	4.4	4.5	4.2	3.9	–	–	–
Nd	17.8	19.5	19	18.3	15.4	–	–	–
Sm	3.3	4.6	3.8	3.4	3.4	–	–	–
Eu	1	1.3	1.1	0.9	1.1	–	–	–
Gd	2.2	3.1	2.6	2.3	2.1	–	–	–
Tb	0.4	0.5	0.5	0.3	0.3	–	–	–
Dy	1.6	2.4	1.8	1.3	1.4	–	–	–
Ho	0.4	0.5	0.4	0.2	0.3	–	–	–
Er	1.8	1.4	1.1	0.8	0.8	–	–	–
Tm	0.2	0.2	0.2	0.1	0.1	–	–	–
Yb	0.8	1.2	0.9	0.5	0.6	–	–	–
Lu	0.2	0.2	0.2	0.1	0.1	–	–	–
(La/Yb) <sub>CN</sub>	19.55	14.21	18.05	32.50	25.28	–	–	–

## Appendix (continued)

GSWA sample	White Flag Lake 117206	Mount Shea 114447	Mount Shea 114443	Pipeline 114450	LED10 114492	Kambalda 114483	Kambalda 114479	114481
Rock type	Rhyolite cgte clast	Andesite breccia	Dacite	Andesite	Amydaloidal basalt flow	Basalt	Amydaloidal basalt	Basalt
Location	W of White Flag Lake	Island S of lake	NE of Mount Shea	Mascotte Ora Banda	Boulder	Democrat	Foster	Democrat
Drillhole					LED10	DHD422	TD 1847	DHD421
Depth (m)					230.4	267.7	122.5	94.5
Map code	3136	3236	3236	3137	3236	3234	3234	3234
Easting	3320	3669	3673	3132	357921	389834	387660	389834
Northing	66098	65770	65763	66328	6591996	6509759	6510245	6509759

	Percentage								
SiO <sub>2</sub>	76.5	61.4	68.2	58.9	40.2	47.5	48.2	51.4	
TiO <sub>2</sub>	0.18	0.47	0.48	0.53	1.01	0.98	1.24	0.84	
Al <sub>2</sub> O <sub>3</sub>	12.1	14.8	15.4	15	12.7	17.9	18.6	15.6	
Fe <sub>2</sub> O <sub>3</sub>	1.03	1.26	2.28	1.8	1.58	4.25	1.42	2.74	
FeO	0.65	3	0.68	3.89	8.75	7.44	4.19	6.15	
MnO	–	0.07	–	0.09	0.18	0.19	0.17	0.08	
MgO	0.6	4.9	1.69	5.21	8.38	5.63	3.07	4.89	
CaO	2.14	6.93	2.14	7.93	7.68	6.86	9.17	6.6	
Na <sub>2</sub> O	4.88	4.58	5.33	4.06	1.22	2.16	5.4	3.63	
K <sub>2</sub> O	1.56	1.22	2.03	0.79	1.14	0.83	1.59	0.28	
P <sub>2</sub> O <sub>5</sub>	0.06	0.28	0.18	0.16	0.08	0.09	0.17	0.08	
LOI	0.64	1.42	1.7	2.29	16.1	6.1	6.97	8.22	
<b>Total</b>	<b>100.34</b>	<b>100.33</b>	<b>100.11</b>	<b>100.65</b>	<b>99.02</b>	<b>99.93</b>	<b>100.19</b>	<b>100.51</b>	
	Parts per million								
Ba	844	972	2 237	621	488	208	331	32	
Cu	6	–	26	–	87	5	37	69	
Cr	37	326	61	304	140	58	24	51	
Ga	13	16	19	17	17	–	23	19	
Hf	–	3.3	–	3	2.1	2.1	3.4	2.2	
Nb	1	2	–	1.7	3.1	4.1	9.3	4.2	
Ni	22	128	39	168	122	109	38	85	
Pb	13.4	6.6	13	3.9	4.7	3.4	8.5	4.3	
Rb	29	31	45	15	32	22	47	6	
Sc	5.2	19.3	8	24.7	41.8	41.1	29.1	31.1	
Sr	678	1 072	923	461	557	154	181	182	
Ta	2	2	–	1.8	0.6	1.1	1.2	1	
Th	4.3	7.8	15	5.8	0.5	0.7	1.8	0.6	
U	1.3	1.8	–	1.4	0.2	0.1	0.4	0.2	
V	36	110	62	128	350	234	195	201	
Y	3	10.3	8	11	12	12.9	13.3	13.3	
Zn	29	38	20	33	206	136	103	103	
Zr	163	221	269	153	119	91	133	93	
La	15.3	46.3	38	30.6	7.4	8.4	16.1	7.3	
Ce	27.3	85.2	71	60	17.4	19.3	31.3	16	
Pr	3.1	8.8	–	5.8	1.9	2	3.6	1.7	
Nd	8.3	36.1	–	25.1	8.9	9.1	13	7.9	
Sm	2.4	7.9	–	4.8	3.1	2.9	3.6	2.5	
Eu	0.6	2.1	–	1.4	1	1.9	1	0.8	
Gd	1.2	5	–	3.7	2.7	3	3.1	2.5	
Tb	0.1	0.7	–	0.5	0.4	0.5	0.5	0.4	
Dy	0.6	2.4	–	2.3	2.5	3	2.8	2.9	
Ho	0.1	0.6	–	0.5	0.5	0.6	0.6	0.6	
Er	0.3	1.3	–	1.4	1.6	1.9	1.9	1.8	
Tm	–	0.3	–	0.2	0.2	0.3	0.3	0.3	
Yb	0.2	1	–	1.2	1.4	1.6	1.8	1.7	
Lu	–	0.3	–	0.2	0.2	0.3	0.3	0.3	
(La/Yb) <sub>CN</sub>	51.58	31.22	–	17.19	3.56	3.54	6.03	2.90	

## Appendix (continued)

GSWA sample	Kambalda						Jeedamya	
	111993	114423	114424	114404	111970	111995	110223	110222
Rock type	Felsic tuff	Dacite tuff	Dacite tuff	Rhyolite	Tuff	Rhyolite lava	Basalt	Basalt
Location	Foster	Loves Find	Loves Find	W of Mandilla Homestead	Mandilla	Morgans Island	ESE of Jeedamya Homestead	NW of 21 Mile Well
Drillhole	TD921	DDH4	DDH4		WID1159A			
Depth (m)	96.8	78.7	53.1		268.5			
Map code	3235	3234	3234	3235	3235	3235	3139	3139
Easting	390763	38233	38233	3595	358903	3704	3352	3336
Northing	6522266	6512801	6512801	65275	6527670	65431	67454	67380
	<b>Percentage</b>							
SiO <sub>2</sub>	62	67.4	67.4	69	69.5	70.1	45.8	47.6
TiO <sub>2</sub>	0.51	0.33	0.33	0.24	0.36	0.23	2.05	1.41
Al <sub>2</sub> O <sub>3</sub>	14.3	16.1	16.1	14.6	14.5	15.1	12.6	14.2
Fe <sub>2</sub> O <sub>3</sub>	1.6	1.4	2.05	1.33	1.2	0.85	3.02	1.92
FeO	2.86	1.9	2.15	0.85	1.49	0.46	13.1	10.9
MnO	0.06	0.13	0.15	–	–	–	0.56	0.32
MgO	2.5	0.71	0.59	0.74	1.33	1.08	4.46	6.16
CaO	4.77	2.49	2.18	1.89	2.36	1.2	14.8	14
Na <sub>2</sub> O	3.21	5.05	5.87	4.65	3.21	5.41	1.8	1.91
K <sub>2</sub> O	3.69	2.69	2.13	4.77	4.04	2.26	0.31	0.36
P <sub>2</sub> O <sub>5</sub>	0.13	0.39	0.23	0.1	0.1	0.09	0.21	0.13
LOI	5.04	1.58	1.21	2.12	2.4	2.26	0.21	0.34
<b>Total</b>	<b>100.67</b>	<b>100.17</b>	<b>100.39</b>	<b>100.29</b>	<b>100.49</b>	<b>99.04</b>	<b>98.92</b>	<b>99.25</b>
	<b>Parts per million</b>							
Ba	483	1 194	846	724	784	1 164	83	54
Cu	–	15	14	–	5	7	4	6
Cr	48	31	27	25	30	23	26	120
Ga	19	18	17	17	15	19	19	19
Hf	–	–	3.6	–	–	1.93	1.65	–
Nb	–	9	8.1	10	1	0.28	5.14	–
Ni	34	13	17	9	22	11	27	114
Pb	–	11	15.4	34	11	37.9	6	–
Rb	100	61	60	157	85	72	9	5
Sc	8	6	9	2	6	1.07	28.4	–
Sr	275	449	567	315	105	650	75	109
Ta	–	–	3.4	–	–	0.19	1.25	–
Th	2	9	6.9	22	11	7.42	0.77	–
U	–	2	0.6	5	–	2	–	–
V	69	62	48	36	44	22	454	391
Y	9	14	10.9	13	9	2.35	38.69	34
Zn	44	49	59	43	40	49	132	92
Zr	129	194	221	184	131	213	146	100
La	11	66	46.4	47	21	18.81	8.42	–
Ce	23	138	63.2	84	36	31.22	21.23	10
Pr	–	–	9.8	–	–	3.79	3.54	–
Nd	–	–	39	–	–	12.55	16.82	–
Sm	–	–	8.7	–	–	2.36	4.99	–
Eu	–	–	2.3	–	–	0.77	1.19	–
Gd	–	–	5.4	–	–	1.58	6.7	–
Tb	–	–	0.7	–	–	0.16	1.22	–
Dy	–	–	2.4	–	–	0.6	8.1	–
Ho	–	–	0.4	–	–	0.09	1.76	–
Er	–	–	1.1	–	–	0.25	5.16	–
Tm	–	–	0.1	–	–	–	0.79	–
Yb	–	–	0.8	–	–	0.16	5.26	–
Lu	–	–	0.1	–	–	–	0.79	–
(La/Yb) <sub>CN</sub>	–	–	39.10	–	–	79.26	1.08	–

## Appendix (continued)

GSWA sample	Jeedamya							
	110221	110231	110230	110228	110229	110226	110227	110224
Rock type	Basalt	Dacitic tuff	Rhyolitic tuff	Rhyolite breccia clast	Rhyolitic breccia	Qtz-fspar porphyry dyke	Qtz-fspar rhyolite	Dacitic lithic crystal tuff
Location	NW of 21 Mile Well	ENE of Dead Horse Rocks	SW of Kurnalpi R'hole	ENE of Dead Horse Rocks	ENE of Dead Horse Rocks	NE of Sandy Well	NE of Sandy Well	SE of Jeedamya Homestead
Drillhole Depth (m)								
Map code	3139	3139	3139	3139	3139	3139	3139	3139
Easting	3320	3356	3356	3346	3346	3363	3344	3350
Northing	67392	67511	67507	67511	67511	67487	67486	67446
	<b>Percentage</b>							
SiO <sub>2</sub>	51.7	62.4	70.1	70.3	71.1	71.9	74	74.4
TiO <sub>2</sub>	0.73	0.64	0.48	0.36	0.36	0.38	0.28	0.24
Al <sub>2</sub> O <sub>3</sub>	13.4	15.1	14.1	12.9	13.7	13.6	12.8	12.5
Fe <sub>2</sub> O <sub>3</sub>	1.01	1.75	1.45	2.06	1.08	1.04	1.08	1.19
FeO	7.78	3.76	1.35	1.05	1.9	1.87	1.56	1.29
MnO	0.25	0.12	0.09	0.11	0.11	0.05	0.06	–
MgO	8.13	3.15	0.62	0.59	1.42	0.77	0.4	0.29
CaO	12.9	7.26	4.58	4.26	2.3	2.4	1.41	1.23
Na <sub>2</sub> O	2.05	4.08	3.64	2.89	3.21	4.37	3.4	4.17
K <sub>2</sub> O	0.17	0.3	3.16	4.44	3.92	2.67	4.05	3.32
P <sub>2</sub> O <sub>5</sub>	0.07	0.14	0.11	0.08	0.09	0.09	0.05	–
LOI	1.03	1.11	0.7	0.73	0.91	0.82	0.75	1.08
<b>Total</b>	<b>99.22</b>	<b>99.81</b>	<b>100.38</b>	<b>99.77</b>	<b>100.1</b>	<b>99.96</b>	<b>99.84</b>	<b>99.71</b>
	<b>Parts per million</b>							
Ba	99	283	690	720	611	621	670	803
Cu	23	8	–	12	9	–	–	21
Cr	587	11	31	59	48–5	–	–	7
Ga	13	16	13	13	13	13	12	13
Hf	0.67	–	–	3.75	–	–	5.16	–
Nb	1.07	7	8	5.7	8	8	5.32	10
Ni	196	6	17	14	27	–	–	–
Pb	4.4	11	12	23.5	48	15	102	5
Rb	15	3	101	188	136	96	149	108
Sc	30.6	–	–	5.94	–	–	4.67	–
Sr	79	317	191	101	105	138	77	117
Ta	0.59	–	–	1.79	–	–	1.63	–
Th	0.44	7	13	10.94	13	12	12.48	15
U	–	–	3	2	3	3	3	4
V	273	126	45	34	37	25	8	7
Y	13.33	19	22	18.7	29	26	19.9	30
Zn	81	71	32	56	158	50	61	15
Zr	46	177	210	193	212	221	241	240
La	1.88	50	27	27.9	36	32	29.83	33
Ce	4.61	108	54	49.59	62	61	55.08	62
Pr	0.85	–	–	6.32	–	–	6.91	–
Nd	4.05	–	–	21.75	–	–	24.07	–
Sm	1.48	–	–	4.54	–	–	4.86	–
Eu	0.56	–	–	0.9	–	–	0.98	–
Gd	2.31	–	–	4.62	–	–	5	–
Tb	0.42	–	–	0.68	–	–	0.76	–
Dy	2.9	–	–	3.86	–	–	4.15	–
Ho	0.64	–	–	0.82	–	–	0.87	–
Er	1.9	–	–	2.44	–	–	2.57	–
Tm	0.28	–	–	0.36	–	–	0.43	–
Yb	1.87	–	–	2.29	–	–	2.85	–
Lu	0.25	–	–	0.34	–	–	0.41	–
(La/Yb) <sub>CN</sub>	0.68	–	–	8.21	–	–	7.06	–

## Appendix (continued)

GSWA sample	Jeedamyra		Melita					
	110225	110232	110247	110249	110243	110236	110238	110242
Rock type	Rhyolitic ignimbrite	Rhyolitic tuff	Basalt	Basalt	Basaltic andesite	?Pillowed basalt	Basaltic andesite	Basaltic andesite
Location	ENE of Sandy Well	NE of Dead Horse Rocks	ESE of Melita Homestead	Westrail Quarry	SW of Melita Homestead	NE of Coron- ation Well	NE of Coron- ation Well	E of Heron Well
Drillhole Depth (m)								
Map code	3139	3139	3139	3139	3139	3139	3139	3139
Easting	3373	3356	3516	3517	3475	3433	3461	3435
Northing	67489	67515	67838	67614	67834	67748	67787	67800
	<b>Percentage</b>							
SiO <sub>2</sub>	75.7	76.1	47.5	49.4	51.1	51.5	53.4	54.1
TiO <sub>2</sub>	0.26	0.21	1.4	0.82	1.08	1.17	1.18	0.79
Al <sub>2</sub> O <sub>3</sub>	11.9	12.4	13.1	14.4	13.8	17.6	14.7	15.5
Fe <sub>2</sub> O <sub>3</sub>	0.72	0.79	1.77	2.33	1.78	3.12	3.39	2.82
FeO	0.75	0.98	9.4	8.84	6.67	5.76	6.49	6.21
MnO	–	–	0.19	0.22	0.16	0.18	0.19	0.16
MgO	0.08	0.25	4.91	7.47	7.92	3.8	5.29	5.11
CaO	1.54	0.88	7.7	11.1	7.72	10.1	8.42	8.88
Na <sub>2</sub> O	2.98	4.47	3.54	2.3	3.22	3.04	3.88	2.65
K <sub>2</sub> O	5.12	3.45	0.23	0.12	2.82	0.41	0.35	0.62
P <sub>2</sub> O <sub>5</sub>	0.05	–	0.27	0.08	0.47	0.2	0.22	0.13
LOI	0.92	0.46	9.16	2.2	2.65	2.84	2.35	2.72
<b>Total</b>	<b>100.02</b>	<b>99.99</b>	<b>99.17</b>	<b>99.28</b>	<b>99.39</b>	<b>99.72</b>	<b>99.86</b>	<b>99.69</b>
	<b>Parts per million</b>							
Ba	672	691	104	37	861	82	164	264
Cu	–	–	19	131	38	70	64	72
Cr	8	–	115	280	353	150	105	87
Ga	12	12	18	17	18	18	16	16
Hf	5.98	–	–	–	4.74	3.44	3.53	–
Nb	5.16	9	–	–	7.27	3.64	6.47	7
Ni	–	–	74	114	204	138	38	88
Pb	21.8	15	–	–	16.6	7.8	7	4
Rb	141	136	3	–	63	15	7	24
Sc	4.88	–	–	–	14.1	25.7	23.3	–
Sr	80	90	183	129	211	165	254	219
Ta	1.37	–	–	–	0.97	0.66	0.93	–
Th	10.64	17	3	–	7.65	2.12	1.7	3
U	3	5	–	–	2	–	–	2
V	5	–	263	254	163	242	225	169
Y	19.4	29	24	17	25.14	14.41	18.93	21
Zn	41	29	81	88	118	106	95	89
Zr	222	205	221	59	182	123	168	134
La	26.79	37	7	–	39.88	9.69	13.52	12
Ce	53.42	71	25	–	70.43	19.77	28.39	22
Pr	6.21	–	–	–	11.6	3.05	4.45	–
Nd	21.43	–	–	–	47.81	12.25	17.67	–
Sm	4.34	–	–	–	10.8	2.85	4.03	–
Eu	0.94	–	–	–	2.94	1.05	1.27	–
Gd	4.63	–	–	–	10.3	3.55	4.57	–
Tb	0.7	–	–	–	1.3	0.54	0.71	–
Dy	3.98	–	–	–	6.03	2.96	4.1	–
Ho	0.84	–	–	–	1.14	0.66	0.89	–
Er	2.59	–	–	–	2.91	1.85	2.7	–
Tm	0.39	–	–	–	0.39	0.26	0.39	–
Yb	2.56	–	–	–	2.58	1.83	2.45	–
Lu	0.35	–	–	–	0.33	0.23	0.38	–
(La/Yb) <sub>CN</sub>	7.06	–	–	–	10.42	3.57	3.72	–

## Appendix (continued)

GSWA sample	Melita							
	114455	110233	110245	110239	110235	110240	110241	110237
Rock type	Dolerite	Basaltic andesite	Dacite crystal tuff	Rhyolitic ignimbrite	Feldsparphyric tuff	Rhyolitic ignimbrite	Crystal tuff	Rhyolite
Location	Coronation Well	W of Coronation Well	SE of Melita Homestead	NW of Snow Well	NE of Coronation Well	Heron Well	NE of Heron Well	ENE of Coronation Well
Drillhole Depth (m)								
Map code	3139	3139	3139	3139	3139	3139	3139	3139
Easting	3423	3401	3493	3461	3425	3416	3429	3439
Northing	67750	67735	67839	67787	67748	67800	67804	67749
	<b>Percentage</b>							
SiO <sub>2</sub>	56	59	65.4	73.4	73.6	73.8	74.4	74.9
TiO <sub>2</sub>	0.75	0.89	0.72	0.16	0.42	0.29	0.24	0.18
Al <sub>2</sub> O <sub>3</sub>	16.1	15.3	13	11.8	11.8	10.5	11.1	12.3
Fe <sub>2</sub> O <sub>3</sub>	2.66	2.5	1.69	0.96	0.92	0.84	1.16	1.16
FeO	4.98	5.23	5.04	2.61	2.4	2.74	2.44	1.49
MnO	0.11	0.11	0.11	–	0.06	0.08	0.06	–
MgO	5.06	3.88	1.28	0.24	0.23	0.08	0.46	0.31
CaO	7.37	5.5	2.79	0.31	1.97	1.19	1.53	1.79
Na <sub>2</sub> O	2.51	2.5	4.7	0.48	3.57	0.82	4.2	3.26
K <sub>2</sub> O	1.49	1.7	1.81	8.58	3.25	7.68	1.99	3.9
P <sub>2</sub> O <sub>5</sub>	0.21	0.25	0.19	–	0.07	–	–	–
LOI	3.19	2.83	3.17	1.03	1.49	1.28	2.12	0.76
<b>Total</b>	<b>100.43</b>	<b>99.69</b>	<b>99.9</b>	<b>99.57</b>	<b>99.78</b>	<b>99.3</b>	<b>99.7</b>	<b>100.05</b>
	<b>Parts per million</b>							
Ba	386	370	466	1 775	636	1 340	450	694
Cu	14	41	9	174	–	7	6	–
Cr	58	14	–	–	5	4	–	5
Ga	17	16	20	12	16	17	24	11
Hf	–	–	–	–	–	17.85	–	–
Nb	–	7	15	11	17	26.98	46	13
Ni	57	17	–	–	–	–	–	–
Pb	4	7	5	6	11	17.1	7	12
Rb	43	53	44	129	82	125	40	90
Sc	22	–	–	–	–	2.89	–	–
Sr	180	248	85	30	78	60	84	93
Ta	–	–	–	–	–	3.02	–	–
Th	3	4	7	14	13	18.01	21	17
U	–	2	–	4	3	5	5	4
V	136	126	13	–	7	4	3	3
Y	19	24	45	50	57	162.4	160	50
Zn	66	96	102	13	97	98	73	52
Zr	150	210	439	266	390	572	572	290
La	15	16	32	41	40	81.64	70	43
Ce	32	40	75	82	94	142.6	167	89
Pr	–	–	–	–	–	23.4	–	–
Nd	–	–	–	–	–	96.63	–	–
Sm	–	–	–	–	–	23.6	–	–
Eu	–	–	–	–	–	3.29	–	–
Gd	–	–	–	–	–	27.8	–	–
Tb	–	–	–	–	–	4.31	–	–
Dy	–	–	–	–	–	28.7	–	–
Ho	–	–	–	–	–	5.81	–	–
Er	–	–	–	–	–	17.9	–	–
Tm	–	–	–	–	–	2.67	–	–
Yb	–	–	–	–	–	17.9	–	–
Lu	–	–	–	–	–	2.47	–	–
(La/Yb) <sub>CN</sub>	–	–	–	–	–	3.07	–	–

## Appendix (continued)

GSWA sample	Perkolilli							
	110234	110248	110246	110244	114157	114152	114155	114149
Rock type	Rhyolitic tuff	Rhyolitic tuff	Rhyolitic ignimbrite	Glassy rhyolite	Rhyolite lava	Rhyolitic tuff	Rhyolite clast in breccia	Rhyolite clast in breccia
Location	NE of Coronation Well	Mount Barton	E of Melita Homestead	E of Melita Homestead	Perkolilli	Perkolilli east	Perkolilli	Perkolilli
Drillhole								
Depth (m)								
Map code	3139	3139	3139	3139	3236	3236	3236	3236
Easting	3423	3522	3524	3497	3713	3736	3712	3708
Northing	67748	67643	67846	67844	66094	66073	66100	66904
	<b>Percentage</b>							
SiO <sub>2</sub>	75.8	76.3	76.4	77.9	77.5	77.7	81.1	81.4
TiO <sub>2</sub>	0.16	0.09	0.15	0.15	0.06	0.15	0.05	0.11
Al <sub>2</sub> O <sub>3</sub>	11.6	11.9	11.4	10.6	12.1	12.5	10.9	10.5
Fe <sub>2</sub> O <sub>3</sub>	0.79	0.46	0.66	0.45	0.22	2.28	0.1	0.16
FeO	1.45	0.61	1.8	1.43	0.24	0.16	0.19	0.16
MnO	–	–	0.11	–	–	–	–	–
MgO	0.2	0.19	0.42	0.31	–	0.99	–	–
CaO	1.05	0.56	0.17	0.55	0.06	–	0.13	0.33
Na <sub>2</sub> O	2.38	2.56	2.2	2.53	0.78	–	2.09	2.63
K <sub>2</sub> O	5.53	6.21	5.57	4.74	9.29	4.62	6.19	4.52
P <sub>2</sub> O <sub>5</sub>	–	–	–	–	–	–	–	–
LOI	0.86	1.23	0.95	1.03	0.62	2.44	0.53	0.91
<b>Total</b>	<b>99.82</b>	<b>100.11</b>	<b>99.83</b>	<b>99.69</b>	<b>100.87</b>	<b>100.84</b>	<b>101.28</b>	<b>100.72</b>
	<b>Parts per million</b>							
Ba	976	932	915	701	635	824	336	1 312
Cu	–	–	–	–	–	–	–	–
Cr	–	17	–	18	–	9	–	–
Ga	13	19	16	13	10	–	10	10
Hf	10.31	–	–	–	–	–	–	4
Nb	9.8	35	15	14	7	12	7	2.31
Ni	–	–	–	–	–	–	–	–
Pb	13.4	10	30	9	11	10	16	17.8
Rb	106	126	101	95	238	149	168	104
Sc	0.99	–	–	–	4	8	4	1.88
Sr	67	44	32	35	42	8	12	69
Ta	1.52	–	–	–	–	–	–	0.36
Th	14.21	18	15	13	11	23	11	8.61
U	4	6	4	3	3	5	4	2
V	–	–	4	–	3	8	–	–
Y	59.98	126	79	63	22	34	22	9.98
Zn	11	21	169	37	8	14	18	18
Zr	269	200	244	245	58	146	51	127
La	43.63	36	49	47	11	20	11	33.09
Ce	89.65	81	102	94	23	33	27	63.5
Pr	11.7	–	–	–	–	–	–	7.11
Nd	44.54	–	–	–	–	–	–	23.43
Sm	10.8	–	–	–	–	–	–	4.27
Eu	1.79	–	–	–	–	–	–	1.03
Gd	12.4	–	–	–	–	–	–	3.61
Tb	2.06	–	–	–	–	–	–	0.49
Dy	12.1	–	–	–	–	–	–	2.27
Ho	2.61	–	–	–	–	–	–	0.44
Er	7.7	–	–	–	–	–	–	1.27
Tm	1.23	–	–	–	–	–	–	0.19
Yb	8.19	–	–	–	–	–	–	1.26
Lu	1.21	–	–	–	–	–	–	0.17
(La/Yb) <sub>CN</sub>	3.59	–	–	–	–	–	–	17.71

## Appendix (continued)

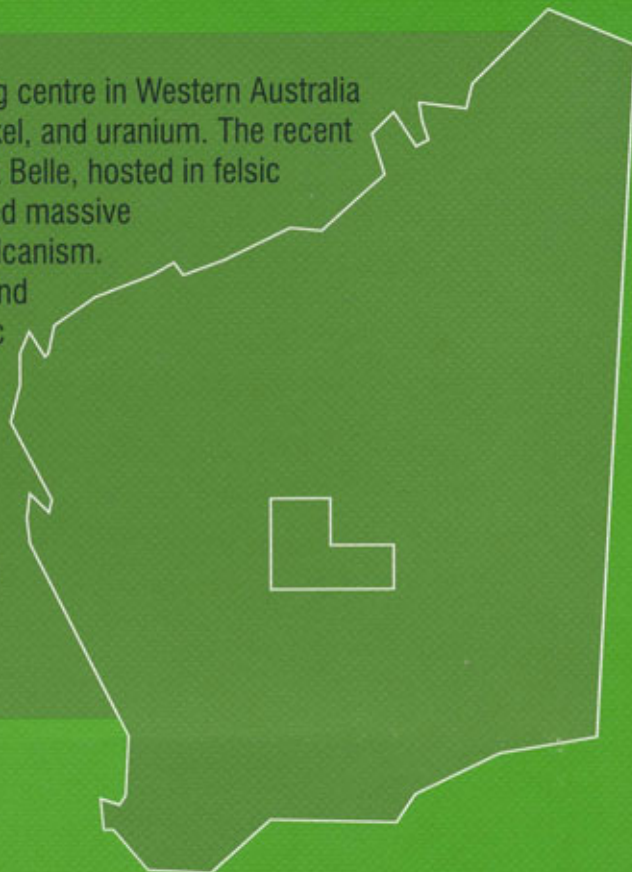
GSWA sample	Perkolilli 114151	Standards				Detection level
		JB-3 CCWA	? Potts et al. (1992)	JA-1 CCWA	? Potts et al. (1992)	
Rock type	Rhyolite clast in breccia					
Location	Perkolilli					
Drillhole						
Depth (m)						
Map code	3236					
Easting	3708					
Northing	66904					
<b>Percentage</b>						
SiO <sub>2</sub>	81.4	—	—	—	—	—
TiO <sub>2</sub>	0.05	—	—	—	—	—
Al <sub>2</sub> O <sub>3</sub>	10.7	—	—	—	—	—
Fe <sub>2</sub> O <sub>3</sub>	—	—	—	—	—	—
FeO	0.14	—	—	—	—	—
MnO	—	—	—	—	—	—
MgO	—	—	—	—	—	—
CaO	—	—	—	—	—	—
Na <sub>2</sub> O	2.16	—	—	—	—	—
K <sub>2</sub> O	5.91	—	—	—	—	—
P <sub>2</sub> O <sub>5</sub>	—	—	—	—	—	—
LOI	0.5	—	—	—	—	—
<b>Total</b>	<b>100.86</b>	—	—	—	—	—
<b>Parts per million</b>						
Ba	466	—	—	—	—	—
Cu	—	—	—	—	—	—
Cr	—	—	—	—	—	—
Ga	8	—	—	—	—	—
Hf	—	—	—	—	—	—
Nb	7	—	—	—	—	—
Ni	—	—	—	—	—	—
Pb	15	—	—	—	—	—
Rb	163	—	—	—	—	—
Sc	4	—	—	—	—	—
Sr	37	—	—	—	—	—
Ta	—	—	—	—	—	—
Th	10	—	—	—	—	—
U	5	—	—	—	—	—
V	—	—	—	—	—	—
Y	21	—	—	—	—	—
Zn	6	—	—	—	—	—
Zr	55	—	—	—	—	—
La	10	8.64	9.1	5.15	5.5	0.06
Ce	30	21.2	20.5	13.8	13.2	0.01
Pr	—	3.49	3.2	2.2	1.5	—
Nd	—	16.2	16.6	11.23	11	0.03
Sm	—	4.8	4.3	3.65	3.6	0.02
Eu	—	1.43	1.3	1.22	1.2	0.01
Gd	—	4.78	4.6	4.47	4.6	0.01
Tb	—	0.79	0.82	0.77	0.77	0.02
Dy	—	4.39	4.4	4.92	4.9	0.01
Ho	—	0.93	0.84	1.04	0.89	0.01
Er	—	2.61	2.5	3.08	3.2	0.01
Tm	—	0.39	0.5	0.45	0.51	0.01
Yb	—	2.55	2.4	2.99	2.9	0.01
Lu	—	0.39	0.38	0.46	0.46	0.01
(La/Yb) <sub>CN</sub>	—	—	—	—	—	—

## References

- MORRIS, P. A., PESCU, L., THOMAS, A., GAMBLE, J., TOVEY, E., MARSH, N., and EVERETT, R., 1991, Geochemical analyses of Archaean mafic and ultramafic volcanics, eastern Yilgarn Craton, Western Australia: Western Australia Geological Survey, Record 1991/8, 78p.
- POTTS, P. J., TINDLE, A. G., and WEBB, P. C., 1992, Geochemical reference material compositions: London, Whittles Publishing, 313p.
- WITT, W. K., DAVY, R., HUNTER, W. M., and PESCU, L., 1996, Geochemical analyses of Archaean acid to intermediate igneous rocks, including granitoids, minor intrusions, and volcanic rocks, southwest Eastern Goldfields Province, Western Australia: Western Australia Geological Survey, Record 1995/2, 55p.

The Eastern Goldfields region is an important mining centre in Western Australia and is highly prospective for gold, base metals, nickel, and uranium. The recent discovery of a significant gold resource at Kanowna Belle, hosted in felsic volcanic rocks, and global interest in volcanic-hosted massive sulfide deposits have stimulated interest in felsic volcanism.

This report discusses the volcanology, chemistry, and regional setting of two major areas of felsic volcanic rocks in the Eastern Goldfields region. Felsic volcanic rocks of the Black Flag Group dominate the upper part of the greenstone stratigraphy in the Kalgoorlie Terrane, and form a major part of this report. A felsic volcanic succession at Melita and Jeedamya, southeast of Leonora, and its strike extension at Kanowna are also described.



**Further details of geological publications and maps produced by the Geological Survey of Western Australia can be obtained by contacting:**

**Information Centre  
Department of Minerals and Energy  
100 Plain Street  
East Perth WA 6004  
Phone: (08) 9222 3459 Fax: (08) 9222 3444  
[www.dme.wa.gov.au](http://www.dme.wa.gov.au)**